

RICE UNIVERSITY

**Modulation of Chondrogenic and Osteogenic
Differentiation of Mesenchymal Stem Cells through
Signals in the Extracellular Microenvironment**

by

Jiehong Liao

A THESIS SUBMITTED
IN PARTIAL FULFILMENT OF THE
REQUIREMENT FOR THE DEGREE

Doctor of Philosophy

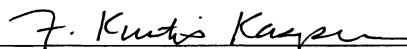
APPROVED, THESIS COMMITTEE:



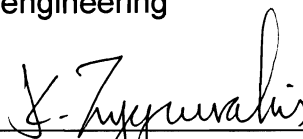
Antonios G. Mikos, Professor (Chair)
Bioengineering



K. Jane Grande-Allen, Associate Professor
Bioengineering



F. Kurtis Kasper, Faculty Fellow
Bioengineering



Kyriacos Zygorakis, Professor
Chemical & Biomolecular Engineering

HOUSTON, TX
DECEMBER 2010

ABSTRACT

Modulation of Chondrogenic and Osteogenic Differentiation of Mesenchymal Stem Cells through Signals in the Extracellular Microenvironment

by

Jiehong Liao

Damage to synovial joints results in osteochondral defects that only heal with inferior fibrous repair tissue. Since mesenchymal stem cells (MSCs) play a vital role in the natural development, maintenance, and repair of cartilage and bone, tissue engineering strategies to enhance functional regeneration by modulating MSC differentiation are a promising alternative to the limitations and potential complications associated with current conventional therapies. In this work, signals present in the native microenvironment were utilized in fabricating polymer/extracellular matrix composite scaffolds to guide chondrogenic and osteogenic differentiation.

In an osteochondral defect environment, interactions exist between bone marrow cell populations. Although MSCs have been extensively utilized for their ability to support hematopoietic stem and progenitor cells (HSPCs), the role of HSPCs in regulating the osteogenic differentiation of MSCs in the bone marrow niche is not well understood, and thus was explored via direct contact co-culture.

HSPCs in a low dose with sustained osteogenic induction by dexamethasone accelerated osteogenesis and enhanced mineral deposition, whereas the lack of induction signals affected the spatial distribution of cell populations and minerals. Thus, HSPCs presumably play an active role in modulating the development and maintenance of the osteogenic niche.

Since physical signals affect cellular activity, flow perfusion culture was employed to deposit mineralized extracellular matrix (ECM) with different maturity and composition on electrospun poly(ϵ -caprolactone) (PCL) microfibers in fabricating mineralized PCL/ECM composite scaffolds. The presence of mineralized matrix induced the osteogenic differentiation of MSCs even in the absence of dexamethasone, and a more mature matrix with higher quantities of collagen and minerals improved osteogenesis by accelerating alkaline phosphatase expression and matrix mineralization.

To determine whether PCL/ECM scaffolds can be applied to support the chondrogenic differentiation of MSCs, cartilaginous PCL/ECM composite scaffolds were fabricated. The presence of cartilaginous matrix reduced fibroblastic phenotype and in combination with transforming growth factor- β 1 (TGF- β 1), further promoted chondrogenesis as evident in elevated levels of glycosaminoglycan synthetic activity. While further investigation is necessary to optimize and test these scaffolds to induce the regeneration of cartilage and bone, this work demonstrates the importance of harnessing signals present in the native microenvironment to modulate chondrogenic and osteogenic differentiation.

ACKNOWLEDGEMENTS

I would like to thank my advisor, Dr. Antonios G. Mikos, for his patience, support, and encouragement in this endeavor. He has taught me what it truly means to be a scientific researcher and I sincerely appreciate the trust and confidence he has shown me throughout my time in the Mikos Research Group. I would also like to thank my thesis committee members, Dr. K. Jane Grande-Allan, Dr. F. Kurtis Kasper, and Dr. Kyriacos Zygourakis, for their valuable counsel and insightful discussions.

My appreciation goes out to Dr. Margaret A. Goodell and Dr. Grant A. Challen at the Baylor College of Medicine for their collaboration and expertise, and also to Dr. Kyle E. Hammerick, especially for his humor in difficult times. I am grateful for my friends and colleagues, all of whom I share fond memories with and who have made my time at Rice University a truly unforgettable and rewarding experience.

To my family and friends, I would like to extend my warmest appreciation for all their support and confidence in me. Thank you, to my volleyball friends who helped provide a great escape from work, and especially to the love of my life, Galen I. Papkov, who has showed me love and encouragement throughout our experience together at Rice University, and whom I look forward to sharing many more life experiences with. Finally, I would like to thank my mother, Jane Lin, who has provided me with this wonderful opportunity, and my father, Han Zhong Liao, who I know has always been with me in spirit.

TABLE OF CONTENTS

Abstract.....	ii
Acknowledgements.....	iv
Table of Contents.....	v
List of Figures.....	viii
List of Tables.....	x
List of Abbreviations.....	xi
CHAPTER I	
OVERVIEW.....	1
CHAPTER II	
BACKGROUND.....	3
BIOLOGY OF CARTILAGE AND BONE.....	3
Cartilage.....	3
Bone.....	7
STEM CELLS.....	12
Mesenchymal Stem Cells.....	13
Hematopoietic Stem Cells.....	15
TISSUE ENGINEERING.....	16
Scaffolds.....	17
Electrospinning.....	19
Bioreactors.....	22
FIGURES.....	26
CHAPTER III	
INVESTIGATING THE ROLE OF HEMATOPOIETIC STEM AND PROGENITOR CELLS IN REGULATING THE OSTEOGENIC DIFFERENTIATION OF MESENCHYMAL STEM CELLS IN VITRO.....	27
ABSTRACT.....	27
INTRODUCTION.....	29
MATERIALS AND METHODS.....	31
MSC Isolation and Expansion.....	31

HSPC Flow Cytometry Purification	32
MSC-HSPC Direct Contact Co-culture.....	33
Scanning Electron Microscopy	34
Staining and Light Microscopy	35
Osteogenic Differentiation Assays	36
Colony-forming Assay	37
Statistical Analysis	38
RESULTS.....	39
Cellularity and Alkaline Phosphatase.....	39
Calcium Deposition and Matrix Morphology.....	41
HSPC Colonies	42
DISCUSSION	42
CONCLUSION	49
FIGURES	50

CHAPTER IV

MODULATION OF OSTEOGENIC PROPERTIES OF BIODEGRADABLE POLYMER/EXTRACELLULAR MATRIX COMPOSITE SCAFFOLDS GENERATED WITH A FLOW PERFUSION BIOREACTOR.....

ABSTRACT.....	57
INTRODUCTION	59
MATERIALS AND METHODS	62
Electrospinning	62
Scaffold Preparation.....	63
PCL/ECM Mineralized Composite Scaffold Generation	64
Mineralized Matrix Characterization.....	66
Osteogenic Differentiation without Dexamethasone	68
Osteogenic Differentiation Assays	69
Scanning Electron Microscopy	71
Statistical Analysis	72
RESULTS.....	72
PCL/ECM Mineralized Composite Characterization.....	72
Cellularity and Alkaline Phosphatase.....	74
Calcium Deposition and Matrix Morphology.....	75

DISCUSSION	76
CONCLUSION	82
FIGURES	84
CHAPTER V	
BIOACTIVE POLYMER/EXTRACELLULAR MATRIX SCAFFOLDS	
FABRICATED WITH A FLOW PERFUSION BIOREACTOR FOR	
CARTILAGE TISSUE ENGINEERING	90
ABSTRACT	90
INTRODUCTION	92
MATERIALS AND METHODS	95
Electrospinning	95
Scaffold Preparation.....	96
PCL/ECM Cartilaginous Composite Scaffold Generation.....	96
Cartilaginous Matrix Characterization	98
Chondrogenic Differentiation with TGF- β 1	100
Chondrogenic Differentiation Assays	102
Scanning Electron Microscopy.....	103
Real-time RT-PCR	103
Statistical Analysis	104
RESULTS.....	106
PCL/ECM Cartilaginous Composite Characterization	106
Cellularity and Glycosaminoglycan	107
Quantitative Gene Expression	108
DISCUSSION	110
CONCLUSION.....	117
FIGURES	119
CHAPTER VI	
CONCLUDING REMARKS.....	127
CHAPTER VII	
BIBLIOGRAPHY.....	130

LIST OF FIGURES

Figure II-1	Schematic diagram and photograph of the flow perfusion bioreactor	26
Figure III-1	Total DNA content of wells cultured with MSCs alone or MSCs and HSPCs in co-culture either with or without the addition of dexamethasone	50
Figure III-2	Representative scanning electron micrographs after 8 and 14 days of wells cultured with MSCs alone or MSCs and HSPCs in co-culture either with or without the addition of dexamethasone	51
Figure III-3	Total alkaline phosphatase activity and normalized alkaline phosphatase activity of wells cultured with MSCs alone or MSCs and HSPCs in co-culture either with or without the addition of dexamethasone	52
Figure III-4	Alkaline phosphatase staining after 8 days of wells cultured with MSCs alone or MSCs and HSPCs in co-culture either with or without the addition of dexamethasone	53
Figure III-5	Total calcium content and fold change in calcium content of wells cultured with MSCs alone or MSCs and HSPCs in co-culture either with or without the addition of dexamethasone	54
Figure III-6	Alizarin Red staining after 24 days of wells cultured with MSCs alone or MSCs and HSPCs in co-culture either with or without the addition of dexamethasone	55
Figure III-7	Colony-forming unit counts of colonies derived in methylcellulose medium from the total cell population after co-culture either with or without the addition of dexamethasone	56
Figure IV-1	Matrix composition showing glycosaminoglycan, collagen, and calcium contents of PE4, PE8, PE12, and PE16 constructs generated in flow perfusion culture	84
Figure IV-2	Matrix morphology showing H&E, x-ray and SEM of PE4, PE8, PE12, and PE16 constructs generated in flow perfusion culture	85

Figure IV-3	Cellularity of plain PCL scaffolds and PE4, PE8, PE12, and PE16 composite scaffolds seeded with MSCs and cultured in static conditions without dexamethasone	86
Figure IV-4	Alkaline phosphatase activity of plain PCL scaffolds and PE4, PE8, PE12, and PE16 composite scaffolds seeded with MSCs and cultured in static conditions without dexamethasone	87
Figure IV-5	Calcium content of plain PCL scaffolds and PE4, PE8, PE12, and PE16 composite scaffolds seeded with MSCs and cultured in static conditions without dexamethasone	88
Figure IV-6	Representative scanning electron micrographs after 4, 8, and 16 days showing plain PCL scaffolds and PE4, PE8, PE12, and PE16 composite scaffolds seeded with MSCs and cultured in static conditions without dexamethasone	89
Figure V-1	Schematic representation of the overall experimental design for the generation, characterization, and evaluation of PCL/ECM composite scaffolds	119
Figure V-2	Morphology showing SEM, hematoxylin, and Safranin-O of PCL/ECM constructs following flow perfusion culture and PCL/ECM composite scaffolds following decellularization	120
Figure V-3	Composition showing glycosaminoglycan and collagen contents of PCL/ECM constructs following flow perfusion culture and PCL/ECM composite scaffolds following decellularization	121
Figure V-4	Biochemical results showing cellularity, glycosaminoglycan, and glycosaminoglycan synthetic activity for MSCs cultured on plain PCL scaffolds and PCL/ECM composite scaffolds either with or without the addition of TGF- β 1	122
Figure V-5	Representative scanning electron micrographs after 9, 15, and 21 days showing plain PCL scaffolds and PCL/ECM composite scaffolds seeded with MSCs and cultured either with or without the addition of TGF- β 1	123
Figure V-6	Quantitative gene expression results showing aggrecan, collagen type II, and collagen type I for MSCs cultured on plain PCL scaffolds and PCL/ECM composite scaffolds either with or without the addition of TGF- β 1	124

LIST OF TABLES

Table V-1	Global effect of experimental factors on biochemical results showing cellularity, glycosaminoglycan, and glycosaminoglycan synthetic activity	125
Table V-2	Global effect of experimental factors on quantitative gene expression results showing aggrecan, collagen type II, and collagen type I	126

LIST OF ABBREVIATIONS

ACI	Autologous Chondrocyte Implantation
ALP	alkaline phosphatase
BGP	bone gla protein
BMP	bone morphogenetic protein
BSP	bone sialoprotein
CC	co-culture
COMP	cartilage oligomeric matrix protein
DEX	dexamethasone
DMEM	Dulbecco's modified Eagle's medium
DMSO	dimethyl sulfoxide
DNA	deoxyribonucleic acid
ECM	extracellular matrix
FBS	fetal bovine serum
FDA	Food and Drug Administration
FGF	fibroblast growth factor
FITC	fluorescein isothiocyanate
GAG	glycosaminoglycan
GAPDH	glyceraldehyde 3-phosphate dehydrogenase
HBSS	Hank's balanced salt solution
HSC	hematopoietic stem cell
HSPC	hematopoietic stem and progenitor cells
IGF	insulin-like growth factors
KSL	c-Kit ⁺ Sca-1 ⁺ Lineage ⁻
MSC	mesenchymal stem cell
OCN	osteocalcin
OPF	oligo(poly(ethylene glycol) fumarate)
OPN	osteopontin
PBS	phosphate buffered saline
PCL	poly(ϵ -caprolactone)
PE	phycoerythrin
PGA	poly(glycolic acid)
PLA	poly(lactic acid)
PLGA	poly(lactic-co-glycolic acid)
PPF	poly(propylene fumarate)
RNA	ribonucleic acid
RT-PCR	reverse transcription polymerase chain reaction
SEM	scanning electron microscopy
SLRP	small leucine-rich proteoglycans
TGF	transforming growth factor
VEGF	Vascular endothelial growth factor
α -MEM	minimum essential medium, alpha modification

CHAPTER I

OVERVIEW

Conventional therapies to repair cartilage and bone defects involve donor grafts, which face challenges in their limited supply along with complications associated with donor site morbidity. With respect to cartilage, procedures to stimulate extrinsic repair typically result in inferior fibrocartilage that lacks the structure and composition required for long-term mechanical stability. Tissue engineering is a promising alternative where cells, bioactive factors, and scaffolds are incorporated to enhance tissue regeneration. Modulating the differentiation response of mesenchymal stem cells (MSCs) is a central concept in tissue engineering strategies since MSCs play a vital role in the natural development, maintenance, and repair of cartilage and bone. MSCs are influenced by signals present in the native microenvironment, and understanding these interactions to engineer key aspects of these signals *ex vivo*, enables the development of inductive scaffolds to facilitate the regeneration osteochondral tissue.

The overall goal of this thesis work is to explore signals present in the native tissue microenvironment and utilize these interactions in fabricating polymer/extracellular matrix (PCL/ECM) composite scaffolds to guide osteogenic and chondrogenic differentiation. This work addresses the following specific objectives:

1. Examine the role of hematopoietic stem and progenitor cells in regulating the osteogenic differentiation of mesenchymal stem cells via cell-cell interactions in direct contact co-culture.
2. Modulate the composition of mineralized PCL/ECM composite scaffolds through flow perfusion culture of osteoblastic cells and investigate how mineralized matrix maturity affects the osteogenic differentiation of mesenchymal stem cells in the absence of dexamethasone supplementation.
3. Fabricate cartilaginous PCL/ECM composite scaffolds through flow perfusion culture of chondrocytes and evaluate the ability of cartilaginous matrix to support the chondrogenic differentiation of mesenchymal stem cells in combination with transforming growth factor- β 1.

This thesis begins with background information on the biology and repair of cartilage and bone, along with considerations for osteochondral tissue engineering. Following chapters present investigations into factors which modulate MSC differentiation in terms of cellular interactions in the bone marrow niche, in addition to mineralized matrix signals and cartilaginous matrix signals incorporated into a biodegradable scaffolding system. Concluding remarks summarize the major findings and provide perspective for future directions.

CHAPTER II

BACKGROUND

Biology of Cartilage and Bone

Skeletal tissues function as the physical support system of the body. Both cartilage and bone serve vital roles in normal physiological activities, with complex biological mechanisms governing their development, maintenance, and repair. For successful strategies to facilitate the regeneration of diseased or damaged tissue, it is necessary to understand the biology of these complex tissues, from their macroscopic structure down to the extracellular composition and cellular interactions.

Cartilage

Articular cartilage is a specialized form of hyaline cartilage which provides a smooth lubricated covering on the articulating ends of bones in synovial joints. This lining of cartilage functions as a compressive load-bearing surface to evenly distribute forces onto bone and to reduce friction during joint movement. The shock-absorbing function of cartilage tissue is attributed to its hydrated nature and ordered structure, from the superficial zone which is the direct articulating surface, down to the calcified zone joining cartilage to bone. Articular cartilage is unique among connective tissues since it is only sparsely populated by cells

(chondrocytes) and lacks blood vessels, nerves, and lymphatics, making cartilage a tissue with low turnover and limited natural healing capacity.

Articular cartilage is composed of both a fluid phase and a solid phase as a biphasic viscoelastic material with high resilience. Mature cartilage is approximately 70% water, 20% collagen, and 6% proteoglycans by weight, with the remainder consisting of non-collagenous proteins and other molecules [1]. The fluid phase of cartilage contributes to its hydrated and lubricating nature, where fluid flow and osmotic pressure are the mechanisms responsible for how cartilage is able to resist high mechanical loads [2]. The solid phase of cartilage consists of cells and extracellular matrix, which in large part is collagen type II and aggrecan, whose interactions impart both tensile and compressive properties to the cartilage matrix [3]. Articular cartilage has a zonal structure (superficial, middle, deep, and calcified zones), where the organization and composition of matrix components differ with depth from the articulating surface to the subchondral bone [4]. This zonal structure influences the biomechanical properties of cartilage and its resilience in repeated loading during joint movement.

The only cells present in articular cartilage are chondrocytes, which have a rounded morphology, and make up less than 10% of the tissue volume [1]. Mature chondrocytes are responsible for the synthesis and maintenance of their surrounding cartilage matrix and rarely divide under normal conditions [5]. Although chondrocytes are embedded in large volumes of extracellular matrix, they respond to a variety of stimuli including growth factors, matrix molecules,

mechanical loads, and hydrostatic pressure changes [2]. Chondrocytes develop from chondroblasts, chondroprogenitor cells differentiated from mesenchymal stem cells in the bone marrow and synovium [6, 7]. Since cartilage tissue is avascular with such low cell density, chondrocytes obtain nutrients through diffusion from the synovial fluid as facilitated by fluid flow during joint movement [8].

While water is the most abundant component of articular cartilage, collagen is the main structural constituent of the cartilage matrix. Collagen type II is the principal collagen in cartilage which provides tensile strength [2]. The tensile properties of cartilage are attributed to the meshwork of collagen type II fibrils formed around a core of collagen type XI aggregates, where fibrillar diameter and crosslinking are modulated by collagen type IX [9, 10]. Aggrecan is the predominant proteoglycan in cartilage which provides compressive strength [10]. The compressive properties of cartilage are attributed to glycosaminoglycan (GAG) chains of chondroitin sulfate and keratan sulfate linked to the core protein of aggrecan, which are responsible for hydrophilic interactions and the osmotic swelling pressure in cartilage [11]. Aggrecan also joins with hyaluronan through link proteins to form proteoglycan aggregates, further enforcing the compressive nature of cartilage [12, 13]. Other proteoglycans in cartilage, such as decorin and fibromodulin, modulate collagen fibril formation and sequester growth factors [4]. Non-collagenous proteins in cartilage, such as cartilage oligomeric matrix protein (COMP) and fibronectin, are involved in matrix-matrix and cell-matrix interactions and signaling [14].

Damage to articular cartilage may result from impact or torsional joint injuries, repetitive loading, or degenerative diseases such as osteoarthritis, where cartilage tissue deteriorates leaving areas of exposed bone. Cartilage has a limited capacity for regeneration as compared to bone, due to its low cellularity and restricted access to stem and progenitor cells. Depending on the severity of damage, cartilage lesions range in depth and thus healing response [15, 16]. Chondral lesions are fissures or tears confined to the cartilage layer which results in intrinsic repair, relying on chondrocytes to proliferate and synthesize extracellular matrix. However, since chondrocytes only increase their synthetic activity as a transient response to injury, chondral lesions do not heal and thus, leave permanent defects that propagate with progressive loss and deterioration of the cartilage matrix [13, 17, 18]. Osteochondral lesions penetrate down to the subchondral bone layer which results in an extrinsic repair, beginning with an inflammatory response and fibrin clot formation, then the recruitment, proliferation, and chondrogenic differentiation of mesenchymal cells, and finally the synthesis of extracellular matrix [18-21]. This extrinsic wound healing response results in the formation of new cartilage tissue that is fibrous in nature and lacks the structure and composition required for long-term mechanical stability [22]. Among the factors involved in cartilage repair, transforming growth factors (TGF- β) modulate the chondrogenic differentiation of mesenchymal cells, while insulin-like growth factors (IGF) and bone morphogenetic proteins (BMP) maintain the differentiated phenotype of chondrocytes and stimulate the production of collagen and proteoglycans [18].

Since cartilage tissue itself has a limited capacity for regeneration, conventional procedures to repair cartilage defects include resurfacing techniques and the transplantation of cartilage grafts or chondrocytes [23]. Resurfacing methods aim to access bone marrow and initiate extrinsic repair by penetrating the subchondral bone layer via abrasion, microfracture, or drilling [24-26]. These methods yield fibrous repair tissue with variable composition, eventually resulting in the formation of fibrocartilage which lacks durability [26-28]. Autologous procedures include the transplantation of cartilage plugs (MosaicPlasty) since mature cartilage tissue consists of the appropriate structure and composition, and also the implantation of chondrocytes (Autologous Chondrocyte Implantation (ACI)) since differentiated cells in mature cartilage tissue exhibit the appropriate chondrocyte phenotype [29, 30]. Challenges in the use of autologous tissue for cartilage repair include the limited availability of donor tissue and consequent donor site morbidity from the harvest of healthy cartilage. Although allogenic sources have been explored for cartilage repair, transplantation of allogenic tissue often results in an immune response, even in the immunologically privileged joint environment [31, 32]. In either case, joint inflammation following these procedures is commonly associated with poor integration and mechanical mismatch between the donor and host tissue [33].

Bone

Bone is the rigid support structure of the body which protects internal organs and provides the framework for load-bearing and motion. The mineralized

nature of bone, with both compact structure in cortical bone, and porous trabecular structure in cancellous bone, allows the transfer of mechanical forces during movement. Bone serves as a reservoir of calcium salts and other minerals that are important for metabolism, and the medullary cavity of long bones is the site where blood and immune cells are generated in the bone marrow. With its vascularized nature and diverse population of cells (osteoblasts, osteocytes, osteoclasts), bone is a dynamic tissue that is constantly remodeled.

Bone is composed of both an organic phase and a mineral phase as a composite material that possesses both flexibility and strength. Mature bone is approximately 20% water, 35% organic molecules, and 45% minerals by weight [34]. The organic phase of bone consists of cells and extracellular matrix, which in large part is collagen type I, with a fibrous structure for elasticity [35, 36]. The hard mineral phase of bone consists of hydroxyapatite that has a calcium phosphate crystal structure for strength [36-38]. The mechanical properties of bone vary with shape and structure (long, short, flat, irregular, or sesamoid) [34]. Depending on the primary mechanism of bone formation, bone has either a woven or lamellar structure. Woven bone is deposited during rapid intramembranous bone formation directly within a mesenchymal cell condensation, or endochondral bone formation through a cartilage intermediate, where collagen bundles are randomly oriented, then later remodeled to lamellar bone [34]. Lamellar bone is deposited during slow appositional bone formation on surfaces of cartilage or bone, where collagen bundles are ordered to form regular sheets [34]. The structural arrangement, along with matrix interactions,

influences the biomechanical properties of bone as a load-bearing tissue and its ability to adapt to physiological conditions through remodeling.

The three types of bone cells in bone tissue are osteoblasts, osteocytes, and osteoclasts, each with specialized functions in bone remodeling. Osteoblasts are bone-forming cells that produce extracellular matrix and secrete factors to control mineralization. Osteocytes are terminally differentiated osteoblasts which become entrapped in bone matrix, and with long cytoplasmic processes, act as mechanoreceptors to coordinate cellular response to mechanical signals in the dense bone tissue [39]. Osteoclasts are large multinucleated bone-resorbing cells that break down bone matrix by secreting hydrogen ions and hydrolytic enzymes to dissolve minerals and digest matrix proteins [40]. Whereas osteoclasts develop from monocytes/macrophages differentiated from hematopoietic stem cells in the bone marrow, osteoblasts and osteocytes develop from osteoprogenitor cells differentiated from mesenchymal stem cells in the bone marrow and periosteum [41]. Since bone tissue has such a dense structure, bone cells obtain nutrients through diffusion from a network of vascular canals from the bone marrow [34].

Collagen is the major constituent of the organic phase in bone matrix, making up approximately 90% of the organic component in bone, with the remainder consisting of non-collagenous proteins, proteoglycans, and other molecules [34]. Collagen type I is the principal collagen in bone, and as a fibril-forming collagen, post-translationally modified collagen type I chains contain hydroxyproline and hydroxylysine residues that allow for crosslinking to form

stable fibers [42, 43]. In much lower quantities, bone also contains collagen types III, V, and XII, which are responsible for controlling collagen type I fibril formation and bundling [35]. Small leucine-rich proteoglycans (SLRPs), such as biglycan and lumican, the most abundant proteoglycans in bone matrix, are also involved in the structural organization of bone and play an essential role in regulating growth factor activity [44]. Together, collagen type I fibrils provide bone its elastic properties and act as a template for the deposition and alignment of mineral crystals, while the process of mineralization is facilitated by non-collagenous proteins, such as osteocalcin or bone gla protein (BGP), bone sialoprotein (BSP), and bone morphogenetic protein (BMP) [34, 35]. The mineral phase in bone matrix, that gives bone its hardness, is composed of crystalline hydroxyapatite ($\text{Ca}_{10}(\text{PO}_4)_6(\text{OH})_2$) made of calcium and phosphate [37]. The process of mineralization in bone is the heterogeneous nucleation of crystals on the collagen type I matrix. Enzymes secreted by bone cells neutralize inhibitors of mineralization, while anionic non-collagenous proteins act as nucleators of initial apatite formation. As mineral crystals agglomerate and grow, crystal size and shape are regulated by matrix proteins [35]. Alkaline phosphatase plays an important role in this process of mineralization as an enzyme that hydrolyzes organic phosphate and calcium substrates to create a supersaturated microenvironment where calcium and phosphate ions are readily available for incorporation into the developing bone matrix [45].

Damage to bone tissue may result from impact injury or degenerative diseases such as osteoporosis, where bone is fragile and susceptible to fracture

due to low bone mass. Surgical resection of bone tumors or traumatic injury typically results in the loss of large regions of bone, creating critical-sized defects or non-unions that do not heal. Depending on the severity of damage, bone tissue may regenerate at various rates or fail to heal at all, and thus require interventions to enhance or facilitate the process of regeneration. Nevertheless, since bone is a vascularized tissue with access to progenitor cells in the marrow and has the capacity for remodeling, regeneration to restore full form and function occurs more readily than for cartilage. The process of bone fracture healing consists of an inflammatory response, leading to the recruitment, proliferation, and osteochondral differentiation of mesenchymal cells responsible for initiating the reparative phase, where woven bone is formed through intramembranous and endochondral ossification, that is finally remodeled to lamellar bone architecture with mechanical strength [46, 47]. Aside from the initial inflammatory factors, bone morphogenetic proteins (BMP) modulate the osteogenic differentiation of mesenchymal cells, while transforming growth factors (TGF- β), insulin-like growth factors (IGF), and fibroblast growth factors (FGF) stimulate the proliferation and synthetic activity of differentiated bone cells [48, 49].

Although the natural process of bone regeneration is sufficient to heal most fractures, larger defects require surgical procedures to enhance or facilitate bone regeneration. Conventional methods to repair bone defects involve the transplantation of bone grafts in the form of autologous bone chips or blocks harvested from healthy bone tissue, since bone matrix itself is both

osteoinductive and osteoconductive [50-52]. While autografts have a high success rate due to the capacity of bone cells to remodel the transplanted bone matrix, harvesting bone tissue results in donor site morbidity [53, 54]. Allografts are alternative options for significant bone repair, but potential complications such as inflammation due to immune response and the risk of infection or disease transmission, limit their application [55, 56].

Stem Cells

Stem cells have the ability of self-renewal to retain stemness and the capacity for differentiation into specialized cell types in the body. Adult stem cells are responsible for the maintenance and regeneration of damaged or diseased tissue. Although the presence of adult stem cells have been confirmed in most differentiated tissues, bone marrow contains the most prominent stem cell compartment, and is the site where both hematopoietic stem cells and mesenchymal stem cells were first discovered [57, 58].

Stem cells in the bone marrow niche possess the capacity to differentiate into multiple cell types. Even though the stem cell population is very rare, as only 1 in 10,000 to 15,000 cells in the bone marrow is considered a stem cell, the stem cell niche contains signals which affect stem cell self-renewal [59]. In order to maintain a pool of progenitor cells, the process of self-renewal relies on the balance between symmetric and asymmetric cell division. This allows the proliferation of differentiated specialized cells while still maintaining a pool of undifferentiated stem cells. Understanding stem cell characteristics and

interactions are essential in utilizing this therapeutic cell source for clinical applications.

Mesenchymal Stem Cells

Mesenchymal stem cells (MSCs) or marrow stromal cells are characterized by their capacity to differentiate into multiple mesodermal lineages, such as cartilage and bone, and also by their ability to support hematopoietic cells even after their differentiation into osteoblasts [60, 61]. MSCs are multipotent progenitors that are not tissue-specific, in that they reside in multiple sites besides bone marrow. MSCs can be efficiently harvested from bone marrow aspirates, identified based on their adhesive properties to tissue culture plastic, isolated via colony formation when propagated in culture, and thus have been considered a heterogeneous population of stromal cells [62, 63]. MSCs play a vital role in the natural development, maintenance, and repair of cartilage and bone, and are often targeted in strategies to enhance tissue regeneration. Chondrogenic and osteogenic differentiation of MSCs are influenced by a broad range of signals, especially those present in the native microenvironment. The relationship between MSCs to both the structural and mechanical environment in which they are exposed, is an important aspect in modulating cellular response for tissue engineering applications.

Chondrogenic differentiation of MSCs *in vitro* is typically initiated by three-dimensional aggregation in high-density culture to maximize cell-cell gap-junctions based on the process of condensation during development, or by three-

dimensional low-density culture to mimic post-condensation where extracellular matrix molecules accumulate in the pericellular environment [64, 65]. Chondrogenic induction can be further stimulated by growth factors such as transforming growth factors (TGF- β), though ascorbic acid is essential for the organization and maturation of the collagen extracellular matrix, and contributions or interactions of other bioactive factors are commonly studied under serum-free culture conditions [66]. Chondrocyte development progresses through sequential stages consisting of proliferation, differentiation and extracellular matrix synthesis, and hypertrophy [67]. As MSCs undergo chondrogenic differentiation, Sox-9 expression is detected at the onset of differentiation, collagen type I expression decreases while collagen type II and aggrecan increase as cartilage matrix is generated, and collagen type X expression increases when chondrocytes become hypertrophic [68]. The end result in terms of tissue formation is a cartilaginous extracellular matrix predominantly consisting of collagen type II and glycosaminoglycan which can be directly quantified *in vitro*.

Osteogenic differentiation of MSCs *in vitro* is typically induced by the glucocorticoid dexamethasone or growth factors such as bone morphogenetic proteins (BMP), while osteoblastic progression and the formation of mineral nodules is dependent on ascorbic acid and β -glycerophosphate [69, 70]. Osteoblast development progresses through sequential stages consisting of proliferation, extracellular matrix synthesis and maturation, and mineralization [71]. As MSCs undergo osteogenic differentiation, collagen type I expression

decreases, whereas alkaline phosphatase (ALP) initially increases then decreases as mineralization is in progress [71-74]. Osteopontin (OPN) expression peaks during proliferation then again at the onset of differentiation, but prior to bone sialoprotein (BSP) which appears in differentiated osteoblasts and osteocalcin (OCN) which is associated with osteoblasts undergoing active mineralization [71-74]. The end result in terms of tissue formation is a mineralized extracellular matrix predominantly consisting of collagen type I and calcium phosphate which can be directly quantified *in vitro*.

Hematopoietic Stem Cells

Hematopoietic stem cells (HSCs) are characterized by their capacity to differentiate into myeloid and lymphoid lineages and also by their ability to generate all the blood and immune cells in the body [75]. HSCs are pluripotent progenitors that reside mainly in the bone marrow compartment, and while they can be activated to enter into circulation, they quickly return to their bone marrow niche or undergo differentiation. HSCs can be efficiently harvested from bone marrow aspirates, identified by their cell surface antigens, and isolated via immunoselection for combinations of receptors which have been confirmed to yield highly enriched cell populations capable of repopulating bone marrow [76, 77]. Due to the therapeutic nature of HSCs in regenerating blood and immune cells, bone marrow transplantation is a routine procedure, although engraftment and repopulation potential are directly related to the number of HSCs

transplanted [78]. Thus, *ex vivo* expansion of HSCs while maintaining their self-renewal and differentiation capacity has significant clinical implications.

Unlike MSCs, HSCs are non-adherent cells that require feeder layers of stromal cells and growth factors to remain viable and retain their stem cell characteristics once removed from the bone marrow niche environment [75]. Consequently, cell-cell interactions and soluble signals not only guide stem cell function but are essential for survival. However, it is unclear whether cell-matrix interactions with extracellular matrix components are sufficient for stem cell maintenance. Understanding the complexity of the bone marrow niche and engineering key aspects of these signals *ex vivo* would allow the maintenance of HSCs *in vitro* and enable the identification of factors involved in HSC expansion to further their therapeutic application. Since the bone marrow niche is a complex environment containing a heterogeneous population of cells, among which MSCs and osteogenic cells are responsible for generating mineralized extracellular matrix, it is important to consider how the cell-cell and cell-matrix interactions that take place within the niche regulate its development and maintenance.

Tissue Engineering

Tissue engineering of osteochondral tissue involves the incorporation of cells, bioactive factors, and scaffolds to either fabricate tissue constructs *in vitro* for implantation, or as means to enhance or facilitate tissue regeneration *in vivo*. The direct microenvironment in which a cell is exposed to plays a vital role in controlling cell function whether *in vitro* or *in vivo*, and thus must be taken into

careful consideration during the tissue engineering process. As cells interact with various components in their extracellular microenvironment, these factors in turn guide cellular response. Particularly in cartilage and bone, changes in the tissue microenvironment provide cues for regeneration remodeling. Understanding the key components in the native microenvironment and how those factors influence cellular function, provides the basis for which to engineer specific interactions *in vitro* to modulate cellular behavior or to design systems that induce tissue regeneration *in vivo*.

Scaffolds

Scaffolds for tissue engineering applications act as temporary structural supports, provide a template for cell growth and extracellular matrix deposition, and may be used as carriers for the delivery of cells or bioactive factors [79]. Scaffolding materials should be biodegradable, maintaining sufficient mechanical properties for temporary support during active tissue regeneration then completely degrading to restore native structure and function. Scaffolding materials and their degradation products must be biocompatible in that they must not be cytotoxic or immunogenic and must not cause unresolved inflammation. Scaffolds should be porous or degrade to provide porosity, with an interconnected pore structure allowing cellular infiltration, attachment, migration, and creating sufficient volume for tissue growth and integration. Natural and synthetic biomaterials are frequently employed in osteochondral tissue engineering since they fulfill many of these criteria or can be tailored accordingly.

Natural matrices are scaffolds consisting of purified extracellular matrix components such as collagen type II or hyaluronan for cartilage and collagen type I or hydroxyapatite for bone [80-83]. Although these natural scaffolds have shown promising results due to their role in native tissue, they can be easily degraded or resorbed in the physiological environment upon implantation. These materials also exhibit low mechanical properties since they are isolated components which lack the structural organization and necessary interactions as present in the native extracellular matrix from which they were derived. Thus, synthetic materials have been investigated for tissue engineering applications due to their ease of synthesis and processing to tailor material properties and degradation kinetics.

Synthetic polymer scaffolds may be injectable for photo polymerization or chemical polymerization *in situ*, or prefabricated with a fixed architecture for implantation. Injectable systems for cartilage such as oligo(poly(ethylene glycol) fumarate) (OPF), has been investigated for the delivery of growth factors and cells in an osteochondral defect [84]. Injectable systems for bone such as poly(propylene fumarate) (PPF), has been investigated with the incorporation of carbon nanostructures for mechanical reinforcement [85]. Porous preformed scaffolds are typically fabricated through processing techniques such as rapid prototyping, salt leaching, emulsion templating, and electrospinning [86, 87]. Common polymers used for cartilage and bone tissue engineering include poly(lactic acid) (PLA) and poly(glycolic acid) (PGA) which have been approved by the Food and Drug Administration (FDA) for certain applications. The

copolymer poly(lactic-co-glycolic acid) (PLGA), where the ratio of PLA to PGA can be adjusted to control degradation and material properties, has been investigated as an electrospun nanofiber scaffold to support both the chondrogenic and osteogenic differentiation of MSCs [88]. These poly(α -hydroxy esters) all undergo bulk degradation through hydrolytic cleavage of ester bonds, resulting in lactic acid and glycolic acid which are natural metabolites that can be physiologically integrated into metabolic pathways. Depending on the degradation rate, the accumulation of acidic degradation products may result in a local inflammatory response [89, 90].

Poly(ϵ -caprolactone) (PCL) is another FDA approved poly(α -hydroxy ester) that has been investigated for cartilage and bone tissue engineering, which has a slower degradation rate on the order of two years [91]. Since PCL also degrades through bulk hydrolysis, degradation rate depends on scaffold structure, particularly the surface to volume ratio. Maximizing surface area increases polymer contact with the aqueous environment and consequently accelerates degradation. PCL has been electrospun into highly porous nonwoven fiber mesh scaffolds which have been shown to support the differentiation of mesenchymal stem cells into cartilage and bone [92, 93].

Electrospinning

Electrospinning is a technique used to create nonwoven fiber mesh scaffolds with high interconnected porosity, large surface to volume ratios, and adjustable fiber diameters. Polymer fibers can be electrospun with diameters

from the micro to nanoscale with porosities as high as 90% [93, 94]. Electrospinning has been applied to produce tissue engineering scaffolds using both natural and synthetic polymers to mimic the fibrous microenvironment in connective tissues. These scaffolds offer three-dimensional fibers for cell attachment and migration, along with accessible volume for cell infiltration and tissue integration.

Electrospinning uses a simple and inexpensive setup typically consisting of a syringe pump, voltage source, and collector [95]. During the electrospinning process, a polymer solution is held at the needle tip by surface tension. When an electric field is applied via the voltage source, repulsive charges are induced within the polymer solution. This electrostatic force opposes the surface tension holding the polymer solution at the needle tip. When this electrostatic force overcomes the surface tension, a thin jet is formed and pulled toward the collector. As the jet of polymer solution travels the distance to the collector, the solvent evaporates leaving a continuous polymer fiber that can be captured on the collector. Both natural and synthetic polymers have been successfully electrospun for tissue engineering applications such as collagen, silk, PLGA, and PCL [96, 97].

The main factors which affect electrospinning include solution properties, processing variables, and ambient conditions [95]. Solution properties are characterized by viscosity or polymer concentration, conductivity or solution charge density, surface tension, polymer molecular weight, and dipole moment and dielectric constant. Processing variables include flow rate, electric field

strength or voltage, distance between the needle tip and collector, needle tip design and placement, and collector composition and geometry. Ambient conditions that affect electrospinning are temperature, humidity, and air flow. Of these factors, fiber diameter and morphology is most dependent upon viscosity as adjusted via polymer concentration in solution. Fiber diameters increase with higher polymer concentration, and increasing viscosity also reduces the appearance of beads or junctions caused by solvent that has not completely evaporated for more uniform fiber morphology [98, 99]. Electric field strength is another important factor controlling fiber diameter and morphology. If the applied voltage is low but sufficient to overcome the surface tension in the droplet suspended at the needle tip, then a single continuous jet is formed. As the applied voltage is increased, the droplet recedes and a larger jet is formed that has been shown to splay into several jets causing inconsistent fiber diameters and the presence of beads [100]. The architecture of electrospun scaffolds can also be tailored by employing various methods of fiber collection, such as aligned fibers using a rotating cylindrical drum collector rather than a stationary target. Aligned fibers affect cell orientation and matrix production and have been applied to model the superficial zone of articular cartilage [101, 102].

Electrospun PCL nanofiber scaffolds support the chondrogenic and osteogenic induction of MSCs when cultured with bioactive factors *in vitro* and have shown promising results when implanted as a construct *in vivo* [103-106]. Not only do electrospun fiber scaffolds mimic the structural features of the

extracellular matrix, with modifications such as surface coatings, these scaffolds can be engineered to provide cells with biological signals.

Bioreactors

Bioreactors in tissue engineering are designed to establish uniform distributions of cells seeded onto a scaffold, facilitate mass transfer to and from cells within a construct, and provide physiologically relevant mechanical signals [107]. The latter is based on the concept that the formation of functional tissue can be enhanced by replicating the mechanical environment of the native tissue. Since articular cartilage formation and endochondral bone formation exists in a fluid environment, joint movement imparts mechanical forces, mainly hydrostatic and direct compression, along with shear and some instances of tension. These forces are positive stimuli for osteochondral differentiation and extracellular matrix synthesis [108].

The two main types of mechanical stimulation most commonly investigated to produce osteochondral tissue of functional quality include hydrostatic compression and direct compression. Hydrostatic compression occurs during joint movement as a result of synovial fluid pressure in the joint capsule. Direct compression occurs when the joint surface is directly compressed by the opposing joint. Bioreactors designed to apply physiological loading and investigations into the magnitude, frequency, and duration of loading have generally shown enhanced matrix synthesis with dynamic stimulation as opposed to constant pressure [109-112].

Three-dimensional constructs for tissue engineering require the delivery of oxygen and nutrients to the interior of the construct for cell growth and tissue formation. In conventional static culture, where constructs are maintained statically in culture dishes, both internal and external mass transfer is through passive diffusion from the surrounding culture medium, which has detrimental effects on cell survival and limit culture duration [113, 114]. In basic dynamic culture, constructs are maintained with convective mixing of culture medium to improve external mass transfer through the surrounding fluid flow and convection over the surfaces of the constructs. Such bioreactors include spinner flasks with turbulent flow that often results in the formation of a fibrous capsule around the construct, and rotating vessels with laminar flow and thus improved peripheral tissue with no fibrous capsule formation [114-116]. Perfusion bioreactors enhance both internal and external mass transport by the flow of culture medium through the interconnected pores of the construct, thereby improving the delivery of oxygen and nutrients to the cells within the construct. In order to ensure that fluid flows through and not around the construct, there must be a tight fit between the construct and the walls of the flow chamber. Although constructs cultured in perfusion bioreactors do not show fibrous capsule formation, non-uniform tissue growth may result due to the unilateral direction of flow causing cells to deposit matrix with more collagen type I at the top surface of the construct in response to more direct fluid shear of higher magnitude [117]. The fluid flow rate can be optimized for tissue growth where lower flow rates may yield more uniform tissue.

Osteochondral tissues experience fluid shear stresses in the physiological environment, as mechanical loading creates fluid flow in the hydrated matrix of cartilage or through the canaliculus microstructure of bone. Fluid shear stresses have been shown to promote both chondroblast and osteoblast phenotype and enhance extracellular matrix deposition [118, 119]. The interconnected porosity of a scaffold creates channels for fluid flow, and cells attached at the walls of these channels experience shear forces directly associated with the rate of fluid flow. These channels can be modeled as cylindrical conduits to calculate the relationship between volumetric flow rate and shear stress at the wall [120]. As cells deposit increasing amounts of extracellular matrix that accumulates in the pore volume, the diameter of the channels or conduits decrease, and therefore results in higher fluid shear stresses over extended culture periods.

The perfusion bioreactor system developed in our laboratory provides direct fluid flow perfusion through tightly press-fitted constructs placed within individual flow chambers (Figure II-1) [121]. This bioreactor consists of a block with six chambers in which a cassette containing the press-fitted scaffold is placed within each chamber. The chambers are sealed with screw tops and connected to an inflow and an outflow medium reservoir via silicone tubing to allow oxygen diffusion. Medium is circulated through the closed system using a peristaltic pump and complete medium changes can be performed periodically to replenish nutrients. Studies in using this perfusion bioreactor have largely been conducted to investigate the osteogenic differentiation of MSCs on titanium fiber mesh scaffolds and starch-based fiber mesh scaffolds with promising results

[119, 122]. Thus efforts are warranted towards the transition to a biodegradable scaffolding system with the capacity to modulate both osteogenic and chondrogenic differentiation of MSCs for osteochondral tissue engineering applications. This thesis work begins with examining cellular interactions that regulate osteogenic differentiation specifically within the bone marrow niche microenvironment, and then explores mineralized extracellular matrix signals incorporated into a biodegradable scaffolding system in modulating osteogenesis, and finally applying the scaffolding system to investigate chondrogenesis through cartilaginous extracellular matrix signals.

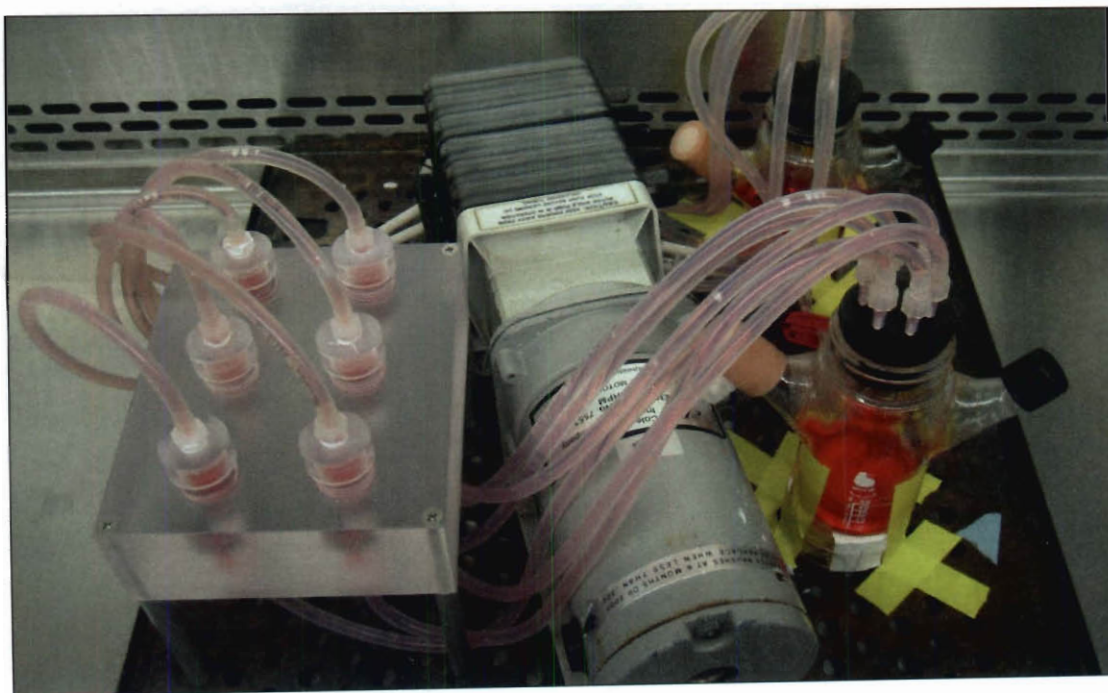
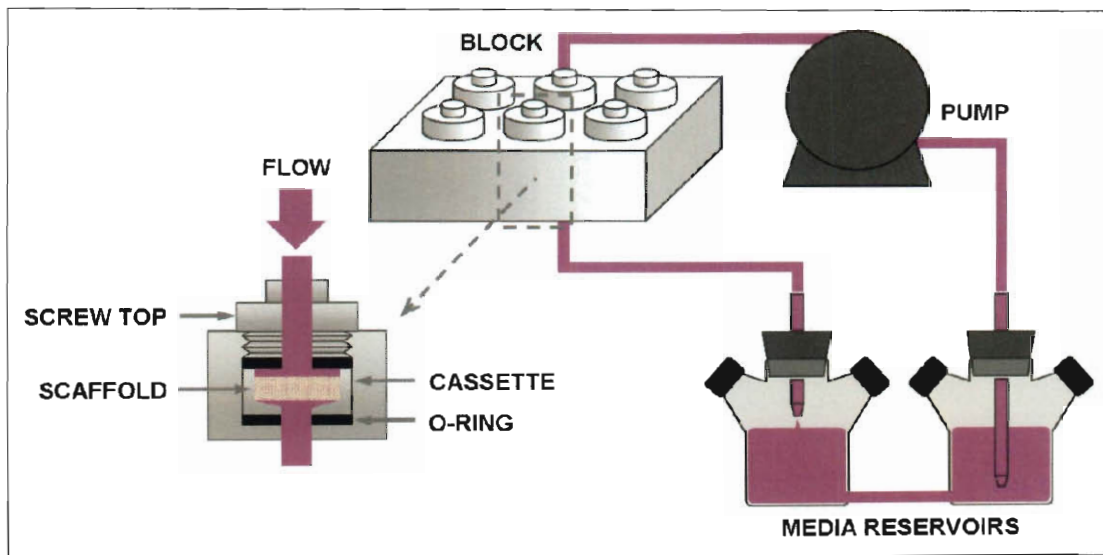


Figure II-1: Schematic diagram and photograph of the flow perfusion bioreactor.

CHAPTER III

INVESTIGATING THE ROLE OF HEMATOPOIETIC STEM AND PROGENITOR CELLS IN REGULATING THE OSTEOGENIC DIFFERENTIATION OF MESENCHYMAL STEM CELLS IN VITRO [†]

Abstract

Significant progress has been made in understanding the hematopoietic supportive capacity of both mesenchymal stem cells (MSCs) and osteogenic cells in maintaining hematopoietic stem and progenitor cells (HSPCs) *in vitro*. However the role of HSPCs in regulating their bone marrow niche environment through influencing the function of neighboring cell populations to complete this reciprocal relationship is not well understood. In this study, we investigated the influence of HSPCs on the osteogenic differentiation of MSCs *in vitro*, using a highly enriched population of hematopoietic cells with the phenotype c-Kit⁺ Sca-1⁺ Lineage⁻ (KSL) and bone marrow derived mesenchymal stromal cells in direct contact co-culture in medium with or without the addition of the osteogenic supplement dexamethasone. The data suggest that a low dose of HSPCs in co-culture with MSCs accelerates the osteogenic progression of MSCs as evidence in the reduced cellularity, earlier peak in alkaline phosphatase activity, and

[†] This chapter was submitted to the Journal of Orthopedic Research as: Liao J, Hammerick KH, Challen GA, Goodell MA, Kasper FK, Mikos AG. Investigating the role of hematopoietic stem and progenitor cells in regulating the osteogenic differentiation of mesenchymal stem cells in vitro.

enhanced calcium deposition compared to cultures of MSCs alone. We found that it is the primitive hematopoietic stem and progenitor cells in the population treated with dexamethasone that are responsible for augmenting the osteogenic differentiation of MSCs. Therefore, our findings further support the concept that HSPCs are actively involved in regulating the development and maintenance of the stem cell niche environment in which they reside.

Introduction

Hematopoietic stem and progenitor cells (HSPCs) have the capacity of self-renewal and are able to generate blood and immune cells to repopulate the bone marrow. However, unlike mesenchymal stem cells (MSCs), hematopoietic cells are difficult to expand *in vitro*. Since HSPCs function in a bone marrow microenvironment and reside near the endosteal surface of trabecular bone, recreating this stem cell niche *in vitro* may enable the expansion of functional hematopoietic cells *ex vivo*. To effectively engineer the marrow microenvironment, it is essential to understand the interactions between resident cell populations, as intimate contact between supporting cells, growth factors, and extracellular matrix cues provide a specific microenvironment that balances stem cell self-renewal versus differentiation and quiescence versus proliferation. The cellular components comprising the stem cell niche contain a heterogeneous population of cells, and in addition to hematopoietic progenitors, include multipotent mesenchymal progenitor cells and osteoblastic cells that may play an integral role within the stem cell niche. While significant progress has been made in understanding the hematopoietic supportive capacity of both MSCs and osteogenic cells [123-126], little is known about the ability of HSPCs to regulate the development and maintenance of their own niche environment by influencing neighboring cells. Since hematopoietic cells and mesenchymal populations reside in such close proximity, it is widely believed that there is substantial crosstalk between HSPCs and the other cellular components of the niche [127-129].

HSPCs and their primitive progeny are primarily located proximal to the endosteal surface of trabecular bone [130, 131]. The exact spatial relationship of HSPCs and stromal progenitor cells within the marrow is not well defined, but both cell populations coexist in close proximity within the marrow, suggesting that they play an interactive role in regulating their microenvironment and influencing the function of the other. HSPC development and localization is directly influenced by factors synthesized during the osteogenic program of MSCs. The differentiation of bone marrow stromal cells toward the osteogenic lineage results in a cascade of events, from the early expression of osteopontin to the development of a mineralized extracellular matrix. For example, osteopontin which is a potent regulator of mineralization and one of the most abundant non-collagenous proteins in bone [132], has been shown as a negative regulator of HSPC proliferation [133, 134], presumably facilitating the maintenance of a pool of hematopoietic progenitor cells within the marrow. Also, the mineral phase of bone is integral to the localization and adhesion of HSPCs within the endosteal niche, as HSPCs lacking the calcium-sensing receptor to detect the ionic content of the mineral phase do not function normally upon transplantation [135]. These examples support the concept that MSCs and osteoblastic cells actively regulate the function of HSPCs. The question remains whether HSPCs participate in completing this reciprocal relationship and how they influence the development and maintenance of the bone marrow niche.

Recent reports suggest that HSPCs regulate bone formation through the production of BMP-2 and BMP-6 [136, 137]. However, these studies emphasize

the effect of soluble signaling as the cell populations were physically separated in culture. Here we investigate the role of HSPCs in regulating the osteogenic differentiation of MSCs *in vitro* by examining the progression of osteogenesis through incorporating direct cell-cell interactions. Specifically, we evaluated the osteogenic differentiation of MSCs induced by dexamethasone treatment, and hypothesized that both cell-cell interactions and paracrine signaling provided by HSPCs would augment the osteogenic response of MSCs. To investigate our hypothesis, MSCs were co-cultured in direct contact with HSPCs in medium with or without the addition of dexamethasone, in order to explore the progression of osteogenesis and examine how HSPCs participate in the physical development of a mineralized niche environment *in vitro*.

Materials and Methods

MSC Isolation and Expansion

MSCs were isolated from bone marrow collected and pooled from the femurs and tibias of twenty 8-10 week old C57BL/6 mice (Jackson Laboratory, Bar Harbor, ME) according to previously established methods [138] and approved by the Institutional Animal Care and Use Committee of Baylor College of Medicine. Mice were anesthetized with isoflurane, euthanized via cervical dislocation, and then immersed in 70% ethanol. Femurs and tibias were excised and cleared of soft tissue. Bones were crushed using a mortar and pestle with Hank's balanced salt solution (HBSS) (Invitrogen, Carlsbad, CA), supplemented

with 2% fetal bovine serum (FBS) (Gemini Bio-Products, West Sacramento, CA), also with the addition of 1% antibiotics containing 10,000 U/mL penicillin and 10,000 µg/mL streptomycin (Invitrogen, Carlsbad, CA). The bone marrow suspension was filtered through a 100 µm cell strainer to remove bone debris, followed by a 40 µm cell strainer to obtain a single-cell suspension. Whole bone marrow was plated in tissue culture flasks with general expansion medium consisting of α-MEM, supplemented with 10% FBS, also with the addition of 1% antibiotics containing penicillin and streptomycin. Adherent cells were cultured for 7 days in general expansion medium with medium changes every 3 days. Following the primary culture period, MSCs were lifted with 0.25% trypsin and plated at low density for subculture expansion [139]. When confluent, MSCs were lifted and frozen in aliquots of medium containing 20% FBS and 10% dimethyl sulfoxide (DMSO). The adherent cells isolated from whole bone marrow and expanded through subculture will be referred to as the MSC population in subsequent co-cultures.

HSPC Flow Cytometry Purification

Following the same procedure described above to collect bone marrow from C57BL/6 mice, the marrow was alternatively suspended in phosphate buffered saline (PBS), supplemented with 2% FBS, 2 mM EDTA, and 10 mM HEPES, also with the addition of 1% antibiotics containing penicillin and streptomycin, then filtered through a 40 µm cell strainer to obtain a single-cell suspension. Whole bone marrow was enriched immunomagnetically for Sca-1+

cells using the EasySep Mouse SCA1 Positive Selection Kit (Stemcell Technologies, Vancouver, BC, Canada) according to the manufacturer's instructions. In addition to labeling cells with phycoerythrin (PE) conjugated Sca-1 as part of the EasySep Kit, cells were incubated on ice for 20 min with the following antibodies all at 1:100 dilution; fluorescein isothiocyanate (FITC) conjugated c-Kit (BD Pharmingen, Franklin Lakes, NJ), PE-Cy5 conjugated Mac-1, Gr-1, CD4, CD8, B220, and Ter-119 (eBioscience, San Diego, CA, USA) as previously described [140]. Cells were sorted for the cell surface phenotype c-Kit⁺ Sca-1⁺ Lineage⁻ (KSL), comprised of hematopoietic stem and progenitor cells, using a Cytomation MoFlo cell sorter (Dako, Carpinteria, CA). The hematopoietic stem and progenitor cells isolated and purified from whole bone marrow will be referred to as the HSPC population in subsequent co-cultures.

MSC-HSPC Direct Contact Co-culture

Cryopreserved MSCs were thawed at 37 °C and plated in tissue culture flasks with general medium for 24 h, then changed to complete osteogenic medium for an additional 6 days with medium changes every 2 days for osteogenic pre-culture [141, 142]. Complete osteogenic medium for osteogenic pre-culture consisted of α -MEM, supplemented with 10% FBS, 10^{-8} M dexamethasone, 10 mM β -glycerophosphate, and 50 mg/L ascorbic acid, also with the addition of 1% antibiotics containing penicillin and streptomycin. In preparation for cell seeding, individual wells of 12-well plates were filled with 1 mL of complete osteogenic medium either with or without the addition of 10^{-8} M

dexamethasone. Following the osteogenic pre-culture period, MSCs were lifted with 0.25% trypsin and seeded into 12-well plates at a density of 4×10^4 cells/well. After allowing 24 h for MSCs to attach and form a monolayer, HSPCs were isolated as described above and seeded into wells designated for direct contact co-culture at either 400 cells/well or 1000 cells/well. The first medium change was performed after 4 days with subsequent medium changes every 2 days thereafter. Sixteen wells were cultured for each culture group (MSC, CC400, CC1000) and dexamethasone treatment (-DEX and +DEX) for each culture time (8, 16, 24 days), at the end of which wells were rinsed with PBS in preparation for analysis. Two wells were fixed for scanning electron microscopy, two wells were stained to visualize alkaline phosphatase activity, and two wells were stained to visualize calcium deposition. Four wells were prepared to quantitatively assess cellularity and alkaline phosphatase activity, four wells to assess calcium content, and two wells to assess colony-forming capacity in methylcellulose medium.

Scanning Electron Microscopy

Culture wells for scanning electron microscopy were fixed with 10% neutral-buffered formalin (Fisher Scientific, Pittsburgh, PA) then rinsed with ddH₂O and air-dried. Wells were cut out from the culture plates using an X-660 Laser Platform laser cutter (Universal Laser Systems, Morningside, QLD, Australia) and mounted on aluminum stubs with conductive copper tape.

Samples were sputter coated with gold for 1 min prior to imaging using a Quanta 400 SEM (FEI, Hillsboro, OR).

Staining and Light Microscopy

Alkaline phosphatase activity was visualized by staining culture wells using a Blue Alkaline Phosphatase Substrate Kit (Vector Laboratories, Burlingame, CA) according to the manufacturer's instructions. Reagents provided with the kit were mixed in recommended proportions into 100 mM Tris-HCl buffer with pH adjusted to 8.2. Cells were incubated with 500 μ L of the substrate solution and developed in the dark for 30 min at 37 °C. Following the staining procedure where cells expressing alkaline phosphatase were stained blue, wells were fixed with 10% neutral-buffered formalin then rinsed with ddH₂O. Plates were placed at an angle to air-dry then stored at 4 °C. Cells were imaged using an Imager.Z2 light microscope with an AxioCam MRc 5 video camera attachment (Zeiss, Thornwood, New York).

Calcium deposition was visualized by staining culture wells with 40 mM Alizarin Red S (Sigma-Aldrich, St. Louis, MO) with pH adjusted to 4.1 using ammonium hydroxide [143]. Cells were fixed with 10% neutral-buffered formalin then rinsed with ddH₂O. Wells were incubated with 500 μ L of the Alizarin Red S solution for 30 min at room temperature. Wells were washed four times with 2 mL of ddH₂O to remove any unincorporated dye. Calcium deposits indicative of matrix mineralization on differentiating cells were stained red. Plates were placed

at an angle to air-dry then stored at 4 °C. Cells were imaged using an Imager.Z2 light microscope with an AxioCam MRc 5 video camera attachment.

Osteogenic Differentiation Assays

Cells from individual culture wells were lifted with 0.25% trypsin and placed in separate microcentrifuge tubes. Cell pellets were washed with PBS then 500 μ L of ddH₂O was added. Cells were lysed via three repetitions of a freeze and thaw cycle, where samples were frozen in liquid nitrogen for 10 min, thawed in a 37 °C water bath for 10 min, and sonicated for 10 min.

As a measure of cellularity, double-stranded DNA was quantified using the fluorometric PicoGreen assay (Invitrogen, Carlsbad, CA) with DNA standards [144]. Fluorescence was measured on an FL x800 plate reader (BioTek, Winooski, VT). DNA content is reported as μ g of DNA per well to assess cellularity. Alkaline phosphatase activity was determined by quantifying the enzyme-mediated dephosphorylation of the substrate p-nitrophenol phosphate to p-nitrophenol in a colorimetric assay (Sigma-Aldrich, St. Louis, MO) with p-nitrophenol standards [145]. Absorbance was measured on a PowerWave x340 plate reader (BioTek, Winooski, VT), with concentrated samples diluted as necessary to ensure absorbance readings within the linear range of the assay. Total alkaline phosphatase activity (ALP) per well is reported as pmol per h and normalized alkaline phosphatase activity (ALP/DNA) was calculated by dividing alkaline phosphatase activity over DNA content for each sample and is reported as pmol per h per μ g DNA as an early marker for osteogenic differentiation.

Calcium content was determined by quantifying free calcium ions in a colorimetric assay by first adding 500 μL of 1 N acetic acid directly into each culture well. After allowing calcium deposits to dissolve, samples were collected and wells were rinsed with an additional 200 μL of 1 N acetic acid. Calcium was quantified using the calcium assay (Genzyme, Cambridge, MA) with calcium chloride standards [146]. Absorbance was measured on a PowerWave x340 plate reader, with concentrated samples diluted as necessary to ensure absorbance readings within the linear range of the assay. Total calcium content is reported as μg of calcium per well and fold change in calcium content at each time point was calculated by normalizing calcium content to that of MSCs alone within each respective dexamethasone treatment to assess matrix mineralization as a late marker for osteogenic differentiation.

Colony-forming Assay

Cells from individual culture wells were lifted with 0.25% trypsin and placed in separate microcentrifuge tubes. The colony-forming capacity of HSPCs after each co-culture period was assessed by plating cells in Methocult GF M3434 methylcellulose-based medium (Stemcell Technologies, Vancouver, BC, Canada), then counting the number of colonies formed after 14 days [147]. Individual samples were first counted using a hemocytometer, aliquots of 10^4 total cells were plated in 35 mm low attachment culture dishes (Stemcell Technologies, Vancouver, BC, Canada) with 1.1 mL of Methocult GF M3434, and then incubated for 14 days. Following the incubation period, colonies were

counted using gridded scoring transparencies on a Stemi 2000 C stereomicroscope (Zeiss, Thornwood, New York). Colony-forming unit counts are reported as colonies per 10^4 total cells to assess the number of functional hematopoietic stem and progenitor cells remaining within the total cell population after co-culture.

Statistical Analysis

Biochemical assay results to assess cellularity, alkaline phosphatase activity, and calcium content are reported as mean \pm standard deviation for $n = 4$. A three-factor ANOVA was first performed to determine significant main effects or interactions between culture group (MSC, CC400, CC1000), dexamethasone treatment (-DEX and +DEX), and culture time (8, 16, 24 days). Multiple pairwise comparisons were then made using the Tukey procedure to determine significant differences. All statistical analyses were performed at a significance level of 5%.

Colony-forming assay results are reported as mean \pm standard deviation for $n = 4$. A two-factor ANOVA was first performed to determine significant main effects or interaction between dexamethasone treatment (-DEX and +DEX) and culture time (8, 16, 24 days). Multiple pairwise comparisons were then made using the Tukey procedure to determine significant differences. All statistical analyses were performed at a significance level of 5%.

Results

Cellularity and Alkaline Phosphatase

The influence of HSPCs on the osteogenic differentiation of MSCs *in vitro* was evaluated through direct contact co-culture with or without the addition of dexamethasone. Total DNA content per culture well was used to assess overall cellularity and proliferation throughout the culture period (Figure III-1). Cellularity remained constant over time at approximately the initial seeding density for cultures of MSCs alone with dexamethasone (MSC+), whereas an increase in cellularity was observed from 8 to 16 days for cultures of MSCs alone without dexamethasone (MSC-). Unlike cultures of MSCs alone, cellularity increased over time for all co-cultures regardless of dexamethasone treatment, with significant differences compared to MSCs alone at 16 and 24 days within both dexamethasone treatments. Co-cultures with dexamethasone (CC400+ and CC1000+) resulted in lower cellularity at 16 and 24 days compared to those without dexamethasone (CC400- and CC1000-).

Scanning electron micrographs were taken to visualize the surface morphology of culture wells with MSCs alone and MSCs and HSPCs in co-culture, as well as changes in the overall topography over time (Figure III-2). MSCs spread over the surface of culture wells forming a monolayer while HSPCs maintained a rounded phenotype. In short-term co-culture over 8 days, HSPCs appeared to grow on the surface of MSCs. In long-term co-culture over 24 days, HSPCs seemed to incorporate into the cell layer with MSCs. The cultures

acquired a rough texture after 24 days with the development of mineralized extracellular matrix containing mineral nodules.

Total alkaline phosphatase activity (ALP) per culture well and alkaline phosphatase activity normalized to DNA content (ALP/DNA) were used to assess early osteogenic differentiation (Figure III-3). Total ALP (Figure III-3A) increased significantly in the first 8 days for all culture groups then remained constant over time for cultures of MSCs alone regardless of dexamethasone treatment. Although co-cultures with dexamethasone showed the same trend and ALP activity levels as MSCs alone, those without dexamethasone resulted in an increase in ALP over time, with significant differences compared to MSCs alone at 16 and 24 days. Co-cultures without dexamethasone resulted in higher ALP activity at 16 and 24 days compared to those with dexamethasone. ALP/DNA (Figure III-3B) remained constant over time at approximately the initial level at seeding for cultures of MSCs alone without dexamethasone, whereas ALP/DNA increased significantly in the first 8 days and peaked at 16 days for cultures of MSCs alone with dexamethasone. Although co-cultures without dexamethasone showed the same trend and ALP/DNA levels as MSCs alone, those with dexamethasone resulted in a peak in ALP/DNA at 8 days. Light micrographs were taken of culture wells stained blue to visualize the ALP expression of MSCs alone and MSCs and HSPCs in co-culture after 8 days (Figure III-4). All cultures showed positive expression of ALP with fairly even distribution within the culture wells overall. Microscopy images revealed that most of the spread MSCs express

ALP with varying intensities of blue staining, while the rounded HSPCs did not appear to express ALP as evident in the lack of blue staining macroscopically.

Calcium Deposition and Matrix Morphology

Total calcium content per culture well and fold change in calcium content as compared to MSCs within each respective dexamethasone treatment were used to assess late osteogenic differentiation (Figure III-5). Total calcium content (Figure III-5A) increased over time for cultures of MSCs alone regardless of dexamethasone treatment, with higher calcium deposition observed for cultures without dexamethasone at 16 and 24 days. Similar to cultures of MSCs alone, calcium content increased over time for all co-cultures regardless of dexamethasone treatment, also with higher calcium deposition observed for cultures without dexamethasone at 16 and 24 days. Fold change in calcium content for co-cultures was calculated by normalizing calcium content to that of MSCs alone within each respective dexamethasone treatment (Figure III-5B). Only the low dose co-culture group with dexamethasone (CC400+) showed a significant difference in calcium content compared to MSCs alone with dexamethasone (MSC+). Fold change in calcium deposition for CC400+ was 5.8 ± 1.2 fold higher than MSC+ at 8 days and 5.5 ± 2.8 fold higher than MSC+ at 16 days. Interestingly, there was no significant difference at 24 days. Light micrographs were taken of culture wells stained red to visualize the calcium deposition of MSCs alone and MSCs and HSPCs in co-culture after 24 days (Figure III-6). Although all cultures showed calcium deposition with varying

intensities of red staining, the distribution of calcium deposits within the culture wells varied overall. Blank regions lacking calcium deposits were most apparent for co-cultures without dexamethasone, whereas calcium deposition appeared more evenly distributed for co-cultures with dexamethasone. Microscopy images revealed that the blank regions indeed had functional cells growing which did not stain red for calcium deposits.

HSPC Colonies

Colony-forming cell growth in methylcellulose medium was used to assess the colony-forming capacity of HSPCs after co-culture (Figure III-7). Although the number of hematopoietic stem and progenitor cells significantly decreased in the first week of co-culture as compared to the initial HSPC population following FACS analysis prior to seeding (data not shown), more colonies remained with dexamethasone treatment in short-term co-culture. After 8 days of co-culture, colony-forming unit counts per 10^4 total cells for CC400+ was 35.3 ± 12.4 and for C400- was 3.3 ± 1.3 . While dexamethasone treatment resulted in this significant difference in colony counts at 8 days, the number of colonies decreased over extended culture periods.

Discussion

The objective of this study was to investigate the influence of HSPCs on the osteogenic differentiation of MSCs through direct contact co-culture, to better understand the interactions of cellular components comprising the stem cell

niche under *in vitro* culture conditions. This study was designed to evaluate the osteogenic differentiation of MSCs *in vitro* induced by dexamethasone treatment, and to examine how the inclusion of HSPCs in co-culture would augment this differentiation response by providing a niche microenvironment consisting of both direct cell-cell interactions and paracrine signaling.

Recent studies have reported that HSPCs actively participate in bone formation by producing BMP-2 and BMP-6 [136], especially when activated by elevated erythropoietin levels induced by acute bleeding [137]. Frequently in studies investigating the crosstalk between HSPCs and MSCs, the effect of soluble signaling is emphasized as HSPCs are cultured separately from MSCs in the top chambers of Transwell plates then assessed for osteoblastic colony formation at the end of culture [136, 148]. Here we investigated the progression of osteogenesis from induction to mineralized matrix production by incorporating direct cell-cell interactions in addition to paracrine signaling, which allowed us to examine how HSPCs participate in the physical development of a mineralized niche environment *in vitro*.

Our results showed that HSPCs influenced the osteogenic differentiation of MSCs under *in vitro* culture conditions with dexamethasone. We observed that low doses of HSPCs co-cultured in direct contact with MSCs and exposed to dexamethasone treatment, reduced overall cellular proliferation, stimulated early alkaline phosphatase activity, and enhanced calcium deposition, thus supporting the progression of osteogenic differentiation *in vitro*. Additionally, we were able to

observe the physical interactions between HSPCs and differentiating MSCs throughout the progression of osteogenesis *in vitro*.

Cellularity and proliferation throughout the culture period was evaluated by quantifying total DNA content per culture well. Cultures of MSCs alone, particularly with dexamethasone treatment, maintained similar cellularity over 24 days of culture. Since cells were induced toward osteogenic differentiation *in vitro* with dexamethasone, we expect to see minimal proliferative activity as cells transition to an osteoblastic phenotype [149]. Although in all co-culture groups, the overall cell population rapidly proliferated, dexamethasone treatment significantly reduced cellularity after 16 and 24 days of culture. Observations from light microscopy and scanning electron microscopy suggest that the HSPC population proliferated quickly in co-culture while the MSC population maintained a confluent cell layer to support the growth and retention of HSPCs *in vitro*. Over an extended culture period however, HSPCs incorporated into the cell layer with MSCs and could possibly outcompete MSCs for space and nutrients. While in this study, the contribution of each cell population to the overall change in cellularity over time was not specifically assessed, we consider that HSPCs proliferate much more rapidly than MSCs in co-culture, as MSCs and osteogenic cells are often used as feeder layers to expand hematopoietic cell numbers *ex vivo* due to their supportive role in the stem cell niche [123-126]. However in those applications, dexamethasone is not included as a culture supplement, and thus the effects of both co-culture and dexamethasone on HSPCs *in vitro* are not known. Studies investigating glucocorticoid treatment through intraperitoneal

injections have shown hematoprotective effects of dexamethasone, promoting the quiescence of stem cells as seen in the maintenance of high colony-forming cell numbers even after cytotoxic chemotherapy [150, 151]. In exploring how HSPCs affect the progression of MSCs initiated toward osteogenic differentiation via dexamethasone exposure, we observed that dexamethasone may play a role in maintaining hematopoietic stem and progenitor cells *in vitro*. This is evidenced in the higher number of functional hematopoietic stem and progenitor cells within the total cell population that remain following short-term co-culture with dexamethasone, albeit those colony-forming cells decrease significantly in number over extended culture periods. Although the expansion of HSPCs *ex vivo* was not the focus of this current study, we found that dexamethasone as a culture supplement may be worth exploring in order to optimize co-culture conditions to permit the sustained expansion of HSPCs *ex vivo*.

Alkaline phosphatase activity was used as an early marker for osteogenic differentiation as enzyme levels peak during the onset of osteogenic differentiation then decrease as cells progress toward an osteoblastic phenotype [149]. Dexamethasone treatment induced a significant increase in ALP/DNA in the first 8 days for all culture groups. While MSCs alone showed a clear peak in ALP/DNA at 16 days, the data suggest that the peak in ALP/DNA for co-culture groups may have occurred sooner within the first 8 days of culture, since ALP/DNA levels were already declining after 8 days. Thus, these trends in ALP/DNA imply that dexamethasone indeed promotes osteogenic differentiation with a characteristic peak in the profile of alkaline phosphatase expression we

typically observe in our osteogenic cultures [152-154], and that co-culture with HSPCs accelerates the osteogenic differentiation of MSCs in their transition to an osteoblastic phenotype.

Since cell populations were not separated following co-culture, total alkaline phosphatase activity of the entire cell population as whole is also reported. Through macroscopic inspection following the staining procedure to visualize ALP expression at 8 days, HSPCs did not appear to stain for ALP activity as most of the staining was much more apparent and intense for the MSCs. While we do not know how the HSPC population contributes to quantitative ALP measurements, ALP expression has been documented for rare hematopoietic cells, particularly plasma cells as terminally differentiated B-cells [155]. This may account for the higher levels of total ALP detected for co-cultures without dexamethasone, as the colony-forming assay revealed that cells rapidly differentiated into mature hematopoietic lineages within the first week of culture without dexamethasone treatment, as evident in the lower numbers of functional hematopoietic stem and progenitor cells remaining within the total cell population after co-culture.

Calcium deposition was used as a late marker for osteogenic differentiation as cells with an osteoblastic phenotype deposit increasing amounts of extracellular matrix which mineralizes over time [149]. Calcium deposition increased over time for all culture groups regardless of dexamethasone treatment. Since mouse MSCs were expanded through a brief osteogenic pre-culture period with dexamethasone in order to direct cells toward

the osteoblastic lineage prior to establishing experimental cultures as with our previous osteogenic studies using rat MSCs [141, 142], this transient exposure may have initiated osteogenic progression with sustained effects even after the removal of dexamethasone in subsequent experimental cultures, similar to what has been documented for human MSCs [156]. Thus, the sustained effects of dexamethasone in initiating a pre-osteoblastic phenotype, likely contributed to the calcium deposition observed in our experimental cultures without dexamethasone. Interestingly, there is a qualitative difference in the distribution of cell populations and calcium deposits within co-cultures not treated with dexamethasone. Mineralized extracellular matrix appears to be localized to the MSC population, with large regions of the cultures wells occupied by the HSPC population that did not stain for calcium, in contrast to the more even staining seen for co-cultures treated with dexamethasone.

When the calcium data for co-culture groups are normalized to that of MSCs alone within each respective dexamethasone treatment and considered as fold change in calcium content, it is apparent that in combination with dexamethasone treatment, a low dose of HSPCs in fact enhance calcium deposition at early time points. Over an extended culture period the signaling effects of HSPCs, which seem to accelerate osteogenic progression, dissipate as MSCs in all culture groups treated with dexamethasone converge to an osteoblastic phenotype. From the colony-forming assay, we see that it is the primitive hematopoietic stem and progenitor cells remaining in the total cell population following co-culture that exert this stimulatory effect on the osteogenic

differentiation of MSCs. On the contrary, if HSPCs differentiate into mature hematopoietic lineages in co-culture, then those hematopoietic cells lose their ability to augment the osteogenic progression of MSCs. Our findings in this study support the concept that not only do osteoblastic cells play a supportive role in maintaining hematopoietic cells, but that there is a reciprocal relationship whereby hematopoietic cells regulate osteoblastic cell function as active participants in the maintenance and development of the stem cell niche [136, 148]. Interestingly, there appears to be an optimal cell density to achieve enhanced mineralization under co-culture conditions, as may be the case in the physiological environment where the balance between cell populations affect overall cell function and tissue morphology. Furthermore, in modeling the osteogenic development of MSCs through dexamethasone exposure, we observe that not only does dexamethasone assist in directing cells towards recreating a mineralized microenvironment *in vitro* via brief exposure in pre-culture, but dexamethasone may also promote the maintenance of functional hematopoietic stem and progenitor cells in short-term co-culture. Thus, our investigation into the reciprocal relationship between the two major cell populations comprising the bone marrow niche under *in vitro* culture conditions, would allow the development of tissue engineering strategies further optimizing co-culture parameters to achieve expansion of hematopoietic cells *ex vivo*. Understanding the development of the bone marrow microenvironment and recreating key components or interactions *in vitro* brings us a step closer towards the realization of medical therapies utilizing culture expanded stem cells.

Conclusion

In this work, we demonstrated that primitive hematopoietic stem and progenitor cells enhance the osteogenic differentiation of mesenchymal stem cells through both cell-cell interactions and paracrine signaling as facilitated through dexamethasone treatment *in vitro*. We were able to examine how HSPCs participate in the physical development of a mineralized niche environment through direct contact co-culture with MSCs. This study further supports the concept that HSPCs actively regulate the development and maintenance of the stem cell niche environment in which they reside.

Acknowledgements

This work has been supported by the National Institutes of Health (R01 AR057083 and R01 EB005173). KE Hammerick was supported by an Alliance for NanoHealth Postdoctoral Fellowship. GA Challen was supported by the National Institutes of Health (K99 DK084259) and is an American Society of Hematology Scholar. We thank Christopher Threton of the Texas Children's Hospital Flow Cytometry Core Laboratory for cell sorting and analysis.

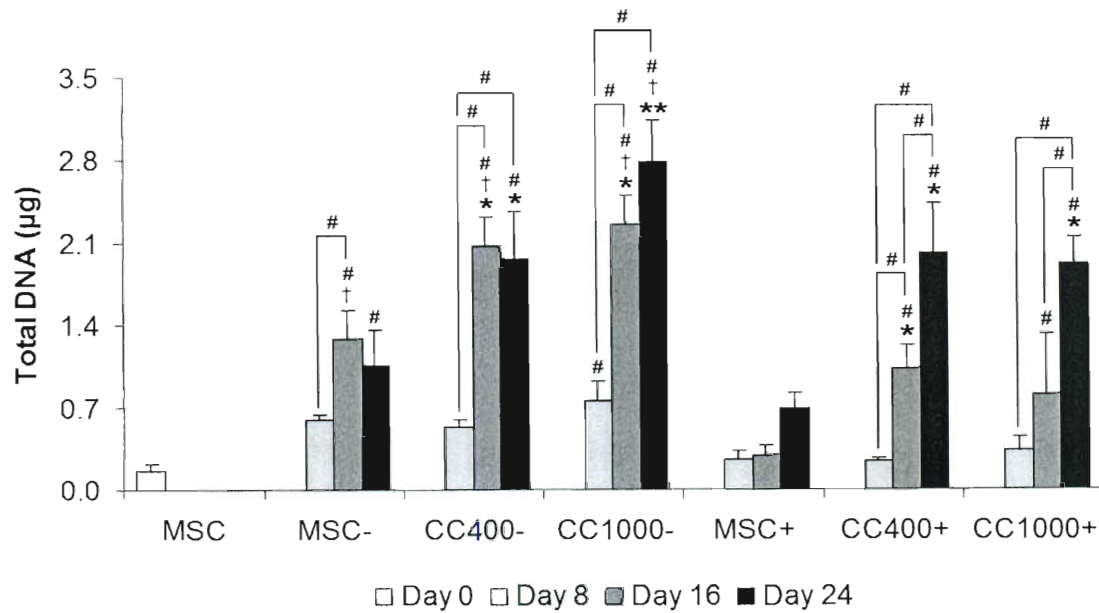


Figure III-1: Total DNA content of wells cultured with MSCs alone (MSC) or MSCs and HSPCs in co-culture (CC) at specified seeding densities (400 or 1000 HSPCs seeded onto 40,000 MSCs) either with (+) or without (-) the addition of dexamethasone. Data are presented as mean \pm standard deviation for $n = 4$. Within a specific treatment group, significant difference ($p < 0.05$) compared to MSCs at seeding and between time points is noted with (#). Within each culture group at a specific time point, significant difference ($p < 0.05$) between dexamethasone treatment is noted with (†). Within each dexamethasone group at a specific time point, significant difference ($p < 0.05$) compared to MSCs alone is noted with (*), with significant difference ($p < 0.05$) compared to all other groups noted with (**).

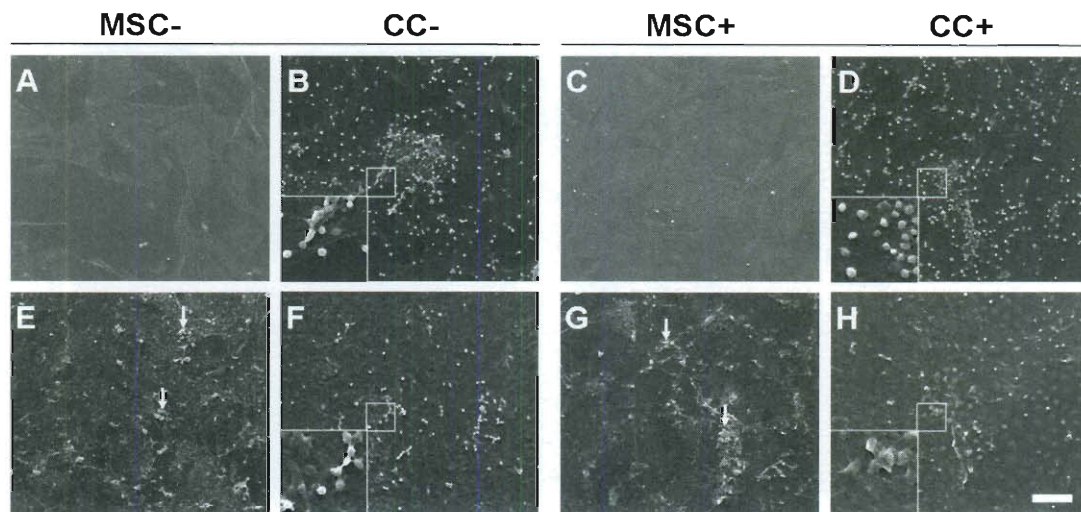


Figure III-2: Representative scanning electron micrographs of wells cultured with MSCs alone (MSC) or MSCs and HSPCs in co-culture (CC) either with (+) or without (-) the addition of dexamethasone after 8 days (A-D) and 24 days (E-H). Arrows indicate areas of mineralization showing mineral nodules. The scale bar represents 100 μm for all images with insets showing a 3x magnified view of HSPCs in more detail.

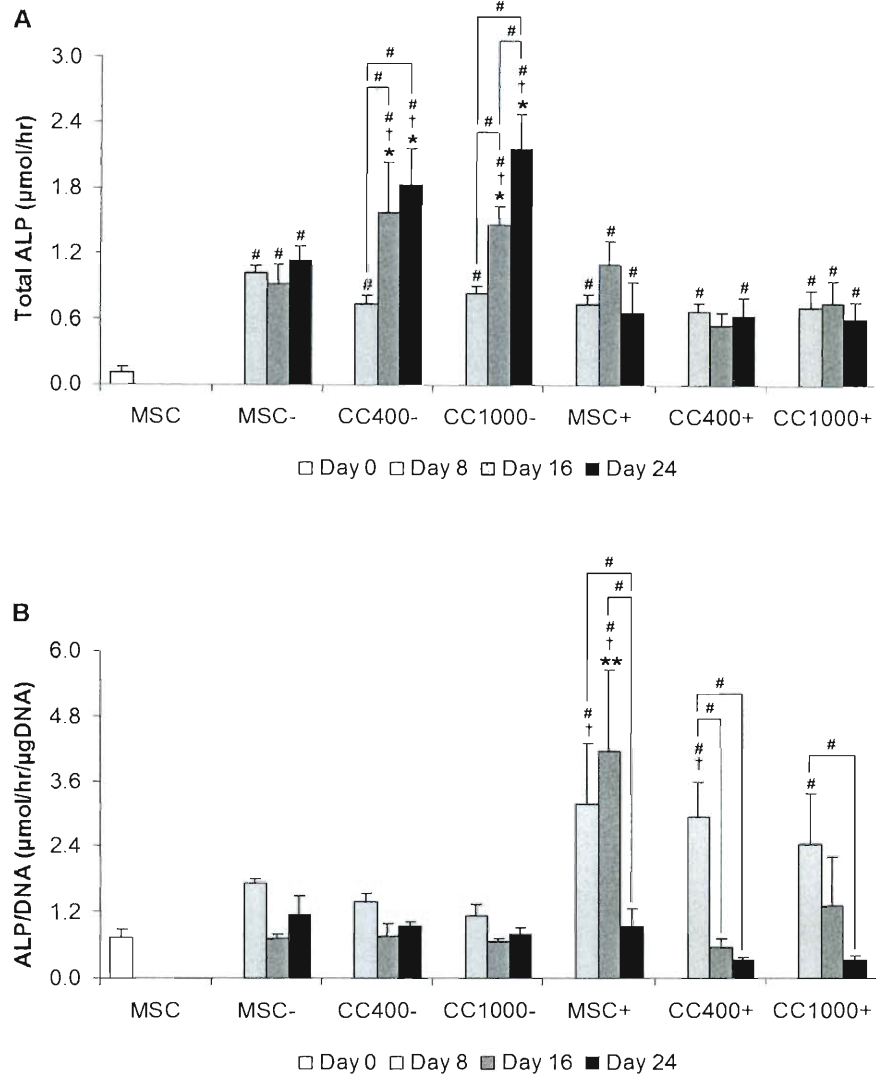


Figure III-3: Alkaline phosphatase activity of wells cultured with MSCs alone (MSC) or MSCs and HSPCs in co-culture (CC) at specified seeding densities (400 or 1000 HSPCs seeded onto 40,000 MSCs) either with (+) or without (-) the addition of dexamethasone. Plots show total alkaline phosphatase activity (A) and alkaline phosphatase activity normalized to DNA content (B). Data are presented as mean \pm standard deviation for $n = 4$. Within a specific treatment group, significant difference ($p < 0.05$) compared to MSCs at seeding and between time points is noted with (#). Within each culture group at a specific time point, significant difference ($p < 0.05$) between dexamethasone treatment is noted with (†). Within each dexamethasone group at a specific time point, significant difference ($p < 0.05$) compared to MSCs alone is noted with (*), with significant difference ($p < 0.05$) compared to all other groups noted with (**).

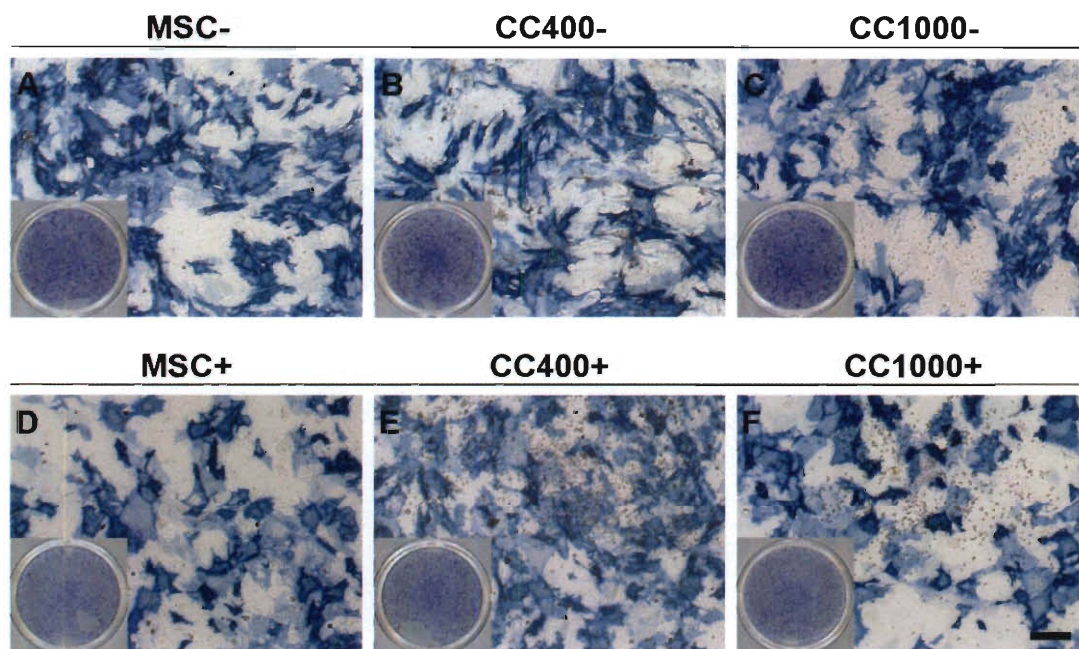


Figure III-4: Alkaline phosphatase staining of wells after 8 days of culture with MSCs alone (MSC) or MSCs and HSPCs in co-culture (CC) at specified seeding densities (400 or 1000 HSPCs seeded onto 40,000 MSCs) either with (+) (D-F) or without (-) (A-C) the addition of dexamethasone. The scale bar represents 200 μm for all microscopy images. Insets show the overall alkaline phosphatase staining of the wells.

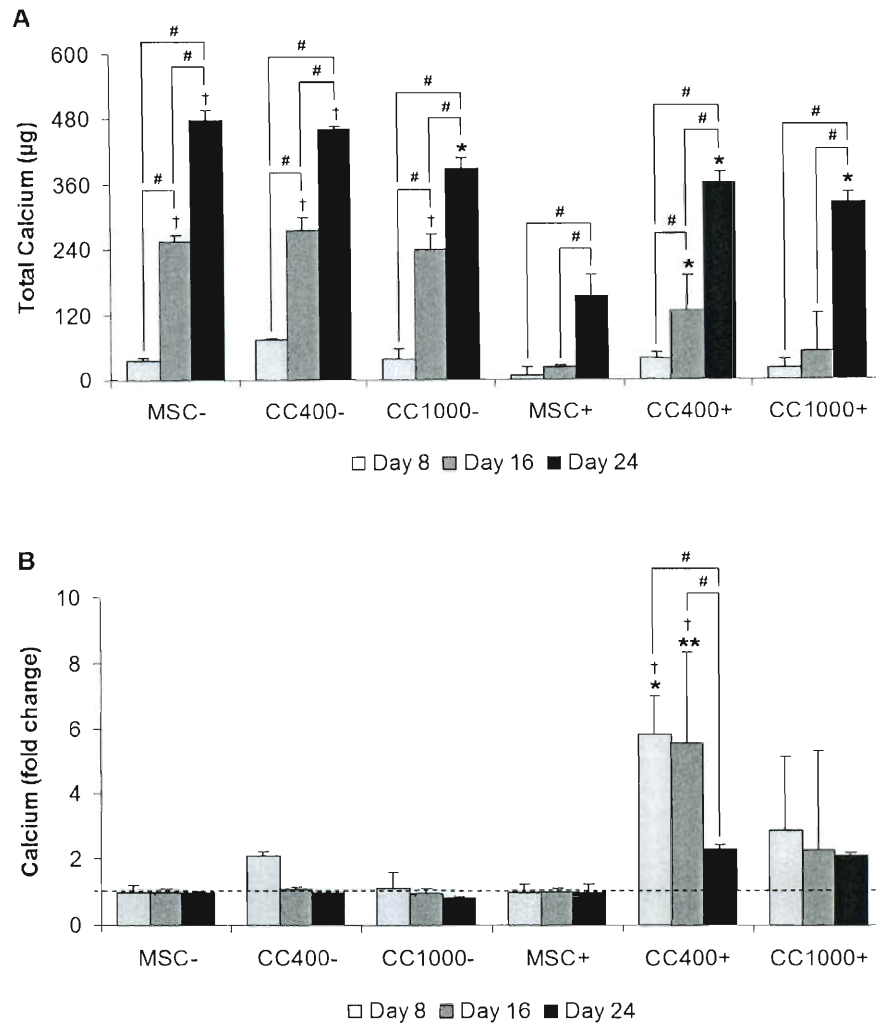


Figure III-5: Calcium content of wells cultured with MSCs alone (MSC) or MSCs and HSPCs in co-culture (CC) at specified seeding densities (400 or 1000 HSPCs seeded onto 40,000 MSCs) either with (+) or without (-) the addition of dexamethasone. Plots show total calcium content (A) and fold change in calcium content as compared to cultures with MSCs for each dexamethasone treatment at each time point (B). Data are presented as mean \pm standard deviation for $n = 4$. Within a specific treatment group, significant difference ($p < 0.05$) between time points is noted with (#). Within each culture group at a specific time point, significant difference ($p < 0.05$) between dexamethasone treatment is noted with (†). Within each dexamethasone group at a specific time point, significant difference ($p < 0.05$) compared to MSCs alone is noted with (*), with significant difference ($p < 0.05$) compared to all other groups noted with (**).

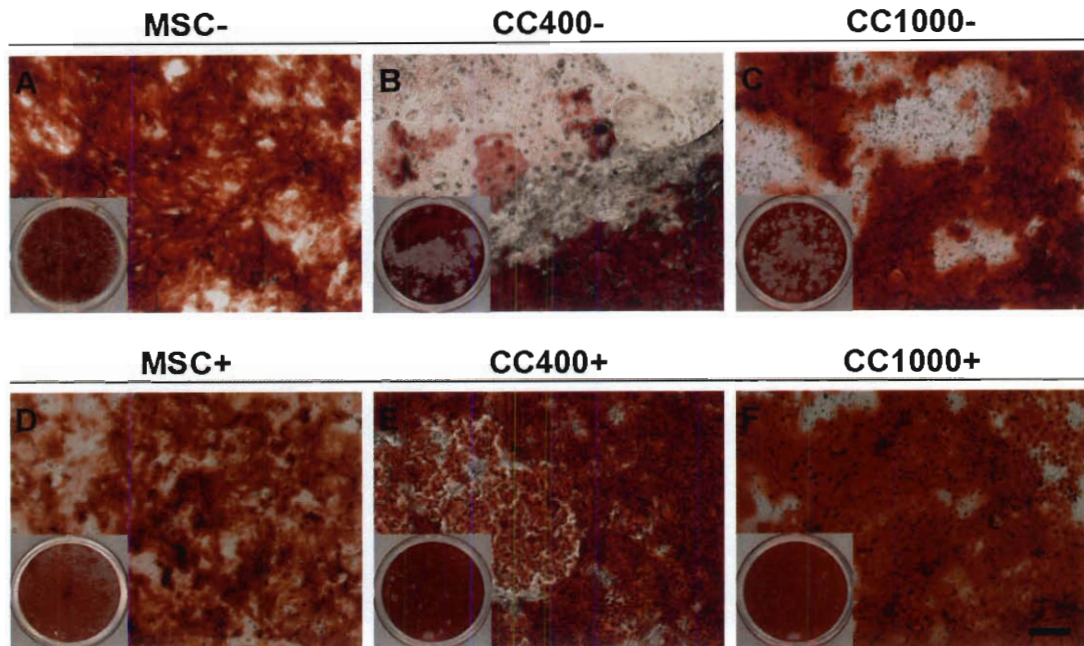


Figure III-6: Alizarin Red staining of wells after 24 days of culture with MSCs alone (MSC) or MSCs and HSPCs in co-culture (CC) at specified seeding densities (400 or 1000 HSPCs seeded onto 40,000 MSCs) either with (+) (D-F) or without (-) (A-C) the addition of dexamethasone. The scale bar represents 200 μm for all microscopy images. Insets show the overall Alizarin Red staining of the wells.

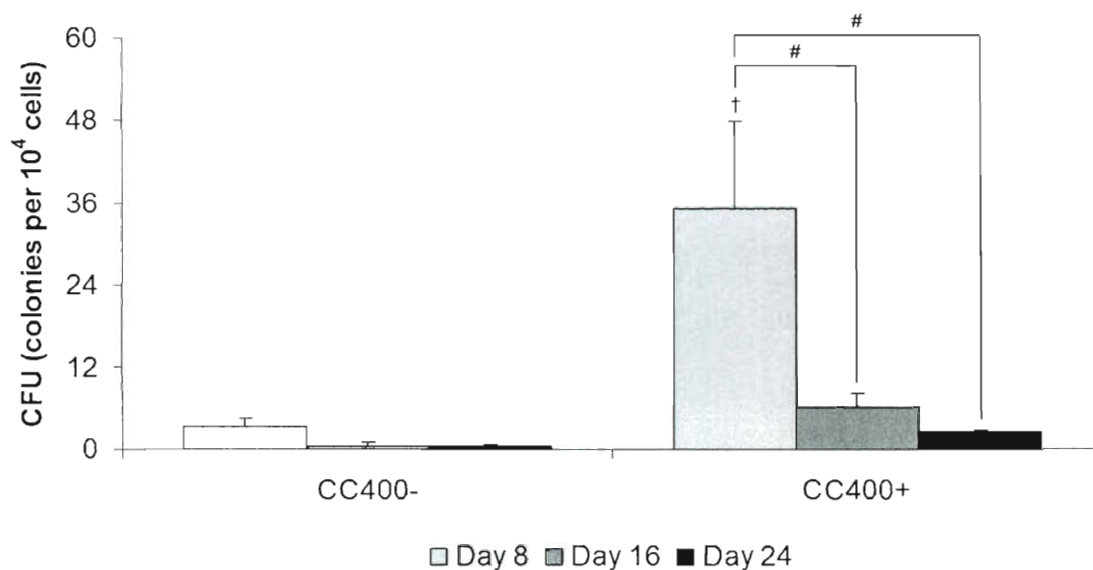


Figure III-7: Colony-forming unit counts of colonies derived in methylcellulose medium from the total cell population after co-culture (CC) at the specified seeding density (400 HSPCs seeded onto 40,000 MSCs) either with (+) or without (–) the addition of dexamethasone. Data are presented as mean \pm standard deviation for $n = 4$. Within a specific treatment group, significant difference ($p < 0.05$) between time points is noted with (#). Significant difference ($p < 0.05$) between dexamethasone treatment is noted with (†).

CHAPTER IV

MODULATION OF OSTEOGENIC PROPERTIES OF BIODEGRADABLE POLYMER/EXTRACELLULAR MATRIX COMPOSITE SCAFFOLDS GENERATED WITH A FLOW PERFUSION BIOREACTOR †

Abstract

In this study, composite scaffolds consisting of both synthetic and natural components with controllable properties were generated by incorporating mineralized extracellular matrix (ECM) and electrospun poly(ϵ -caprolactone) (PCL) microfiber scaffolds. Mesenchymal stem cells (MSCs) were cultured on PCL scaffolds under flow perfusion conditions with culture medium supplemented with dexamethasone to investigate the effect of culture duration on mineralized extracellular matrix deposition. MSCs differentiated down the osteogenic lineage and produced extracellular matrix with different compositions of mineral, collagen, and glycosaminoglycan with distinct morphologies at various stages of osteogenesis. To determine whether the presence and maturity of mineralized extracellular matrix influences osteogenic differentiation *in vitro*, PCL/ECM constructs were decellularized to yield PCL/ECM composite scaffolds that were

† This chapter was published as follows: Liao J, Guo X, Nelson D, Kasper FK, Mikos AG. Modulation of osteogenic properties of biodegradable polymer/extracellular matrix scaffolds generated with a flow perfusion bioreactor. *Acta Biomater* 2010; 6(7): 2386-2393.

subsequently seeded with MSCs and cultured in the absence of dexamethasone. The presence of mineralized matrix reduced cellular proliferation while stimulating alkaline phosphatase activity with increasing amounts of calcium deposition over time. PCL/ECM composite scaffolds containing the most mature mineralized matrix resulted in the most rapid increase and highest levels of alkaline phosphatase activity and calcium deposition compared to all other scaffold groups. Therefore, we demonstrate that mineralized extracellular matrix generated under controlled flow perfusion conditions can impart osteogenic properties to an osteoconductive polymer scaffold, and that the maturity of this matrix influences osteogenic differentiation *in vitro*, even in the absence of dexamethasone.

Introduction

Bone has an innate ability to heal due to its vasculature and access to stem and progenitor cell populations. Although this innate healing response may repair bone fractures, large defects often require the aid of some scaffolding material to bridge the void space and facilitate bone regeneration. Currently, the most successful treatment for bone defects is autologous bone graft, which integrates well with the surrounding bone tissue and can be remodeled to restore structure and function. The success of autologous bone graft as a scaffold for bone regeneration is due to its osteoconductivity and osteoinductivity, as it not only supports stem and progenitor cell attachment, but also stimulates their osteogenic differentiation and bone formation. However, since autologous bone graft is harvested from healthy donor sites, drawbacks associated with its use include donor site morbidity and limited tissue availability [157]. Therefore, the need for alternative scaffolding materials with both osteoconductive and osteoinductive properties has launched the development of diverse biomaterials for bone regeneration applications.

An ideal scaffold to facilitate bone regeneration should be biocompatible, provide structural support to the repair region, allow cell attachment and infiltration, induce osteogenic differentiation of stem and progenitor cells, stimulate bone formation, and be degradable over time, ultimately leaving bone tissue with native structure and function. The three main classes of scaffolding materials that have been investigated for bone regeneration include metals, ceramics, and polymers [158]. Of these materials, metals do not degrade (with

very few exceptions) and most ceramics are quite brittle. Polymer scaffolds on the other hand, can be synthesized with a wide variety of chemical and physical properties through tailored processing conditions. In particular, electrospun polymer scaffolds with a nonwoven fiber mesh structure are promising candidates for bone regeneration applications due to their large surface-to-volume ratio for cell attachment and high interconnected porosity for cell and tissue infiltration. Here, we explore the application of electrospun poly(ϵ -caprolactone) (PCL) microfiber scaffolds for bone regeneration, since PCL is a clinically applicable material regulated by the Food and Drug Administration that is both biocompatible and biodegradable. Electrospun PCL nanofiber scaffolds have been shown to support osteogenesis when seeded with mesenchymal stem cells (MSCs) and cultured in osteogenic cell culture medium containing dexamethasone [92]. As with many other porous scaffolds, electrospun PCL scaffolds are only osteoconductive, as they lack osteoinductive properties to stimulate osteogenesis on their own, and thus require the presence of exogenous induction agents such as dexamethasone or growth factors.

Drawing from the success of bone matrix, whose osteoinductivity is attributed to the presence and association of native organic and inorganic components, we seek to impart osteogenic properties to electrospun PCL microfiber scaffolds by incorporating mineralized extracellular matrix generated by differentiating bone marrow derived MSCs under engineered conditions *in vitro*. Previously, we have successfully differentiated MSCs down the osteogenic lineage and demonstrated the deposition of bone-like extracellular matrix (ECM)

on titanium (Ti) fiber mesh scaffolds in a flow perfusion bioreactor system [153, 159]. After decellularization, Ti/ECM composite scaffolds were shown to support osteogenic differentiation with enhanced calcium deposition [119, 152]. Although these studies with titanium scaffolds demonstrate osteogenic differentiation *in vitro* with either the application of fluid shear stresses or the delivery of dexamethasone, and have also shown promising results *in vivo* when implanted with cells, titanium is not degradable and will remain in the defect even after bone has regenerated [160, 161].

Ultimately, we envision creating a biodegradable osteoinductive scaffold that, when implanted, would recruit infiltrating host cells and induce their osteogenic differentiation and bone formation, either as a stand alone bone scaffold or as a vehicle for cell transplantation. Since MSCs are self-renewing multipotent stem cells that can be easily isolated from bone marrow, we stimulate their differentiation down the osteogenic lineage under flow perfusion culture conditions to where they deposit increasing amounts of mineralized extracellular matrix on electrospun PCL microfiber scaffolds. In this study, we capture the state of mineralized matrix at various stages of osteogenesis in generating PCL/ECM (PE) composite scaffolds of various maturities, in order to evaluate how the presence and maturity of mineralized matrix influences the osteogenic differentiation of MSCs *in vitro* without the osteogenic cell culture supplement dexamethasone. For the fabrication of PCL/ECM composite scaffolds, we hypothesized that exposing MSCs to dexamethasone and fluid shear stresses for various culture durations would stimulate the deposition of ECM containing

various quantities of minerals and signaling molecules. To evaluate the osteogenic properties of PCL/ECM composite scaffolds, we hypothesized that the presence of mineralized matrix would induce MSC differentiation down the osteogenic lineage even without the addition of dexamethasone, by providing cells with a more biological microenvironment compared to plain PCL scaffolds. Furthermore, we hypothesized that the maturity of this mineralized matrix would modulate osteogenic differentiation through physical interaction with various compositions of matrix signals. To investigate our hypotheses, rat MSCs were seeded on electrospun PCL microfiber scaffolds and cultured in medium containing dexamethasone in the flow perfusion bioreactor to characterize the effect of culture duration on mineralized matrix composition and morphology. Resulting PCL/ECM constructs were decellularized to yield PCL/ECM composite scaffolds, which along with plain PCL scaffolds, were seeded with rat MSCs and cultured in medium without dexamethasone to determine how mineralized matrix maturity influences osteogenic differentiation *in vitro* as assessed through cellular proliferation, alkaline phosphatase activity, and calcium deposition.

Materials and Methods

Electrospinning

Nonwoven PCL microfiber mats were fabricated using a horizontal electrospinning setup previously described, consisting of a 10 mL syringe fitted with a blunt tip needle and set on a syringe pump, an 18 gauge copper ring 19

cm in diameter placed 6 cm in front of the needle tip, a power supply with the positive lead split and connected to both the needle and copper ring, and a 0.3 cm thick grounded copper plate covered with a glass collector plate [162]. Mats were electrospun to a targeted fiber diameter of 10 μm using PCL (Sigma-Aldrich, St. Louis, MO) with $M_n = 73,000 \pm 9,000$ and $M_w = 154,000 \pm 26,000$ from three samples relative to polystyrene as determined by gel permeation chromatography (Waters, Milford, MA) using a Phenogel 50 mm column (Phenomenex, Torrance, CA). Polymer was dissolved at 14 wt % in a solution with 5:1 volume ratio of chloroform to methanol. The polymer solution was pumped through a 16 gauge blunt tip needle at a flow rate of 18 mL/h while charged with an applied voltage of 25.5 kV. The copper ring served to stabilize the electric field as the charged polymer jet whipped through the air toward the grounded copper plate positioned 33 cm away from the needle tip. The resulting PCL mat was then removed from the glass collector plate and dried in a desiccator. Prior to use, mats were inspected through scanning electron microscopy to visualize microfiber morphology and to confirm the average fiber diameter.

Scaffold Preparation

PCL scaffolds were die-punched from electrospun mats into 8 mm diameter disks with thicknesses between 0.95 and 1.05 mm. As previously characterized through mercury porosimetry, these scaffolds have a porosity of 87% with an average pore size of 45 μm [162]. PCL scaffolds were prepared for

cell culture by first sterilizing with ethylene oxide gas for 14 h, then aerating overnight to remove residual fumes. Scaffolds were then pre-wetted through a gradient series of ethanol from 100% to 70%, followed by three rinses in phosphate buffered saline (PBS), and incubated in cell culture medium overnight. To ensure complete wetting in each solution, scaffolds were centrifuged at each step of the pre-wetting process. Finally, PCL scaffolds were press-fitted into cassettes designed to confine the cell suspension during seeding and to be used in the flow perfusion bioreactor to generate PCL/ECM composite scaffolds [121]. Cassettes holding the press-fitted scaffolds were placed in 6-well plates in preparation for seeding.

PCL/ECM Mineralized Composite Scaffold Generation

MSCs were harvested and pooled from the tibiae and femora of male Fischer 344 rats (Charles River, Wilmington, MA) weighing 150-175 g according to previously established methods [153, 163]. Rats were anesthetized with 4% isoflurane in oxygen then euthanized by carbon dioxide asphyxiation. The tibiae and femora were excised, cleared of soft tissue, then cut and flushed using an 18 gauge needle with 5 mL of complete osteogenic medium consisting of α -MEM, supplemented with 10% fetal bovine serum (Cambrex, Walkersville, MD), 10^{-8} M dexamethasone, 10 mM β -glycerophosphate, and 50 mg/L ascorbic acid, also with the addition of 1.25 mg/L amphotericin-B, 50 mg/L gentamicin, and 100 mg/L ampicillin. Marrow pellets were triturated and plated in tissue culture flasks. Non-adherent cells were washed away after 24 h, and adherent cells were

cultured for 7 days in complete osteogenic medium with medium changes every 2 days. After this primary culture period, MSCs were lifted with 2 mL of a 0.25% trypsin solution and suspended in culture medium for seeding onto press-fitted scaffolds at a seeding density of 250,000 cells in 200 μ L of medium within each cassette. Scaffolds were incubated with the seeding solution for 2 h, after which 10 mL of medium was added to each well of the 6-well plates to fill the cassettes in which the scaffolds were held.

PCL/ECM constructs containing mineralized extracellular matrix of various maturities were generated by culturing MSCs on electrospun PCL scaffolds for 4, 8, 12, or 16 days under flow perfusion conditions with complete osteogenic medium containing dexamethasone. PCL/ECM constructs were decellularized to yield PCL/ECM composite scaffolds designated as PE4, PE8, PE12, and PE16 experimental groups corresponding to their matrix maturities. To generate each batch of PCL/ECM constructs, MSCs were first harvested and pooled from five rats as described above and expanded through primary culture in complete osteogenic medium. Cells were then seeded onto PCL scaffolds and allowed to attach for 24 h, after which constructs were kept in their cassettes and transferred directly into the flow perfusion bioreactor, whose design and operation has been previously described in detail [121]. Medium was perfused through the press-fitted constructs at a flow rate of 0.7 mL/min with medium changes every 2 days. This flow rate was chosen to match the fluid shear stress applied in our previous study using titanium fiber mesh scaffolds [119]. At the end of each culture period, constructs were rinsed with PBS (without calcium and

magnesium) and stored in 1.5 mL ddH₂O at -80 °C. In addition to those PCL/ECM constructs generated to assess osteogenic differentiation, three constructs from each culture period were prepared for calcium, collagen, and glycosaminoglycan assays to characterize matrix composition and thus maturity, and two constructs from each culture period were prepared for x-ray imaging, histology, and scanning electron microscopy to visualize mineralized matrix morphology.

PCL/ECM constructs were decellularized to yield PCL/ECM composite scaffolds via three consecutive cycles of a freeze and thaw process, in which constructs were frozen for 10 min in liquid nitrogen then thawed for 10 min in a 37 °C water bath [164]. This decellularization process has been shown to yield acellular constructs [152]. The resulting PCL/ECM composite scaffolds were then air-dried overnight, press-fitted into cassettes, sterilized with ethylene oxide gas for 14 h and aerated overnight in preparation for seeding.

Mineralized Matrix Characterization

After culturing MSCs on electrospun PCL microfiber scaffolds for 4, 8, 12, or 16 days under flow perfusion conditions, the resulting PCL/ECM constructs were characterized for their mineralized extracellular matrix composition and morphology. Calcium content was determined by extracting calcium in an acetic acid solution then measuring free calcium ions using the Calcium assay, further described in the following section.

Total collagen content was determined by measuring hydroxyproline in a colorimetric assay [165]. Samples taken from culture and rinsed with PBS were placed in 0.75 mL of a proteinase K solution and digested in a 56 °C water bath for 16 h. The proteinase K solution consisted of 1 mg/mL proteinase K, 0.01 mg/mL pepstatin A, and 0.185 mg/mL iodoacetamide, in a tris-EDTA buffer made by dissolving 6.055 mg/mL tris(hydroxymethyl aminomethane) and 0.372 mg/mL EDTA with pH adjusted to 7.6. Digested matrix components were extracted via three repetitions of a freeze, thaw, and sonication cycle, where samples were frozen for 30 min at -80 °C, thawed at room temperature for 30 min, and sonicated for 30 min to allow matrix components into the solution. Hydroxyproline was quantified using a hydroxyproline assay as previously described [119]. After incubation for 30 min at 60 °C, absorbance at 570 nm corresponding to hydroxyproline concentration was measured on a plate reader (BioTek PowerWave x340, Winooski, VT) and compared to a standard curve generated from known concentrations of hydroxyproline standards. Resulting hydroxyproline measurements in µg were finally converted to collagen contents for each construct following a 1:10 ratio of hydroxyproline to collagen [166].

Glycosaminoglycan content was determined by measuring glycosaminoglycan in a colorimetric assay [167]. Glycosaminoglycan was quantified in the supernatant previously obtained via proteinase K digestion using the dimethylmethylene blue assay (Sigma-Aldrich) as previously described [168]. After incubation for 10 min at room temperature, absorbance at 520 nm corresponding to glycosaminoglycan concentration, was measured on a plate

reader (BioTek PowerWave x340) and compared to a standard curve generated from known concentrations of chondroitin sulfate standards. Resulting glycosaminoglycan measurements in μg were finally determined for each construct.

Samples for x-ray imaging and histology were fixed in 10% neutral buffered formalin then cut in half and rinsed with 70% ethanol. Sample halves for x-ray imaging were air-dried overnight and imaged via x-ray (SkyScan 1172, Kontich, Belgium) according to the manufacturer's recommended voltage of 40 kV with a current of 250 μA as previously described [169]. Sample halves for histology were cryo-embedded in HistoPrep freezing medium (Fisher Scientific, Pittsburgh, PA) and stored at $-80\text{ }^{\circ}\text{C}$. Frozen sections 5 μm thick were cut using a cryostat (Microm HM 500, Ramsey, MN), mounted onto Superfrost Excell glass slides, and placed on a $37\text{ }^{\circ}\text{C}$ slide warmer to facilitate adhesion. Sections were stained with hematoxylin and eosin to visualize the distribution of cells and extracellular matrix proteins. After mounting with Permount (Fisher Scientific), images were obtained using a light microscope (Nikon Eclipse E600, Melville, NY) with a video camera attachment (Sony DXC950P, New York, NY). Samples for scanning electron microscopy were fixed in glutaraldehyde and prepared for imaging as described in the scanning electron microscopy section.

Osteogenic Differentiation without Dexamethasone

To assess osteogenic differentiation on PCL/ECM composite scaffolds of various maturities, MSCs were first harvested and pooled from eight rats as

described above and expanded through primary culture in complete osteogenic medium. Cells were then seeded onto press-fitted experimental scaffolds PE4, PE8, PE12, and PE16, and also plain PCL control scaffolds at a seeding density of 250,000 cells in 200 μ L of medium without dexamethasone within each cassette. Scaffolds were incubated for 2 h with the seeding solution, after which 10 mL of medium without dexamethasone was added to each well of the 6-well plates to fill the cassettes in which the scaffolds were held. After allowing 24 h for cell attachment, constructs were removed from their cassettes and transferred into 12-well plates with 3 mL of medium without dexamethasone and cultured static conditions for 4, 8, or 16 days with medium changes every 2 days. Five samples were cultured for each scaffold group (PCL, PE4, PE8, PE12, PE16) for each culture time (4, 8, 16 days), at the end of which, samples were rinsed with PBS (without calcium and magnesium) and stored for later analysis. Four samples were prepared for assessing construct cellularity, alkaline phosphatase activity, and calcium content, and one sample was prepared for scanning electron microscopy.

Osteogenic Differentiation Assays

Construct cellularity was determined by measuring double-stranded DNA in a fluorometric assay [144]. Samples taken from culture and rinsed with PBS were placed in 1 mL of ddH₂O, where DNA was extracted by lysing cells via three repetitions of a freeze and thaw cycle, in which samples were frozen for 10 min in liquid nitrogen then thawed for 10 min in a 37 °C water bath, and finally

sonicated for 10 min to allow DNA into the solution. DNA was quantified using the PicoGreen assay (Invitrogen, Carlsbad, CA) according to the manufacturer's instructions as previously described [152]. After incubation for 10 min room temperature, fluorescence at 520 nm corresponding to DNA concentration was measured on a plate reader (BioTek FL x800, Winooski, VT) and compared to a standard curve generated from known concentrations of DNA standards. Resulting DNA measurements in μg were finally converted to cell numbers by correlating to DNA extracted from a known number of MSCs in order to assess cellular proliferation.

Alkaline phosphatase activity was determined by measuring the enzyme-mediated conversion of the substrate p-nitrophenyl phosphate to p-nitrophenol in a colorimetric assay [170]. ALP enzymatic activity was quantified in the supernatant previously obtained via freeze, thaw, and sonication, using the Alkaline Phosphatase assay (Sigma-Aldrich) as previously described [153]. After allowing the reaction to progress for 1 h at 37 °C, absorbance at 405 nm corresponding to p-nitrophenol concentration was measured on a plate reader (BioTek PowerWave x340) and compared to a standard curve generated from known concentrations of p-nitrophenol standards. Concentrated samples were diluted as needed to ensure readings within the linear range of the assay. Resulting ALP enzymatic activities as measured in pmol/hr corresponding to p-nitrophenol production were finally normalized to cell numbers in order to assess ALP enzymatic activity per cell as an early stage marker for osteogenic differentiation.

Calcium content was determined by measuring free calcium ions in a colorimetric assay. After completing both DNA and ALP assays, samples were transferred into 1 mL of a 1 N acetic acid solution and placed on a shaker table at 37 °C overnight to dissolve calcium deposited in the constructs. Calcium was quantified in the acetic acid solution using the Calcium assay (Genzyme, Cambridge, MA) as previously described [153]. After incubation for 10 min at room temperature, absorbance at 650 nm corresponding to calcium concentration was measured on a plate reader (BioTek PowerWave x340) and compared to a standard curve generated from known concentrations of calcium chloride standards. Concentrated samples were diluted as needed to ensure readings within the linear range of the assay. Resulting calcium measurements in μg were finally determined for each construct in order to assess calcium deposition as a late stage marker for osteogenic differentiation.

Scanning Electron Microscopy

Samples for scanning electron microscopy were fixed in 2.5% glutaraldehyde for 1 h, dehydrated through a gradient series of ethanol from 70% to 100%, air-dried overnight then cut and mounted on aluminum stubs to visualize the top surface of the constructs. Samples were sputter coated with gold for 1 min prior to imaging via SEM (FEI Quanta 400, Hillsboro, OR).

Statistical Analysis

Characterization results for the composition of mineralized extracellular matrix contained within PCL/ECM constructs following flow perfusion culture are reported as mean \pm standard deviation for $n = 3$. A one-factor ANOVA was performed to determine whether culture duration (4, 8, 12, 16 days) had a significant effect. Comparisons were then made using the Tukey procedure to determine significant differences.

Biochemical assay results to assess osteogenic differentiation following static culture without dexamethasone are reported as mean \pm standard deviation for $n = 4$. A two-factor ANOVA was first performed to determine significant main effects or interaction between scaffold group (PCL, PE4, PE8, PE12, PE16) and culture time (4, 8, 16 days). Multiple pairwise comparisons were then made using the Tukey procedure to determine significant differences. All statistical analyses were performed at a significance level of 5%.

Results

PCL/ECM Mineralized Composite Characterization

Mineralized extracellular matrix deposited on electrospun PCL microfiber scaffolds (fiber diameter $9.86 \pm 0.56 \mu\text{m}$) in generating PCL/ECM (PE) constructs were characterized for their composition and morphology prior to decellularization. Calcium content, collagen content, and glycosaminoglycan content following flow perfusion culture for 4, 8, 12, and 16 days to generate

PE4, PE8, PE12, and PE16 constructs, respectively (Figure IV-1). Calcium content significantly increased over time, with PE16 constructs containing the most calcium as compared to both PE4 and PE8 constructs. Although PE12 constructs contained more calcium than PE4 constructs, the calcium content of PE12 constructs was not statistically different from PE8 or PE16 constructs. In terms of extracellular matrix protein composition, the amount of collagen in PE16 constructs was significantly higher than all other PCL/ECM constructs, while glycosaminoglycan content was not significantly different among the PCL/ECM constructs. Taking mineral content and glycosaminoglycan and collagen contents together, there was no significant difference between PE4 and PE8 constructs or between PE8 and PE12 constructs. However, there was a significant difference between PE12 and PE16 constructs in that PE16 constructs contained more collagen.

Flow perfusion culture enhanced the distribution of cells and extracellular matrix proteins over time, as seen in the histological sections stained with hematoxylin and eosin (Figure IV-2A). Radiopaque regions of mineralized matrix increased over time, with PE16 constructs demonstrating the most minerals visible through x-ray imaging (Figure IV-2B). The surface morphology of PCL/ECM constructs was visualized through scanning electron microscopy (Figure IV-2C). Extracellular matrix developed sparsely on PE4 constructs into a smooth surface seen on PE8 constructs. Mineral nodules on PE12 constructs eventually incorporated into a rough textured matrix on PE16 constructs.

Cellularity and Alkaline Phosphatase

After PCL/ECM constructs were decellularized, the resulting PCL/ECM composite scaffolds along with plain PCL control scaffolds were seeded with MSCs to investigate how mineralized matrix maturity influences osteogenic differentiation in the absence of dexamethasone. Cellularity results showed that cell numbers remained constant over time at approximately the initial seeding density on all PCL/ECM composite scaffolds, whereas an increase in cellularity was observed on PCL scaffolds from 4 to 8 days of culture (Figure IV-3). Although cellularity peaked at 8 days on PCL scaffolds ($0.56 \times 10^6 \pm 0.14 \times 10^6$ cells/construct) and was the highest compared to all PCL/ECM composite scaffolds, there was no statistical difference in cellularity among all scaffold groups after 16 days of culture.

Alkaline phosphatase (ALP) activity per cell was used as an early stage marker for osteogenic differentiation (Figure IV-4). Cells cultured on PCL scaffolds did not show a statistically significant increase in ALP activity over time, whereas those cultured on all PCL/ECM composite scaffolds demonstrated a significant increase in ALP activity from 4 to 16 days of culture with no observable peak. Furthermore, cells cultured on PE16 composite scaffolds also displayed a significant increase in ALP activity from 4 to 8 days of culture. Statistically significant differences in ALP levels compared to plain PCL controls were seen beginning at 8 days for PE16 and at 16 days for PE4, PE8, and PE12 composite scaffolds. Cells cultured on PE16 composite scaffolds exhibited the

highest ALP activity compared to all other scaffold groups at 8 days (9.4 ± 1.0 pmol/hr/cell) and 16 days (12.9 ± 5.0 pmol/hr/cell).

Calcium Deposition and Matrix Morphology

Calcium deposition per construct was used as a late stage marker for osteogenic differentiation (Figure IV-5). Cells cultured on PCL scaffolds and PE4 composite scaffolds did not show a statistical increase in calcium deposition over time, whereas those cultured on PE8, PE12 and PE16 composite scaffolds demonstrated a significant increase in calcium deposition from 4 to 16 days of culture. Statistically significant differences in calcium content compared to plain PCL controls were seen beginning at 4 days for PE16 and at 8 days for PE8 and PE12 composite scaffolds. PE16 composite scaffolds showed the highest calcium content compared to all other scaffold groups at 4 days (764 ± 150 μg), 8 days (799 ± 136 μg), and 16 days (1324 ± 253 μg).

Scanning electron micrographs were taken of the top surfaces of constructs to visualize the overall quality of the resulting extracellular matrix (Figure IV-6). Though PCL/ECM composite scaffolds started with an initial mineralized matrix while PCL scaffolds did not, the density and overall coverage of extracellular matrix on all scaffold groups increased over time, eventually to where scaffold fibers were no longer visible. The most striking differences in matrix quality were seen after 16 days of culture, where both PE12 and PE16 composite scaffolds developed a distinguishingly rough texture, whereas all other scaffold groups retained a smooth appearance. PE16 composite scaffolds

seemed to take on this rough surface characteristic sooner than all other scaffold groups beginning after 8 days of culture.

Discussion

The objective of this study was to evaluate the osteogenic capacity of PCL/ECM composite scaffolds *in vitro*. This study was designed to investigate the effects of mineralized extracellular matrix maturity on MSC differentiation down the osteogenic lineage in the absence of the osteogenic cell culture supplement dexamethasone. In order to determine whether exposing cells to a biomimetic microenvironment containing various compositions of matrix signals could influence their osteogenic differentiation response, PCL/ECM composite scaffolds were generated by coating electrospun PCL microfiber scaffolds with natural mineralized extracellular matrix of various maturities, then seeded with MSCs and cultured in medium without the addition of dexamethasone.

Exposing MSCs to both dexamethasone and fluid shear stresses in flow perfusion culture has been shown to synergistically enhance osteogenic differentiation and the distribution of mineralized extracellular matrix [153, 159]. Thus in this study, flow perfusion culture with dexamethasone was employed to generate PCL/ECM constructs. In generating these PCL/ECM constructs, we found that cells were able to penetrate throughout the interconnected porosity of electrospun PCL microfiber scaffolds and deposit increasing amounts of mineralized extracellular matrix with distinct compositions and morphologies over time. Since PCL/ECM constructs were generated with MSCs induced down the

osteogenic pathway through exposure to osteogenic culture conditions, the resulting constructs at the end of each culture period contains extracellular matrix secreted by cells at various stages of osteogenesis after 4, 8, 12, and 16 days. As evident in our characterization of calcium, collagen, and glycosaminoglycan contents, we were able to generate PE4, PE8, PE12, and PE16 constructs containing various quantities of minerals and proteins by exposing MSCs to dexamethasone and fluid shear stresses for various culture durations. In addition to this quantitative difference in matrix composition, PCL/ECM constructs also differed in appearance, as seen through x-ray images and scanning electron micrographs demonstrating mineralized matrix. Overall, the trends observed here using electrospun PCL microfiber scaffolds are consistent with previous studies in our group using titanium fiber mesh scaffolds, nonwoven poly(L-lactic acid) scaffolds, and fiber bonded starch-poly(ϵ -caprolactone) scaffolds [159, 171, 172]. Although the flow rate in this study was chosen to match the fluid shear stress applied in our previous study using titanium fiber mesh scaffolds, electrospun PCL microfiber scaffolds have smaller pore sizes as compared to our previous scaffolding materials. Therefore, as extracellular matrix accumulates in the pore space over time, higher fluid shear forces are generated throughout the culture period. As a result, we were able to achieve much higher calcium deposition as compared to our previous scaffolding materials, since higher fluid shear stresses stimulate cells to deposit increasing amounts of matrix which mineralizes over time [153, 154].

PCL/ECM constructs were decellularized to yield PCL/ECM composite scaffolds containing mineralized matrix of various maturities. In order to evaluate osteogenic properties and the influence of mineralized matrix maturity on the osteogenic differentiation of MSCs *in vitro*, we seeded PCL/ECM composite scaffolds along with plain PCL control scaffolds with MSCs and cultured them under static conditions without the addition of dexamethasone. Since dexamethasone is a potent synthetic glucocorticoid that is often necessary to drive osteogenic differentiation *in vitro*, we sought to isolate the effects of mineralized matrix on osteogenic differentiation by omitting this osteogenic supplement from the culture medium.

Our results showed that the presence of mineralized matrix in PCL/ECM composite scaffolds was able to induce the differentiation of MSCs down the osteogenic lineage as compared to plain PCL scaffolds. In general, we observed that mineralized matrix reduced cellular proliferation while stimulating alkaline phosphatase activity with increasing amounts of calcium deposition over time, thus indicating the progression of osteogenesis *in vitro*. Cells cultured on plain PCL scaffolds, on the other hand, exhibited minimal alkaline phosphatase activity and calcium deposition as expected, since they were not presented with any osteoinductive stimuli, specifically dexamethasone or extracellular matrix signals.

Mineralized matrix maturity did not seem to differentially influence cellular proliferation since all PCL/ECM composite scaffolds maintained similar cellularity over 16 days of culture. In fact, cells did not appear to proliferate on PCL/ECM composite scaffolds as compared to the proliferation seen on plain PCL

scaffolds. This could be due to a difference in the physical morphology of the scaffolds, where PCL/ECM composite scaffolds are coated with mineralized matrix that may promote cell spreading to a confluent layer, while plain PCL scaffolds present a fiber morphology with a more open pore structure to support cellular proliferation. It is likely that cells seeded on the surface of PCL/ECM composite scaffolds grew to confluence since the layer of mineralized matrix may have been too dense for cells to remodel and penetrate under static culture conditions, as confirmed through histology (data not shown). Though in this study, in order to isolate the effects of mineralized matrix, it was necessary to evaluate osteogenic differentiation under static conditions and minimize confounding factors, namely fluid shear stresses introduced through flow perfusion culture, which would have facilitated cell penetration but also affected cellular response.

Alkaline phosphatase is an enzyme responsible for the dephosphorylation of phosphates, and is used as an early stage marker for osteogenic differentiation. ALP levels peak as cells progress from a proliferative stage to depositing a mature extracellular matrix containing calcium phosphate [149]. Since PE16 composite scaffolds induced significantly higher levels of ALP activity as compared to all other scaffold groups after just 8 days, with the highest levels achieved among scaffold groups at 8 and 16 days of culture, it appears that a more mature mineralized matrix containing greater quantities of calcium and collagen induces a more rapid and robust osteogenic differentiation response. As compared to our previous studies on titanium fiber mesh scaffolds,

higher ALP levels were achieved in this study using extracellular matrix signals than with dexamethasone in static culture, while fluid shear stresses in flow perfusion culture without dexamethasone induced more ALP activity [119, 152, 153].

Although our results did not show a peak in ALP activity for PCL/ECM composite scaffolds, enzyme levels did not significantly increase from 8 to 16 days of culture, implying that cellular activity may just be starting to shift toward the synthesis of a more mature matrix. This shift in cellular activity is supported by the calcium deposition results, used here as a late stage marker of osteogenic differentiation. An increase in calcium content was only observed after 16 days of culture for PE8, PE12, and PE16 composite scaffolds. It is important to emphasize that PCL/ECM composite scaffold groups each began with different amounts of calcium deposited during the generation of mineralized matrix in flow perfusion culture. Although the initial quantity of minerals was characterized following each culture period, the actual mineral content of PCL/ECM composite scaffolds may be reduced following the freeze-thaw decellularization process. Nevertheless, even though minerals present in PCL/ECM composite scaffolds inherently contribute to the enhanced calcium contents seen for more mature scaffold groups, the increase in ALP activity is indicative of osteogenic differentiation, which is especially apparent in MSCs cultured for only 8 days on PE16 composite scaffolds. Due to the initial variation in calcium content among PCL/ECM composite scaffolds, it is difficult to compare the resulting calcium content between scaffold groups, but rather more informative to note the change

in calcium content over time for each scaffold group. In doing so, we see that cells cultured on plain PCL scaffolds and PE4 composite scaffolds do not produce much matrix even after 16 days of culture. In contrast, cells cultured on PE8, PE12, and PE16 composite scaffolds require exposure to matrix signals for at least 16 days in order to differentiate and lay down a mineralized extracellular matrix of their own. The progression in matrix maturation is further observed through scanning electron micrographs showing the initial deposition of a smooth collagen matrix which eventually develops into a rough mineralized matrix over time.

We presume that the osteoinductive effects of mineralized extracellular matrix observed in this study involve specific cell-matrix interactions, since foreseeable confounding effects due to dexamethasone supplementation and fluid shear stresses were excluded from this study. In addition to the characterized presence of calcium, collagen, and glycosaminoglycan, mineralized matrix generated in the same flow perfusion bioreactor system has been shown to contain active bone-related growth factors, particularly BMP-2, FGF-2, VEGF, and TGF- β 1, found to be localized and most prevalent at the surfaces of constructs as detected through immunohistochemical analysis [173]. Therefore, in generating PCL/ECM composite scaffolds of various maturities that contain increasing quantities of minerals and proteins with increasing culture duration, we expect the presence of these signaling molecules to increase as well. Cells seeded onto PCL/ECM composite scaffolds would directly interact with not only physical matrix components but also localized growth factors that

together, regulate osteogenic differentiation. In addition to cell-matrix interactions with native bone tissue components, surface roughness due to calcium phosphate incorporation into the mineralized matrix on PCL/ECM composite scaffolds may have also influenced cellular response. The difference in surface morphology down to nanoscale features could affect cell attachment and migration, with possible effects on osteogenic differentiation [174-176]. Accordingly, we found that a more mature mineralized matrix containing more minerals, collagen, and glycosaminoglycan possesses greater osteogenic ability than less developed matrices, possibly due to the presence of more bone signaling molecules and increased surface roughness.

Conclusion

In this work, we demonstrate that the presence of mineralized extracellular matrix on electrospun PCL microfiber scaffolds imparts osteogenic properties to an otherwise inert biomaterial, as evident in its ability to stimulate osteogenic differentiation of MSCs *in vitro* in the absence of the osteogenic supplement dexamethasone. Furthermore, we show that the maturity of this mineralized matrix modulates osteogenic differentiation, providing insight towards the development of osteoinductive scaffolding materials with controllable characteristics for bone regeneration.

Acknowledgements

This work has been supported by the National Institutes of Health (R01 AR057083). We thank Dr. Galen I. Papkov for assistance with statistical analysis.

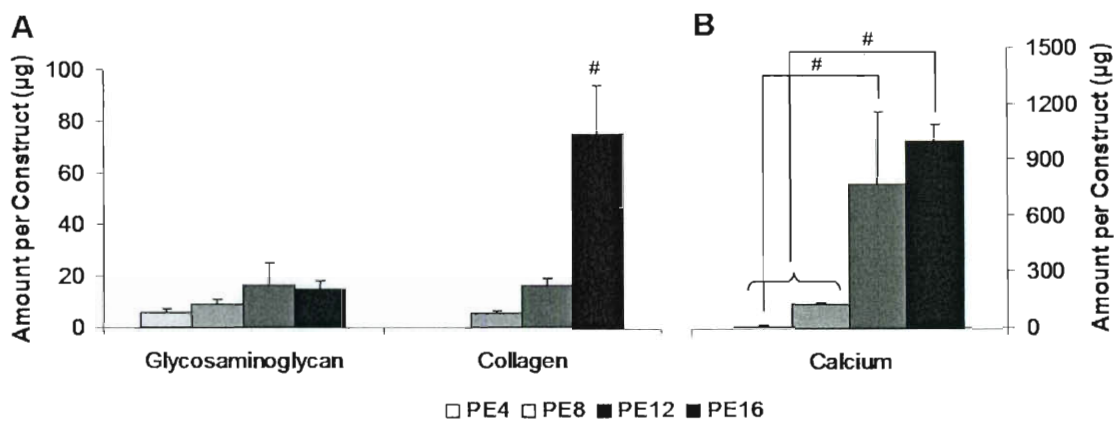


Figure IV-1: Matrix composition of PCL/ECM (PE) constructs generated in flow perfusion culture of increasing durations (4, 8, 12, and 16 days) for PE4, PE8, PE12, and PE16 constructs. Plots show (A) glycosaminoglycan and collagen contents and (B) calcium content as mean \pm standard deviation for $n = 3$. Significant difference ($p < 0.05$) between time points is noted with (#).

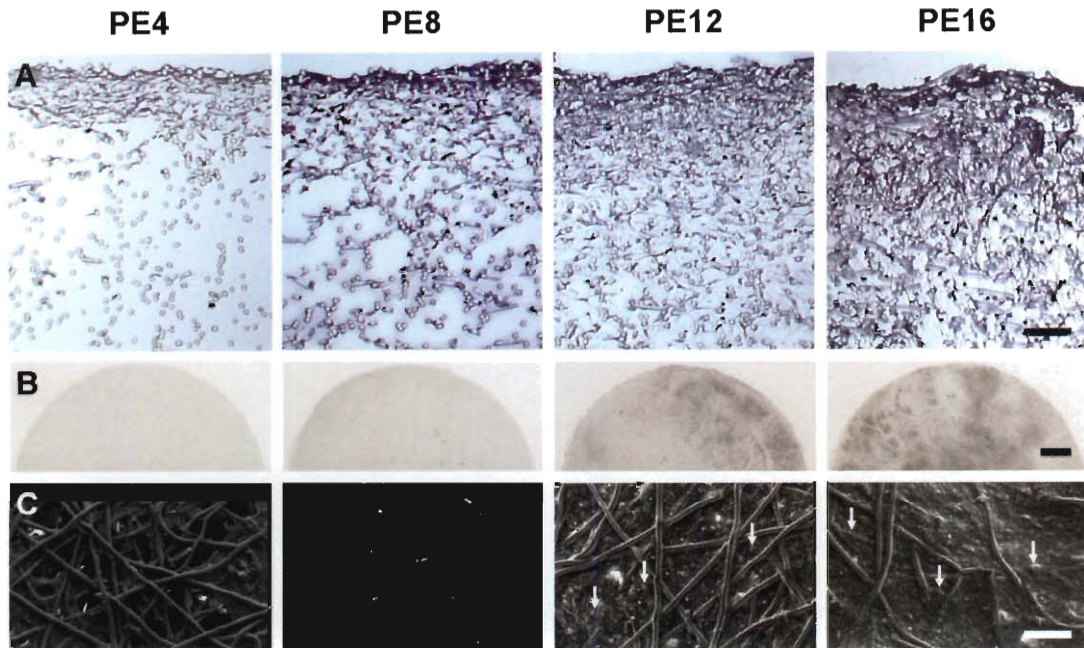


Figure IV-2: Matrix morphology of PCL/ECM (PE) constructs generated in flow perfusion culture of increasing durations (4, 8, 12, and 16 days) for PE4, PE8, PE12, and PE16 constructs. Histological sections stained with hematoxylin and eosin to visualize the distribution of cells and extracellular matrix proteins are shown in (A) with the scale bar representing 100 μm . X-ray images depicting radiopaque regions of mineralized matrix are shown in (B) with the scale bar representing 1 mm. Scanning electron micrographs of the top surface illustrating surface characteristics are shown in (C) with arrows indicating mineral nodules and the scale bar representing 100 μm .

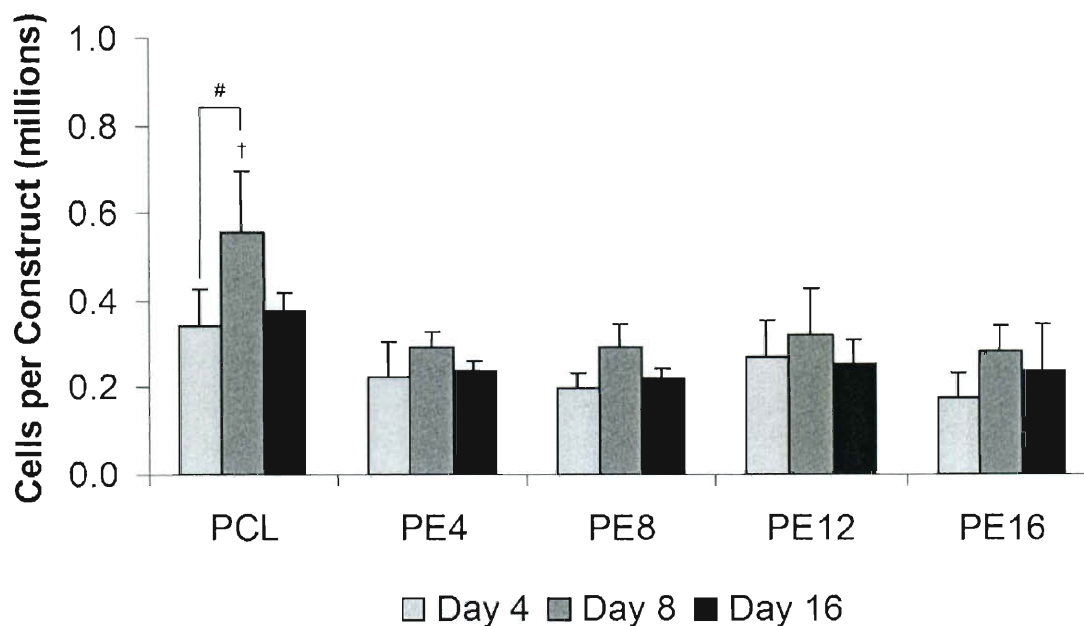


Figure IV-3: Cellularity of plain PCL scaffolds and PCL/ECM (PE) composite scaffolds seeded with MSCs and cultured in static conditions without dexamethasone for 16 days. PE4, PE8, PE12, and PE16 composite scaffolds contain mineralized matrix of various maturities generated in flow perfusion culture of increasing durations. Data are presented as mean \pm standard deviation for $n = 4$. Within a specific scaffold group, significant difference ($p < 0.05$) between time points is noted with (#). At a specific time point, significant difference ($p < 0.05$) compared to all other scaffold groups is noted with (†).

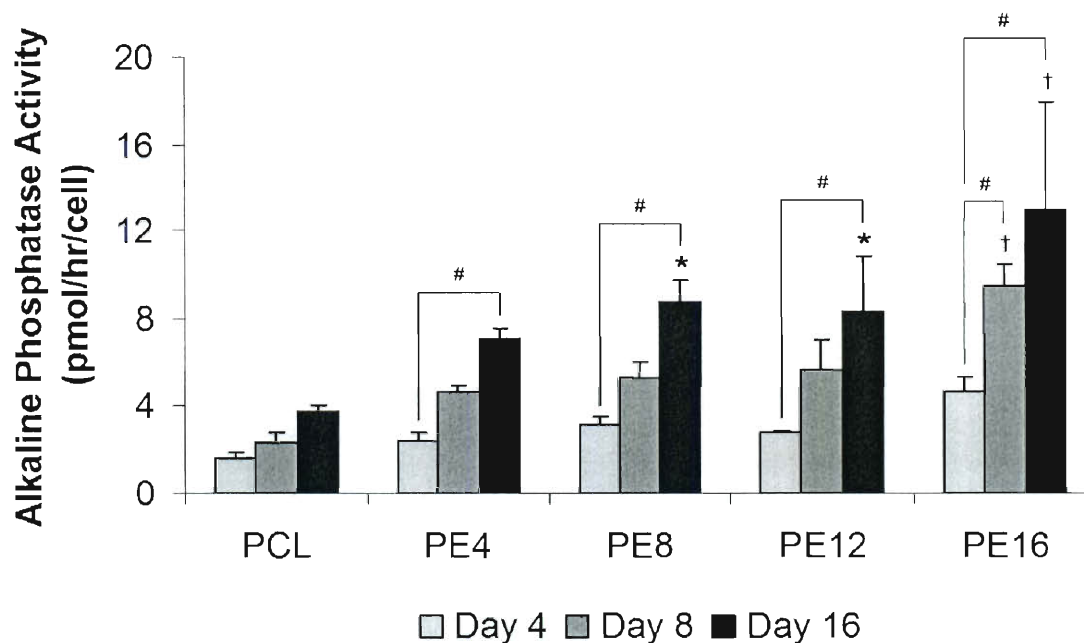


Figure IV-4: Alkaline phosphatase activity of plain PCL scaffolds and PCL/ECM (PE) composite scaffolds seeded with MSCs and cultured in static conditions without dexamethasone for 16 days. PE4, PE8, PE12, and PE16 composite scaffolds contain mineralized matrix of various maturities generated in flow perfusion culture of increasing durations. Data are presented as mean \pm standard deviation for $n = 4$. Within a specific scaffold group, significant difference ($p < 0.05$) between time points is noted with (#). At a specific time point, significant difference ($p < 0.05$) compared to plain PCL controls is noted with (*), with significant difference ($p < 0.05$) compared to all other scaffold groups noted with (†).

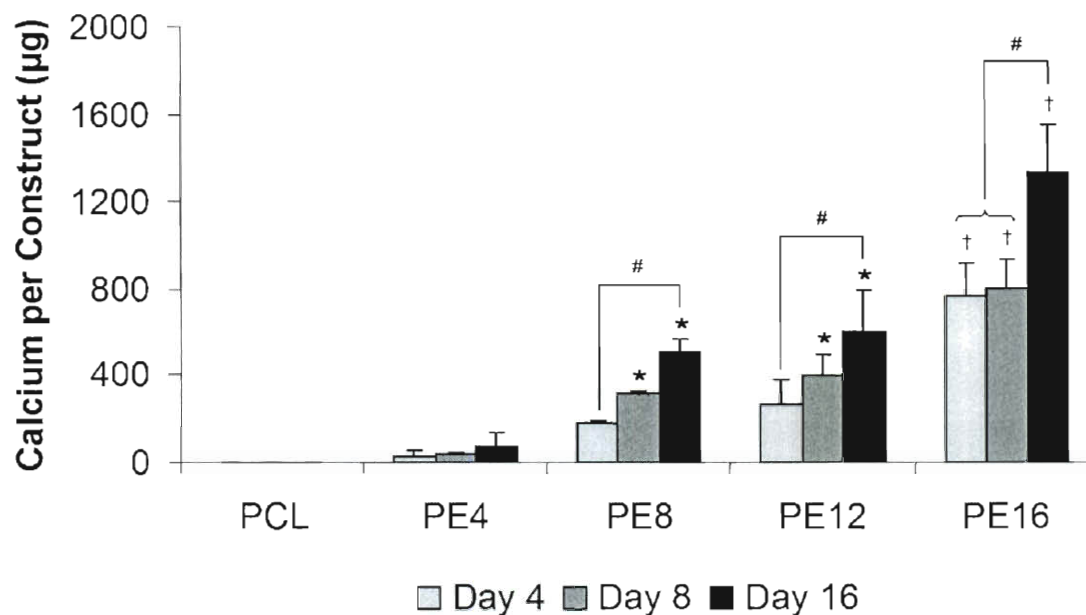


Figure IV-5: Calcium content of plain PCL scaffolds and PCL/ECM (PE) composite scaffolds seeded with MSCs and cultured in static conditions without dexamethasone for 16 days. PE4, PE8, PE12, and PE16 composite scaffolds contain mineralized matrix of various maturities generated in flow perfusion culture of increasing durations. Data are presented as mean \pm standard deviation for $n = 4$. Within a specific scaffold group, significant difference ($p < 0.05$) between time points is noted with (#). At a specific time point, significant difference ($p < 0.05$) compared to plain PCL controls is noted with (*), with significant difference ($p < 0.05$) compared to all other scaffold groups noted with (†).

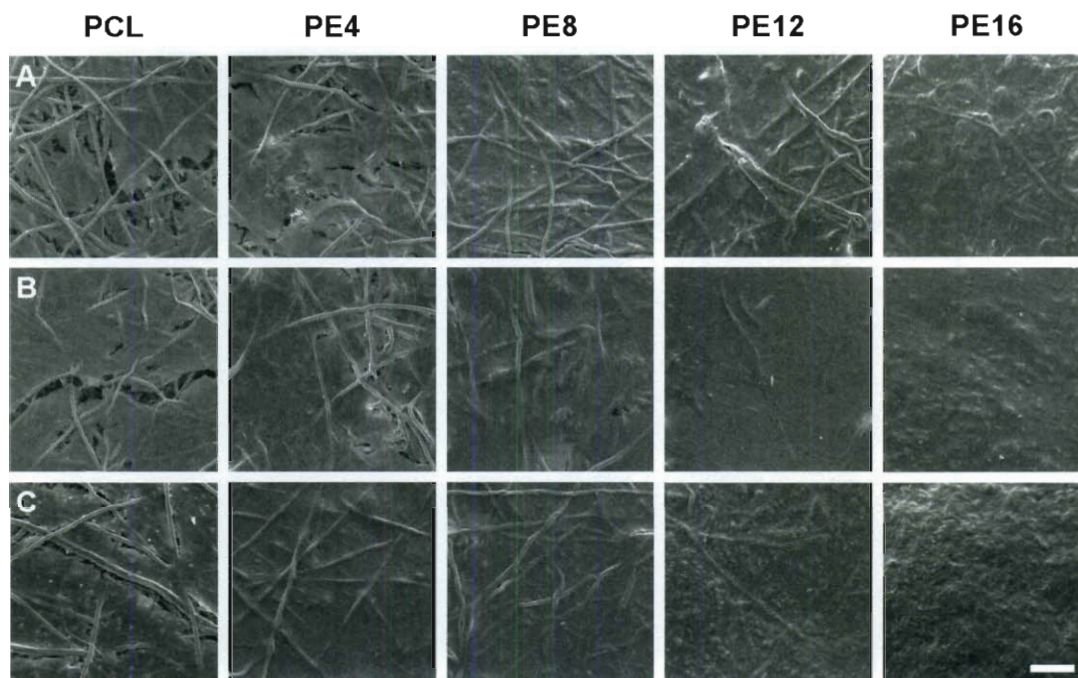


Figure IV-6: Representative scanning electron micrographs of the top surfaces of plain PCL scaffolds and PCL/ECM (PE) composite scaffolds seeded with MSCs and cultured in static conditions without dexamethasone for 16 days. PE4, PE8, PE12, and PE16 composite scaffolds contain mineralized matrix of various maturities generated in flow perfusion culture of increasing durations. For each scaffold group, three rows of images are shown for constructs after (A) 4 days of culture, (B) 8 days of culture, and (C) 16 days of culture. The scale bar shown represents 100 μm and applies to all images.

CHAPTER V

BIOACTIVE POLYMER/EXTRACELLULAR MATRIX SCAFFOLDS FABRICATED WITH A FLOW PERFUSION BIOREACTOR FOR CARTILAGE TISSUE ENGINEERING [†]

Abstract

In this study, electrospun poly(ϵ -caprolactone) (PCL) microfiber scaffolds, coated with cartilaginous extracellular matrix (ECM), were fabricated by first culturing chondrocytes under dynamic conditions in a flow perfusion bioreactor and then decellularizing the cellular constructs. The decellularization procedure yielded acellular PCL/ECM composite scaffolds containing glycosaminoglycan and collagen. PCL/ECM composite scaffolds were evaluated for their ability to support the chondrogenic differentiation of mesenchymal stem cells (MSCs) *in vitro* using serum-free medium with or without the addition of transforming growth factor- β 1 (TGF- β 1). PCL/ECM composite scaffolds supported chondrogenic differentiation induced by TGF- β 1 exposure, as evidenced in the up-regulation of aggrecan (11.6 ± 3.8 fold) and collagen type II (668.4 ± 317.7 fold) gene expression. The presence of cartilaginous matrix alone reduced collagen type I gene expression to levels observed with TGF- β 1 treatment. Cartilaginous matrix

[†] This chapter was published as follows: Liao J, Guo X, Grande-Allen KJ, Kasper FK, Mikos AG. Bioactive polymer/extracellular matrix scaffolds fabricated with a flow perfusion bioreactor for cartilage tissue engineering. *Biomaterials* 2010; 31(34): 8911-8920.

further enhanced the effects of growth factor treatment on MSC chondrogenesis as evidenced in the higher glycosaminoglycan synthetic activity for cells cultured on PCL/ECM composite scaffolds. Therefore, flow perfusion culture of chondrocytes on electrospun microfiber scaffolds is a promising method to fabricate polymer/extracellular matrix composite scaffolds that incorporate both natural and synthetic components to provide biological signals for cartilage tissue engineering applications.

Introduction

Articular cartilage serves a vital role in normal joint function, but has a limited capacity for regeneration once injured or damaged due to its avascular nature and sparse cell population. Clinical procedures that penetrate the subchondral bone to trigger an intrinsic wound healing response, such as abrasion or microfracture, typically result in fibrous tissue which lacks the structure and function of native cartilage [177]. Other clinical approaches involving the transplantation of osteochondral grafts or autologous chondrocytes require tissue biopsies that damage otherwise healthy cartilage [178, 179]. Therefore, tissue engineering strategies incorporating scaffolds, cells, and bioactive factors to regenerate functional cartilage tissue have emerged as a promising alternative.

Mesenchymal stem cells (MSCs) and chondrocytes are often targeted for cartilage tissue engineering due to their vital role in native cartilage formation and function. Since their cellular processes are influenced by both physical and biological signals, effective biomaterial scaffolds for cartilage repair must not only act as temporary supports for tissue growth, but also as instructive microenvironments to guide cellular function. Thus extracellular matrix components, either as isolated proteins or with complex compositions, have been investigated as scaffolding materials for cartilage tissue engineering in an effort to stimulate chondrogenesis by culturing cells within a biological microenvironment [180].

Recently, sponge-like scaffolds fabricated using collagen and glycosaminoglycan, or purely from native cartilage extracellular matrix components, have been shown to support MSC chondrogenic differentiation [181, 182]. Although MSCs were exposed to chondroinductive growth factors either during expansion or throughout the culture period, these studies demonstrate the application of natural matrices with promising results. Fabricating cartilaginous scaffolds typically entails reconstituting proteins and may even involve crosslinking to strengthen the matrix; processing conditions which can affect matrix biochemistry. Still these scaffolds, even after prolonged culture *in vitro*, lack sufficient mechanical properties to support joint function during tissue regeneration [182].

Synthetic polymers on the other hand, are more robust scaffolding materials whose physical properties can be easily controlled through tailored processing conditions. Electrospun polymer scaffolds, in particular, are promising candidates for tissue engineering applications due to their nonwoven fiber mesh structure, which imparts a large surface-to-volume ratio for cell attachment and offers a high interconnected porosity for cell and tissue infiltration. Electrospun poly(ϵ -caprolactone) (PCL) nanofiber scaffolds have been shown to support the attachment and proliferation of chondrocytes and also MSC differentiation along the chondrogenic lineage when cultured with transforming growth factor- β 1 (TGF- β 1) [103, 183].

Previously, we have demonstrated that culturing MSCs in a flow perfusion bioreactor on fiber mesh scaffolds in the presence of osteogenic cell culture

supplements, promotes the deposition of an extracellular matrix (ECM) containing both structural matrix proteins and bioactive growth factors [173]. Upon decellularization, composite scaffolds containing mineralized matrix were capable of inducing MSC osteogenic differentiation even in the absence of dexamethasone, the cell culture supplement often required to stimulate osteogenic differentiation *in vitro* [119, 184]. Here, we seek to develop composite scaffolds for cartilage repair by incorporating cartilaginous matrix generated under fluid flow perfusion conditions on electrospun PCL microfiber scaffolds. By employing both natural and synthetic components in a tissue engineering scaffold, we aim to provide a more physiological microenvironment containing both structural and biological signals to guide MSC chondrogenic differentiation, while at the same time maintaining physical scaffolding properties in a controllable polymeric system.

In this study, we fabricate PCL/ECM composite scaffolds consisting of electrospun microfibers coated with cartilaginous extracellular matrix, and evaluate their ability to support the chondrogenic differentiation of MSCs *in vitro*. For the fabrication of PCL/ECM composite scaffolds, we hypothesized that culturing chondrocytes on PCL scaffolds under dynamic conditions in a flow perfusion bioreactor would stimulate the deposition of cartilaginous ECM that remains even after decellularization. In an effort to evaluate the chondrogenic properties of PCL/ECM composite scaffolds, we hypothesized that PCL/ECM scaffolds would support MSC differentiation along the chondrogenic lineage induced by TGF- β 1 exposure, and that the presence of cartilaginous matrix

would further enhance this differentiation response by providing cells with a more biological microenvironment compared to plain PCL scaffolds. To investigate our hypotheses, bovine chondrocytes were seeded on electrospun PCL microfiber scaffolds and cultured in a flow perfusion bioreactor. The resulting PCL/ECM constructs were decellularized to yield PCL/ECM composite scaffolds, which were characterized for their cartilaginous matrix morphology and composition in response to the decellularization procedure. PCL/ECM composite scaffolds as well as plain PCL scaffolds were seeded with rabbit MSCs and cultured in serum-free medium either with or without the addition of TGF- β 1. Constructs were evaluated for cellularity, glycosaminoglycan content (GAG) and synthetic activity (GAG/DNA), and gene expression through real-time reverse transcription polymerase chain reaction (RT-PCR), to determine how physical matrix interactions and biochemical signaling influence chondrogenic differentiation *in vitro*.

Materials and Methods

Electrospinning

Nonwoven PCL microfiber mats were fabricated using a horizontal electrospinning setup with a copper ring to stabilize the electric field as previously described [162]. Mats were electrospun to a targeted fiber diameter of 10 μ m using a solution of 14 wt % PCL (Sigma-Aldrich, St. Louis, MO) in a 5:1 volume ratio of chloroform to methanol. PCL with $M_n = 73,000 \pm 9,000$ and $M_w =$

154,000 \pm 26,000 was characterized by gel permeation chromatography (Waters, Milford, MA) from three samples relative to polystyrene. The polymer solution was pumped at a flow rate of 18 mL/h while charged with an applied voltage of 25.5 kV to draw microfibers toward the collector plate [184]. The resulting PCL mat was aerated, inspected for consistent microfiber morphology, and stored in a desiccator.

Scaffold Preparation

PCL mats were die-punched into scaffolds 6 mm in diameter with thicknesses between 0.95 and 1.05 mm. As previously characterized through scanning electron microscopy and mercury porosimetry, these scaffolds had an average fiber diameter of 9.86 \pm 0.56 μ m and a porosity of 87% with an average pore size of 45 μ m [162, 184]. Prior to use, PCL scaffolds were sterilized with ethylene oxide gas for 14 h and aerated overnight to remove residual fumes. Scaffolds were pre-wetted by centrifuging through a graded series of ethanol from 100% to 70%, followed by three rinses in phosphate buffered saline (PBS), and incubated in cell culture medium overnight. In preparation for cell seeding, scaffolds were press-fitted into cassettes designed to confine the cell suspension and to be used in the flow perfusion bioreactor [121].

PCL/ECM Cartilaginous Composite Scaffold Generation

Chondrocytes were harvested and pooled from cartilage collected from the femoral condyle area of four young calves through tissue obtained from

Research 87 (Research 87, Boylston, MA) according to previously established methods [185]. Cartilage was collected from the condyles, washed with PBS, and digested in culture medium containing 2 mg/mL collagenase (Worthington, Lakewood, NJ) while incubating at 37 °C overnight. Chondrocytes were frozen in aliquots of medium containing 20% fetal bovine serum (FBS) and 10% dimethyl sulfoxide (DMSO).

PCL/ECM constructs containing cartilaginous extracellular matrix were generated by culturing chondrocytes on electrospun microfiber scaffolds under dynamic conditions in the flow perfusion bioreactor for 9 days, then decellularized through a freeze and thaw procedure to yield PCL/ECM composite scaffolds (Figure V-1). Cryopreserved chondrocytes were first thawed at 37 °C and plated in tissue culture flasks with chondrocyte culture medium consisting of DMEM, supplemented with 10% FBS (Gemini Bio-Products, West Sacramento, CA), 1% non-essential amino acids, 0.4 mM proline, 10 mM HEPES buffer, and 50 mg/L ascorbic acid, also with the addition of penicillin, streptomycin, and fungizone (Invitrogen, Carlsbad, CA). Primary chondrocytes were cultured for 7 days in chondrocyte culture medium with medium changes every 3 days. Chondrocytes were lifted with 0.05% trypsin and suspended in culture medium for seeding onto press-fitted scaffolds at a seeding density of 150,000 cells in 200 μ L of medium within each cassette. Scaffolds were incubated with the seeding solution for 2 h then medium was added to fill each cassette. After allowing 24 h for cell attachment, constructs in their cassettes were transferred directly into the flow perfusion bioreactor and cultured for 9 days with medium changes every 3 days.

Medium was perfused through the press-fitted constructs at a flow rate of 0.3 mL/min to provide cells with some mechanical stimulation and enhance metabolic transport [121].

At the end of culture, constructs were rinsed with PBS and stored in 1.5 mL ddH₂O at -80 °C. PCL/ECM constructs were decellularized to yield PCL/ECM composite scaffolds via three consecutive cycles of a freeze and thaw procedure, in which constructs were frozen for 10 min in liquid nitrogen then thawed for 10 min in a 37 °C water bath [164]. Even though this decellularization procedure has been shown to yield acellular constructs [152], samples were prepared for scanning electron microscopy, histology, and glycosaminoglycan and collagen assays to assess matrix morphology and composition before and after decellularization. The resulting PCL/ECM composite scaffolds were air-dried overnight, press-fitted into cassettes, sterilized with ethylene oxide gas for 14 h and aerated overnight in preparation for seeding.

Cartilaginous Matrix Characterization

Samples for histology were fixed in 10% neutral buffered formalin (Fisher Scientific, Pittsburgh, PA) then immersed in 70% ethanol prior to embedding in HistoPrep freezing medium (Fisher Scientific, Pittsburgh, PA) and stored at -80 °C. Frozen sections 5 µm thick were cut using a cryostat (Leica Biosystems, Richmond, IL), mounted onto Superfrost Excell glass slides (Fisher Scientific, Pittsburgh, PA), and placed on a 37 °C slide warmer to facilitate adhesion. Sections were stained with hematoxylin to visualize the distribution of cells, and

Safranin O to visualize the distribution of cartilaginous extracellular matrix. Images were obtained using a light microscope (Nikon Eclipse E600, Melville, NY) with a video camera attachment (Sony DXC950P, New York, NY).

Samples for biochemical assays were digested in 500 μ L of a proteinase K solution while incubating in a 56 °C water bath for 16 h. The proteinase K solution consisted of 1 mg/mL proteinase K, 0.01 mg/mL pepstatin A, and 0.185 mg/mL iodoacetamide, in a tris-EDTA buffer made by dissolving 6.055 mg/mL tris(hydroxymethyl aminomethane) and 0.372 mg/mL EDTA with pH adjusted to 7.6. Matrix components were extracted via three repetitions of a freeze, thaw, and sonication cycle, where samples were frozen for 30 min at -80 °C, thawed for 30 min at room temperature, and sonicated for 30 min in order to allow matrix components into the solution.

Total collagen content was determined by quantifying hydroxyproline using the colorimetric hydroxyproline assay and hydroxyproline standards as previously described [184]. Absorbance was measured on a plate reader (BioTek PowerWave, Winooski, VT). Resulting hydroxyproline measurements in μ g were converted to collagen contents for each sample following a 1:10 ratio of hydroxyproline to collagen [165].

Glycosaminoglycan content was determined by quantifying GAG using the colorimetric dimethylmethylene blue assay (Sigma-Aldrich, St. Louis, MO) and chondroitin sulfate standards as previously described [184]. Absorbance was measured on a plate reader (BioTek PowerWave, Winooski, VT). Resulting GAG measurements in μ g were determined for each sample. For glycosaminoglycan

synthetic activity, the resulting GAG amounts were normalized to the amount of DNA for each sample.

Chondrogenic Differentiation with TGF- β 1

MSCs were harvested from bone marrow aspirates taken from the tibiae of six male New Zealand white rabbits (Charles River, Wilmington, MA) weighing 2.8-3.0 kg according to previously established methods [186]. Bone marrow from each leg was aspirated into a 10 mL syringe containing 5,000 U/mL heparin to prevent coagulation. The experimental protocol for this study was reviewed and approved by the Institutional Animal Care and Use Committee of Rice University, and all procedures were conducted according to the *Principles of Laboratory Animal Care* (NIH Publication No. 85-23, Revised 1985). The bone marrow was plated in tissue culture flasks with general expansion medium consisting of DMEM, supplemented with 10% FBS (Gemini Bio-Products, West Sacramento, CA), also with the addition of penicillin, streptomycin, and fungizone (Invitrogen, Carlsbad, CA). Non-adherent cells were washed away after 72 h, and adherent cells were cultured for 14 days in general expansion medium with medium changes every 3 days. After this primary culture period, MSCs were lifted with 0.05% trypsin and pooled from all six rabbits then frozen in aliquots of medium containing 20% FBS and 10% DMSO, in order to reduce variation between individual animals [187].

Cryopreserved MSCs were thawed at 37 °C, plated in tissue culture flasks, and expanded to passage three with general expansion medium for the

differentiation study (Figure V-1). MSCs were then trypsinized and seeded onto press-fitted experimental PCL/ECM composite scaffolds and also plain PCL control scaffolds at a density of 150,000 cells in 200 μ L of medium within each cassette. Scaffolds were incubated with the seeding solution for 2 h then serum-free chondrogenic medium was added to fill each cassette consisting of DMEM, supplemented with 1% ITS+ Premix (BD Biosciences, San Jose, CA), 10^{-7} M dexamethasone, 1 mM sodium pyruvate, 50 mg/L ascorbic acid, also with the addition of penicillin, streptomycin, and fungizone (Invitrogen, Carlsbad, CA). After allowing 24 h for cell attachment, constructs were removed from their cassettes and transferred into 24-well plates with 1 mL of medium and cultured under static conditions for 9, 15, and 21 days with serum-free chondrogenic medium either with or without the addition of 10 ng/mL TGF- β 1 replenished every 3 days. Eight samples were cultured for each scaffold group (PCL and PCL/ECM) and growth factor treatment (-TGF and +TGF) for each culture time (9, 15, and 21 days), at the end of which samples were rinsed with PBS and stored for later analysis. Three samples were prepared for assessing construct cellularity and glycosaminoglycan content and synthetic activity, one sample was prepared for scanning electron microscopy, and four samples were prepared for assessing gene expression through real-time reverse transcription polymerase chain reaction.

Chondrogenic Differentiation Assays

Samples for biochemical assays were digested in 500 μ L of a proteinase K solution while incubating in a 56 °C water bath for 16 h. The proteinase K solution consisted of 1 mg/mL proteinase K, 0.01 mg/mL pepstatin A, and 0.185 mg/mL iodoacetamide, in a tris-EDTA buffer made by dissolving 6.055 mg/mL tris(hydroxymethyl aminomethane) and 0.372 mg/mL EDTA with pH adjusted to 7.6. DNA and matrix components were extracted via three repetitions of a freeze, thaw, and sonication cycle, where samples were frozen for 30 min at -80 °C, thawed for 30 min at room temperature, and sonicated for 30 min in order to allow DNA and matrix components into the solution.

Glycosaminoglycan content was determined by quantifying GAG using the colorimetric dimethylmethylene blue assay (Sigma-Aldrich, St. Louis, MO) and chondroitin sulfate standards as previously described [184]. Absorbance was measured on a plate reader (BioTek PowerWave, Winooski, VT). Resulting GAG measurements in μ g were determined for each sample. For glycosaminoglycan synthetic activity, the resulting GAG amounts were normalized to the amount of DNA for each sample.

Cellularity was determined by quantifying double-stranded DNA using the fluorometric PicoGreen assay (Invitrogen, Carlsbad, CA) and DNA standards as previously described [184]. Fluorescence was measured on a plate reader (BioTek FL x800, Winooski, VT). Resulting DNA measurements in μ g were converted to cell numbers by correlating to DNA extracted from a known number of MSCs.

Scanning Electron Microscopy

Samples for scanning electron microscopy were fixed in 2.5% glutaraldehyde, dehydrated through a graded series of ethanol from 70% to 100%, air-dried overnight then mounted on aluminum stubs to visualize the top surface. Samples were sputter coated with gold for 1 min prior to imaging via SEM (FEI Quanta 400, Hillsboro, OR).

Real-time RT-PCR

Samples for real-time reverse transcription polymerase chain reaction were stored in RNAlater (Qiagen, Valencia, CA) at -20 °C to stabilize and protect RNA. After all samples were collected, total RNA was extracted using the RNeasy mini kit (Qiagen, Valencia, CA) according to the manufacturer's instructions as previously described [168]. Constructs were placed in lysis buffer to lyse cells. After gentle mixing to allow RNA into the solution, the lysate was transferred to a QIAshredder column (Qiagen, Valencia, CA) for homogenization. An equal volume of 70% ethanol was added to the lysate and the mixture was transferred to an RNeasy mini spin column (Qiagen, Valencia, CA) where RNA was isolated and purified according to the manufacturer's animal cell protocol, with additional washes as previously described to improve the purity of total RNA [188]. Reverse transcription was then carried out to synthesize cDNA from purified RNA samples using Oligo(dT) primers (Promega, San Luis Obispo, CA) and SuperScript III reverse transcriptase (Invitrogen, Carlsbad, CA). Finally, cDNA was subjected to real-time PCR (Applied Biosystems 7300 Real-Time

PCR System, Foster City, CA) to quantify the gene expression of aggrecan, collagen type II, and collagen type I.

Results were analyzed using the $2^{-\Delta\Delta Ct}$ method to determine relative changes in target gene expression as compared to untreated controls [189]. Target gene expression was first normalized to the expression of the housekeeping gene glyceraldehyde 3-phosphate dehydrogenase (GAPDH) then converted to a fold ratio as compared to the baseline expression of that target gene measured in MSC controls taken directly after expansion just prior to seeding onto scaffolds. The sequences of primers used in this analysis are as follows:

GAPDH: 5'-TCACCATCTTCCAGGAGCGA-3', 5'-CACAATGCCGAAGTGGTCGT-3';

aggrecan: 5'-GCTACGGAGACAAGGATGAGTTC-3', 5'-CGTAAAAGACCTCACCTCCAT-3';

collagen type II: 5'-AACACTGCCAACGTCCAGAT-3', 5'-CTGCAGCACGGTATAGGTGA-3';

collagen type I: 5'-ATGGATGAGGAACTGGCAACT-3', 5'-GCCATCGACAAGAACAGTGTAAGT-3'.

Statistical Analysis

Both characterization and chondrogenic differentiation studies were performed each with two separate and independent experiments. Although the trends were similar between experimental runs, the data presented here for both characterization and chondrogenic differentiation studies are derived from one experiment to mitigate potential differences between cell harvests. For each

experiment, cells from six rabbits were pooled together in effort to reduce variation between individual animals [187].

Characterization results for the glycosaminoglycan and collagen contents of cartilaginous extracellular matrix within PCL/ECM constructs generated in flow perfusion culture, and subsequent PCL/ECM composite scaffolds obtained following decellularization, are reported as mean \pm standard deviation for $n = 3$. A Student's t-test at a significance level of 5% was performed to determine whether the decellularization procedure (Construct vs. Scaffold) had a significant effect on glycosaminoglycan and collagen contents.

Chondrogenic differentiation in static culture was assessed through biochemical assays to evaluate cellularity and glycosaminoglycan content and synthetic activity with $n = 3$ and quantitative gene expression of aggrecan, collagen type II, and collagen type I with $n = 4$. Results are reported as mean \pm standard deviation. A three-factor ANOVA was first performed to determine significant global effects or interactions among scaffold group (PCL and PCL/ECM), growth factor treatment (-TGF and +TGF), and culture time (9, 15, 21 days). Multiple pairwise comparisons were then made using the Tukey procedure to determine significant differences. All statistical analyses were performed at a significance level of 5%.

Results

PCL/ECM Cartilaginous Composite Characterization

PCL/ECM constructs and PCL/ECM composite scaffolds were visualized to assess overall morphological appearance in response to the decellularization procedure. Bovine chondrocytes cultured on electrospun microfiber scaffolds under dynamic conditions in the flow perfusion bioreactor for 9 days to generate PCL/ECM constructs, are most prevalent at the top surface in scanning electron micrographs (Figure V-2A), with some cells present within the construct seen through hematoxylin staining (Figure V-2B). Cartilaginous matrix is predominantly localized to the chondrocytes with a sparse distribution of Safranin O staining evident within the construct (Figure V-2C). Following the decellularization procedure to yield PCL/ECM composite scaffolds, which included three cycles of freeze and thaw, air-dry overnight, and sterilization via ethylene oxide exposure, chondrocytes are no longer apparent at the top surface in scanning electron micrographs (Figure V-2D), as well as within the scaffold as seen through hematoxylin staining (Figure V-2E). A layer of cartilaginous matrix remains visible at the top surface of the scaffold in scanning electron micrographs (Figure V-2D), while retaining a similar distribution within the scaffold as shown through Safranin O staining (Figure V-2F).

Cartilaginous matrix composition in terms of glycosaminoglycan and collagen contents for PCL/ECM constructs and PCL/ECM composite scaffolds were characterized (Figure V-3). Although there is no significant difference in the

collagen content between constructs and scaffolds, constructs contain more glycosaminoglycan than scaffolds, indicating a reduction in glycosaminoglycan content in response to the decellularization procedure.

Cellularity and Glycosaminoglycan

PCL/ECM composite scaffolds along with plain PCL control scaffolds were seeded with rabbit MSCs and cultured under static conditions for 9, 15, and 21 days in serum-free medium with or without the addition of TGF- β 1 to evaluate the chondrogenic properties of PCL/ECM composite scaffolds. Table 1 summarizes the global effect of each experimental factor on the biochemical results. TGF- β 1 treatment had a significant effect on the glycosaminoglycan synthetic activity (GAG/DNA) of MSCs differentiating along the chondrogenic lineage but only on PCL/ECM composite scaffolds. The presence of cartilaginous extracellular matrix on electrospun microfiber scaffolds had a significant effect on cellularity, glycosaminoglycan content (GAG), and GAG/DNA.

Cellularity results showed that cell numbers were not statistically different between treatment groups at each time point, whether cells were cultured with or without TGF- β 1 on PCL scaffolds or PCL/ECM composite scaffolds (Figure V-4A). Cellularity remained constant over time without TGF- β 1 exposure, while all constructs treated with TGF- β 1 exhibited a decrease in cellularity from 9 to 21 days of culture. Glycosaminoglycan content remained constant over time for PCL constructs and was not statistically different between PCL constructs cultured with or without TGF- β 1 (Figure V-4B). PCL/ECM constructs contained more GAG

than PCL constructs at 9 days, with PCL/ECM constructs cultured with TGF- β 1 containing the most GAG at 9 days. Though PCL/ECM composite scaffolds started with an initial amount of GAG ($7.45 \pm 0.59 \mu\text{g}$) in addition to the amount of GAG inherent for the seeded cells ($2.77 \pm 0.73 \mu\text{g}$), a reduction in GAG was observed sooner at 9 days for cultures without TGF- β 1 and later at 15 days for cultures with TGF- β 1. Glycosaminoglycan synthetic activity remained constant over time for all treatment groups (Figure V-4C). Interestingly, although cells cultured on PCL scaffolds did not exhibit higher GAG/DNA in response to TGF- β 1 exposure, those cultured on PCL/ECM composite scaffolds and treated TGF- β 1 did however demonstrate higher GAG/DNA at 9 and 21 days.

Scanning electron micrographs were taken of the top surface of constructs to visualize the overall morphology throughout the culture period (Figure V-5). Though PCL/ECM composite scaffolds started with an initial cartilaginous matrix while PCL scaffolds did not, MSCs did not visibly accumulate extracellular matrix over time on either scaffold. In contrast to constructs with chondrocytes where rounded cell bodies were well distinguished, MSCs were flat and spread forming a smooth coat over the construct surface. Those constructs treated with TGF- β 1 appeared to develop a striated texture with a rippled appearance after 21 days of culture.

Quantitative Gene Expression

Aggrecan, collagen type II, and collagen type I gene expression was measured by real-time reverse transcription polymerase chain reaction to assess

the chondrogenic properties PCL/ECM composite scaffolds. Table 2 summarizes the global effect of each experimental factor on the quantitative gene expression results. TGF- β 1 had a significant effect on the expression of aggrecan, collagen type II, and collagen type I. The presence of cartilaginous extracellular matrix on electrospun microfiber scaffolds had a significant effect on the expression of collagen type I.

Aggrecan gene expression was significantly higher for cells cultured with TGF- β 1 and exhibited an increasing trend over time (Figure V-6A). In cultures without TGF- β 1, aggrecan expression was not statistically different than MSCs at day 0 and remained constant from 9 to 21 days of culture, with no statistical difference between cells cultured on PCL scaffolds or PCL/ECM composite scaffolds. In cultures with TGF- β 1 however, statistical differences in aggrecan expression compared to MSCs at day 0 were detected beginning at 9 days for PCL/ECM composite scaffolds and later at 15 days for PCL scaffolds. While cells cultured with TGF- β 1 exhibited the highest levels of aggrecan expression at 21 days, there was no statistical difference between cells cultured on PCL scaffolds (10.0 ± 2.7 fold) or PCL/ECM composite scaffolds (11.6 ± 3.8 fold).

Similar to aggrecan gene expression, collagen type II gene expression was significantly higher for cells cultured with TGF- β 1 and exhibited an increasing trend over time (Figure V-6B). In cultures without TGF- β 1, collagen type II expression was not statistically different than MSCs at day 0 and remained constant from 9 to 21 days of culture, with no statistical difference between cells cultured on PCL scaffolds or PCL/ECM composite scaffolds. In

cultures with TGF- β 1, statistical differences in collagen type II expression compared to MSCs at day 0 were detected beginning at 15 days for both PCL scaffolds and PCL/ECM composite scaffolds. While cells cultured with TGF- β 1 exhibited the highest levels of collagen type II expression at 21 days, there was no statistical difference between cells cultured on PCL scaffolds (629.3 ± 135.6 fold) or PCL/ECM composite scaffolds (668.4 ± 317.7 fold).

In contrast to aggrecan and collagen type II gene expression, collagen type I gene expression was significantly lower for cells cultured with TGF- β 1 and remained constant over time, with no statistical difference between cells cultured on PCL scaffolds or PCL/ECM composite scaffolds (Figure V-6C). In cultures without TGF- β 1, collagen type I expression increased over time and was the highest for cells cultured on PCL scaffolds at 15 and 21 days (6.9 ± 1.0 fold and 9.0 ± 1.1 fold), while cells cultured on PCL/ECM composite scaffolds on the other hand, demonstrated significantly lower collagen type I expression (4.5 ± 1.5 fold and 5.8 ± 0.8 fold). Furthermore, the level of collagen type I expression for cells cultured on PCL/ECM composite scaffolds was comparable to the expression observed with TGF- β 1 treatment.

Discussion

The objective of this study was to fabricate PCL/ECM composite scaffolds consisting of electrospun microfibers coated with cartilaginous extracellular matrix, and evaluate their ability to support the chondrogenic differentiation of MSCs *in vitro*. This study was designed to investigate the fabrication of

PCL/ECM composite scaffolds through dynamic culture of bovine chondrocytes in a flow perfusion bioreactor, and to determine how the decellularization procedure affects matrix morphology and composition. PCL/ECM composite scaffolds were evaluated for their ability to support the chondrogenic differentiation of rabbit MSCs *in vitro* induced by TGF- β 1 exposure, and to determine whether the presence of cartilaginous matrix would further enhance this differentiation response by providing cells with a more biological microenvironment compared to plain PCL scaffolds.

Culturing chondrocytes under direct flow perfusion conditions providing a low level of fluid shear stress has been shown to stimulate proliferation and accumulation of glycosaminoglycan and collagen [118, 166, 190, 191]. Thus in this study, dynamic culture in a flow perfusion bioreactor was employed to generate PCL/ECM constructs. With our electrospun microfiber scaffolds and the chosen flow rate, we observed that bovine chondrocytes deposited cartilaginous extracellular matrix predominately localized to their pericellular space with a sparse distribution of matrix throughout the thickness of the constructs. Although with our present scaffold geometry and culture parameters, cartilaginous matrix was not very well distributed throughout the depth of our constructs, the optimal combination of seeding density, flow rate, and pore size may be further investigated to balance cell retention and matrix distribution throughout the constructs.

From scanning electron micrographs and histological sections, it appears that chondrocytes may have proliferated quickly to occlude the surface porosity

of the electrospun microfiber scaffolds, and thus resulted in a large amount of cartilaginous matrix at the surface of the constructs, consisting of glycosaminoglycan and collagen. In decellularizing PCL/ECM constructs to yield PCL/ECM composite scaffolds, we observed a decrease in glycosaminoglycan content with collagen content unaffected. Safranin O staining revealed that the reduction in glycosaminoglycan is likely associated with the chondrocytes removed from the surface of the constructs via the decellularization procedure. However, since cartilaginous matrix was visibly present in PCL/ECM composite scaffolds, and due to the amount of glycosaminoglycan and collagen detected through biochemical assays, we sought to evaluate PCL/ECM composite scaffolds for their ability to support the chondrogenic differentiation of MSCs *in vitro*.

PCL/ECM composite scaffolds along with plain PCL control scaffolds were seeded with rabbit MSCs and cultured in serum-free medium either with or without the addition of TGF- β 1. Serum-free culture was applied in this study in order to strictly investigate the effects of physical matrix interactions and biochemical signaling on chondrogenic differentiation. Although serum-free culture is beneficial for studying chondrogenic differentiation in a controlled manner *in vitro*, serum deprivation has been shown to affect cell attachment and inhibit proliferation [192]. As such, we observed a decrease in cellularity for cells cultured on both PCL scaffolds and PCL/ECM composite scaffolds driven toward chondrogenic differentiation through TGF- β 1 exposure.

Our results demonstrated that while MSCs did not accumulate a detectable amount of glycosaminoglycan over time, culturing MSCs on both PCL scaffolds and PCL/ECM composite scaffolds with TGF- β 1 significantly enhanced chondrogenic differentiation, as seen in the up-regulation of aggrecan and collagen type II gene expression over time relative to the baseline expression of MSCs at day 0. This differentiation response is further supported by the minimal collagen type I expression throughout the 21 days of culture, where collagen type I expression indicates pre-chondrogenic undifferentiated MSCs or a fibroblastic phenotype [193]. As previously shown with electrospun PCL nanofiber scaffolds (average fiber size 500 to 700 nm) [102, 103], we prove here that microfiber scaffolds (average fiber size 10 μ m) also support MSC chondrogenesis induced by TGF- β 1. Additionally, we demonstrate that PCL/ECM composite scaffolds, containing cartilaginous matrix generated by chondrocytes, are also capable of supporting the chondrogenic differentiation of MSCs *in vitro*.

While the presence of cartilaginous matrix did not seem to enhance chondrogenic gene expression beyond the levels seen with TGF- β 1 exposure, it did however promote an up-regulation in aggrecan expression sooner than plain scaffolds without cartilaginous matrix. Furthermore, cells cultured on composite scaffolds containing cartilaginous matrix exhibited significantly lower collagen type I expression comparable to the minimal levels seen with TGF- β 1 treatment. Therefore, the presence of cartilaginous matrix alone without the addition of growth factors may provide biological signals to reduce the fibroblastic phenotype

of differentiating MSCs as marked in the collagen type I expression levels observed for cells cultured on PCL/ECM composite scaffolds.

The up-regulation in aggrecan gene expression in response to TGF- β 1 treatment did not translate to an increase in glycosaminoglycan content in the constructs. Given that both GAG content and GAG/DNA levels remained constant over time, it is likely that the soluble proteoglycans produced by differentiating cells were not incorporated into the constructs but rather released into the medium, which has been reported in other studies with both chondrocytes and stem cells cultured on polymer scaffolds [194, 195]. Thus, the absence of glycosaminoglycan accumulation may be attributed to the controlled *in vitro* culture conditions and regular medium changes. Although different outcomes may be likely under physiological conditions *in vivo*, assessment of chondrogenesis *in vivo* was beyond the scope of this present study.

PCL/ECM composite scaffolds contained an initial cartilaginous matrix deposited by chondrocytes in flow perfusion culture. Since the cartilaginous matrix was not crosslinked or physically conjugated to the polymer scaffolds, we observed a reduction in GAG content particularly within the first two weeks of culture, where proteoglycans may be leaching into the aqueous environment; similar to what has been observed with cartilage explants in culture [196, 197]. Interestingly, we found that PCL/ECM constructs cultured with TGF- β 1 retained a higher amount of GAG in the first week of culture than those cultured without TGF- β 1. Thus, the combination of cartilaginous matrix and growth factor treatment promotes the retention of GAG either originally present in PCL/ECM

composite scaffolds or produced by the cultured cells. Furthermore, we discovered that only when cells were cultured in the presence of cartilaginous matrix in PCL/ECM composite scaffolds, did TGF- β 1 treatment result in higher GAG/DNA. Therefore, it appears that cartilaginous matrix facilitates chondrogenesis by enhancing the effects of TGF- β 1 *in vitro*.

The cartilaginous matrix deposited by chondrocytes in fabricating PCL/ECM composite scaffolds proved to be too dense for MSCs to remodel and penetrate under static culture conditions, as confirmed through histology (data not shown). While specific cell-matrix interactions are important in regulating the initial attachment of MSCs, the lack of cell penetration through the dense layer of cartilaginous matrix at the surface of PCL/ECM composite scaffolds limits their spatial contact with extracellular matrix proteins to essentially two-dimensions. Thus in this study, although a complex set of matrix molecules were presented, the full potential of these biological signals to guide chondrogenic differentiation might not be experienced by cells in three-dimensions.

Though the porous nature of sponge-like scaffolds fabricated using native cartilage components facilitate cell seeding, hence promoting three-dimensional interactions [181, 182], the precise mechanisms leading to chondrogenesis are unclear. That is, since the entire scaffold structure is comprised of matrix proteins, it is difficult to distinguish whether MSC chondrogenic differentiation is simply due to maintaining cells in a three-dimensional geometry, or whether chondrogenesis is particularly attributed to specific cell-matrix interactions with biological signals in the matrix. Alternatively, the composite nature of our

PCL/ECM scaffolds, with a porous fiber mesh structure as the base material, makes it possible to examine the underlying mechanisms of chondrogenesis; as in this study where we observed that the presence of cartilaginous matrix in PCL/ECM composite scaffolds in fact augmented the effect of growth factor treatment otherwise not seen for plain PCL controls. By tailoring scaffold properties through controllable electrospinning parameters, together with adjusting the morphology and composition of cartilaginous matrix in varying the conditions of chondrocyte seeding and culture, we may be able to engineer PCL/ECM composite scaffolds with sufficient porosity to support chondrogenesis. Maintaining adequate porosity to facilitate subsequent cell seeding and infiltration would allow us to investigate MSC chondrogenic differentiation in a purely structural three-dimensional environment (PCL), or in an instructive cartilaginous microenvironment containing complex arrays of biological signals (PCL/ECM), to gain a better understanding of the mechanisms regulating chondrogenesis.

In this study we utilized a xenogenic source of chondrocytes to generate cartilaginous matrix in fabricating PCL/ECM composite scaffolds. While limited research has been done to explore the potential inductive properties of xenogenic cartilaginous matrix, xenogenic osteochondral grafts decellularized through a photooxidation technique have been shown to repair cartilage defects with no adverse immune response [198]. Also, acellular bovine cartilage matrix molded through freeze-drying and crosslinked via ultraviolet irradiation, showed good biocompatibility with rabbit MSCs and no cytotoxic effects in both direct contact and extraction assays [199]. Chondrocytes can be stimulated to deposit

large amounts of cartilaginous matrix under engineered culture conditions as demonstrated with the fabrication of PCL/ECM composite scaffolds in this study. Due to the limitations and drawbacks with autogenic or allogenic chondrocyte harvest, xenogenic chondrocytes are a potentially clinically applicable cell source in generating acellular cartilaginous scaffolds to guide cartilage repair, provided that the decellularization procedure effectively removes cellular components [200].

Conclusion

In this work, we fabricated PCL/ECM composite scaffolds consisting of electrospun microfibers coated with cartilaginous extracellular matrix, and evaluated their ability to support the chondrogenic differentiation of MSCs *in vitro*. PCL/ECM composite scaffolds supported chondrogenic differentiation induced by TGF- β 1 exposure, as evidenced in the up-regulation of aggrecan and collagen type II gene expression. The presence of xenogenic cartilaginous matrix alone reduced collagen type I gene expression to levels comparable to those observed with TGF- β 1 treatment. Cartilaginous matrix further enhanced the effects of growth factor treatment as evidenced in the higher glycosaminoglycan synthetic activity for cells cultured on PCL/ECM composite scaffolds with TGF- β 1, whereas TGF- β 1 treatment alone did not translate to higher GAG/DNA levels for cells cultured on plain PCL scaffolds. The present study demonstrated the fabrication of polymer/extracellular matrix composite scaffolds using a flow perfusion

bioreactor to incorporate biological signals in a synthetic scaffolding system for cartilage tissue engineering applications.

Acknowledgements

This work has been supported by the National Institutes of Health (R01 AR057083). We thank Dr. Galen I. Papkov for assistance with statistical analysis.

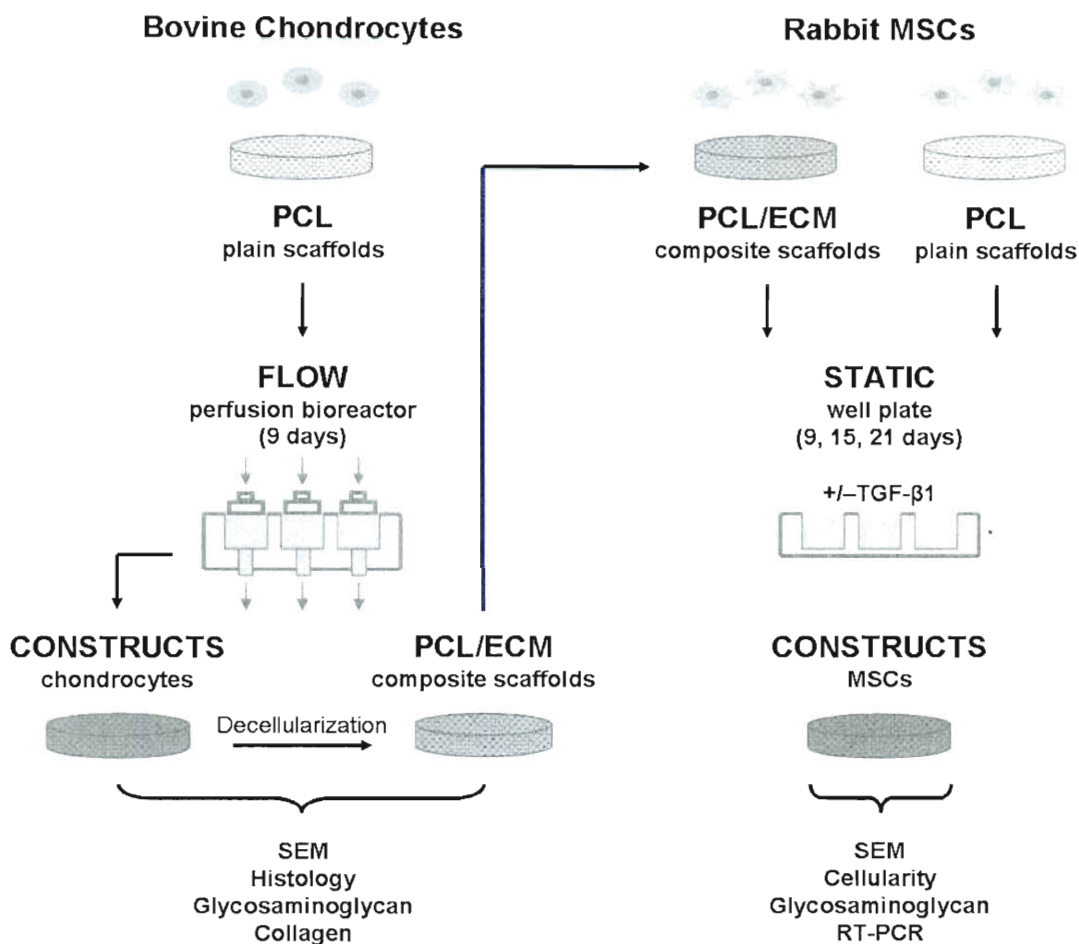


Figure V-1: Schematic representation of the overall experimental design. PCL/ECM constructs were generated through flow perfusion culture of bovine chondrocytes, then decellularized and characterized for matrix morphology and composition in response to the decellularization procedure. PCL/ECM composite scaffolds along with plain PCL polymer scaffolds were seeded with rabbit MSCs and evaluated for their ability to support chondrogenic differentiation in static culture with or without the addition of TGF- β 1.

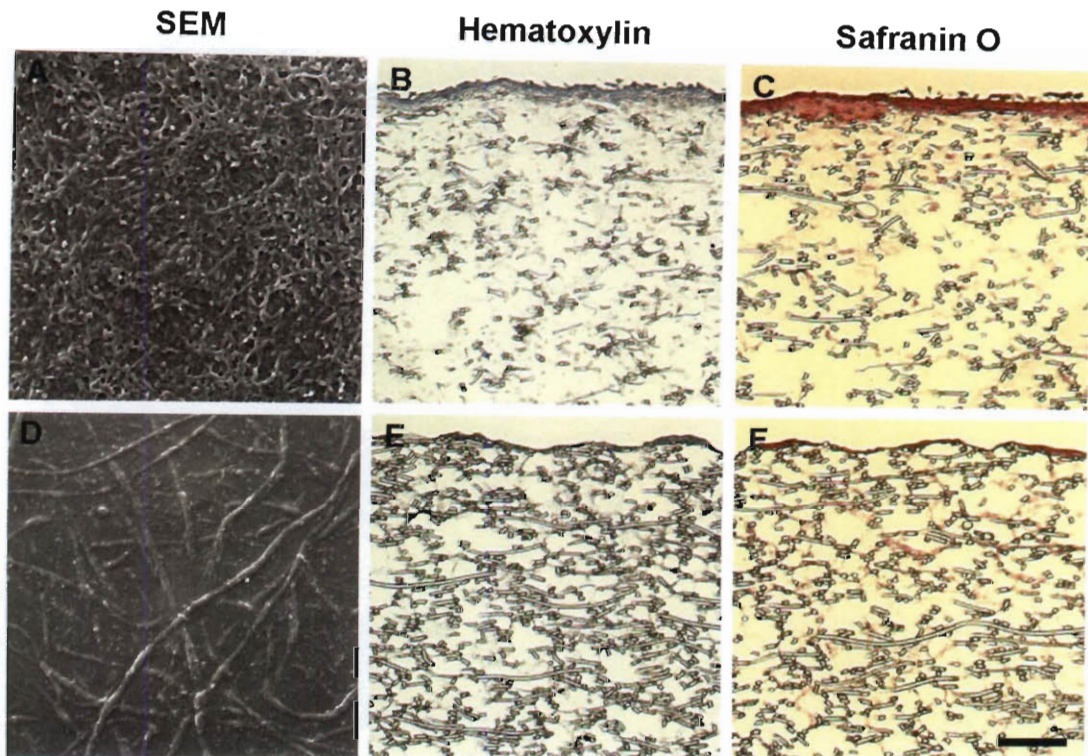


Figure V-2: Morphology of PCL/ECM constructs generated through flow perfusion culture of bovine chondrocytes (A-C) and PCL/ECM composite scaffolds obtained following decellularization (D-F). Images show scanning electron micrographs illustrating surface characteristics (A & D), histological sections stained with hematoxylin to visualize cells (B & E), and histological sections stained with Safranin O to visualize cartilaginous matrix (C & F). The scale bar represents 100 μm for all images.

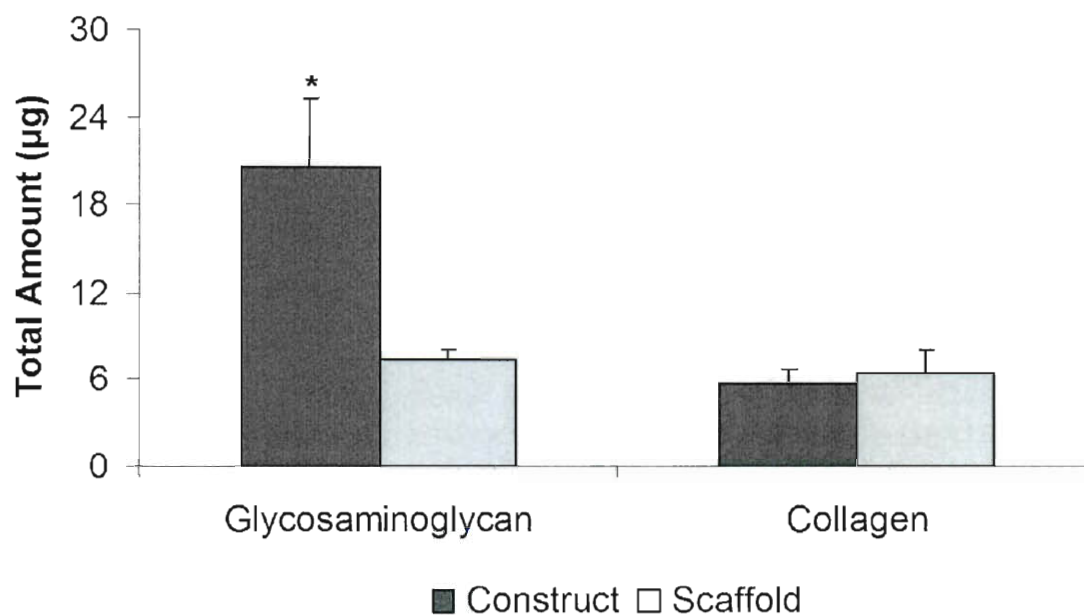


Figure V-3: Composition of PCL/ECM constructs generated through flow perfusion culture of bovine chondrocytes and PCL/ECM composite scaffolds obtained following decellularization. Plots show glycosaminoglycan and collagen contents as mean \pm standard deviation for $n = 3$ from one experiment, although similar trends were observed in two independent experiments. Significant difference ($p < 0.05$) between treatments is noted with (*).

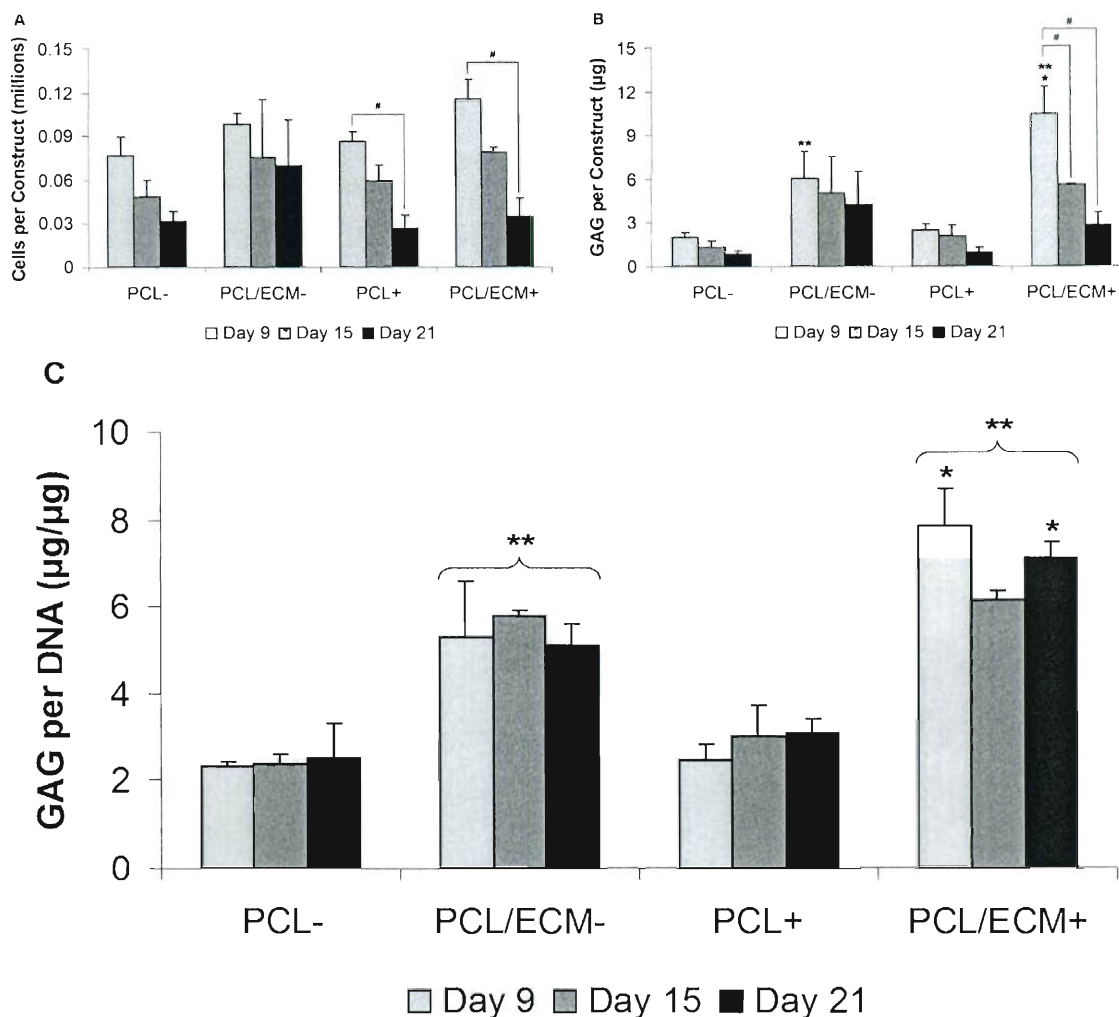


Figure V-4: Biochemical results for MSCs cultured on plain polymer scaffolds (PCL) and composite scaffolds (PCL/ECM) either with (+) or without (–) the addition of TGF- β 1. Plots show cellularity (A), glycosaminoglycan content (B), and glycosaminoglycan synthetic activity (C), as mean \pm standard deviation for $n = 3$ from one experiment, although similar trends were observed in two independent experiments. Within a specific treatment group, significant difference ($p < 0.05$) between time points is noted with (#). At a specific time point for each scaffold group, significant difference ($p < 0.05$) compared to –TGF- β 1 controls is noted with (*). At a specific time point for each growth factor treatment group, significant difference ($p < 0.05$) compared to PCL controls is noted with (**).

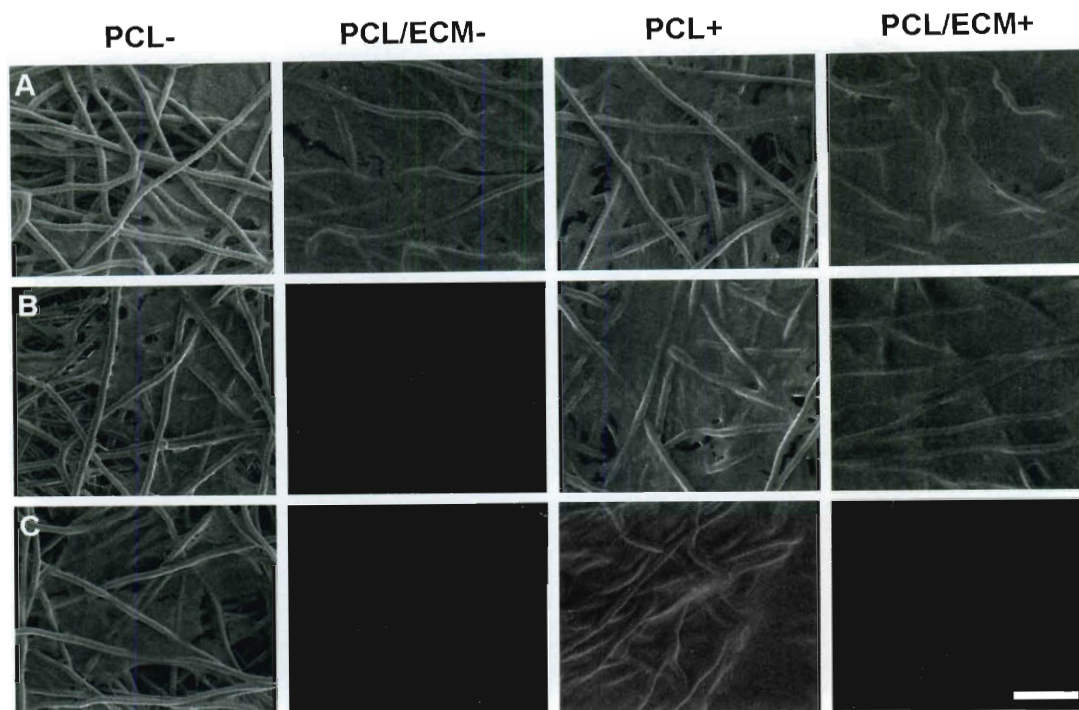


Figure V-5: Representative scanning electron micrographs of the top surface of plain polymer scaffolds (PCL) and composite scaffolds (PCL/ECM) seeded with MSCs and cultured either with (+) or without (–) the addition of TGF- β 1. For each treatment group, three rows of images are shown for constructs after (A) 9 days of culture, (B) 15 days of culture, and (C) 21 days of culture. The scale bar represents 100 μ m for all images.

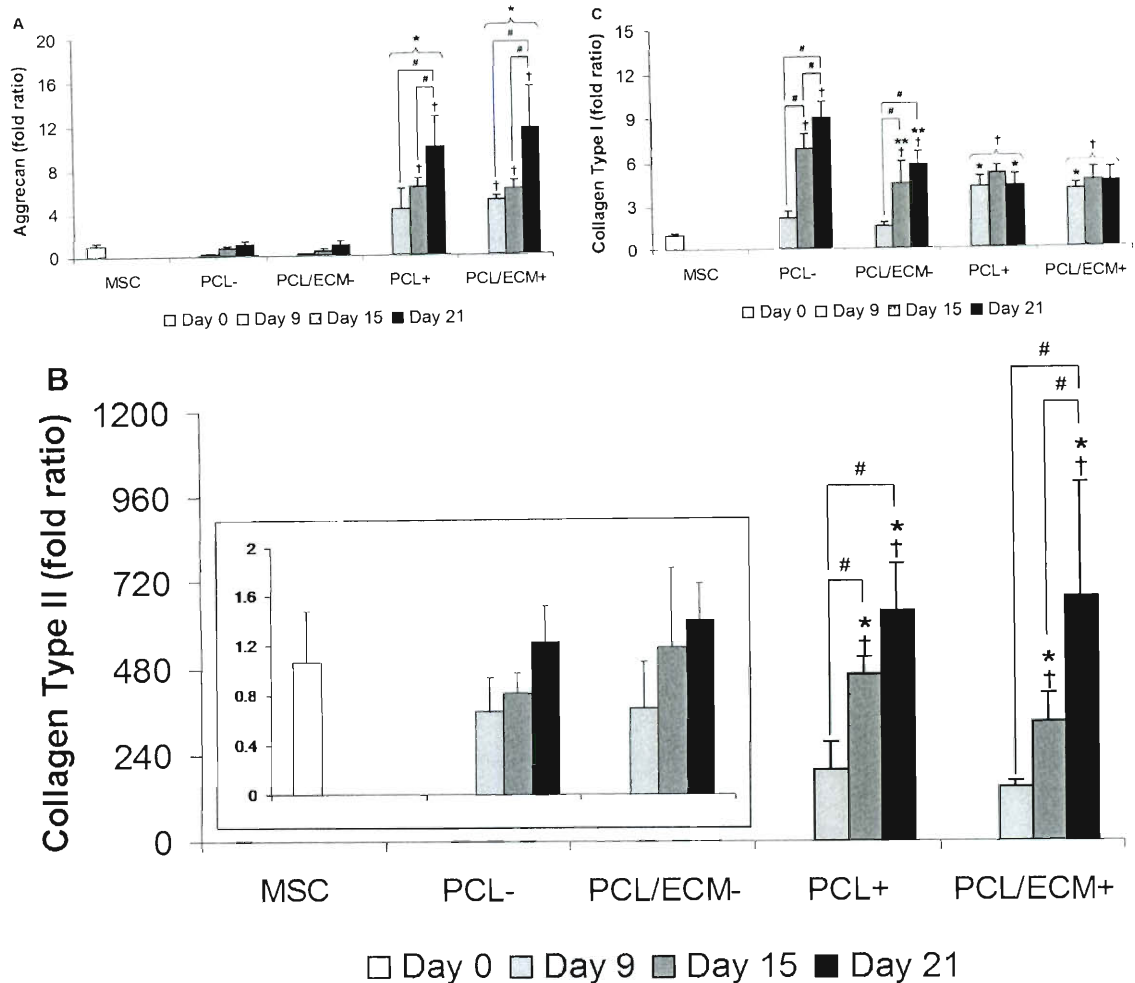


Figure V-6: Quantitative gene expression results for MSCs cultured on plain polymer scaffolds (PCL) and composite scaffolds (PCL/ECM) either with (+) or without (-) the addition of TGF- β 1. Plots show aggrecan expression (A), collagen type II expression with the inset on a rescaled axis (B), and collagen type I expression (C). Data are presented as fold ratio after being normalized to the expression of GAPDH. Fold ratios are shown as mean \pm standard deviation for $n = 4$ from one experiment, although similar trends were observed in two independent experiments. Significant difference ($p < 0.05$) compared to the gene expression of MSCs at day 0 is noted with (\dagger). Within a specific treatment group, significant difference ($p < 0.05$) between time points is noted with ($\#$). At a specific time point for each scaffold group, significant difference ($p < 0.05$) compared to -TGF- β 1 controls is noted with (*). At a specific time point for each growth factor treatment group, significant difference ($p < 0.05$) compared to PCL controls is noted with (**).

Table V-1. Global effect of experimental factors on biochemical results. Significance levels were determined using a three-factor ANOVA and the Tukey procedure. Not significant is abbreviated as NS.

Factor Comparison	Cellularity	GAG	GAG/DNA
-TGF- β 1 vs. +TGF- β 1	NS	NS	$p < 0.05$
PCL vs. PCL/ECM	$p < 0.05$	$p < 0.05$	$p < 0.05$
Day 9 vs. Day 15	$p < 0.05$	$p < 0.05$	NS
Day 9 vs. Day 21	$p < 0.05$	$p < 0.05$	NS
Day 15 vs. Day 21	$p < 0.05$	NS	NS

Table V-2. Global effect of experimental factors on quantitative gene expression results. Significance levels were determined using a three-factor ANOVA and the Tukey procedure. Not significant is abbreviated as NS.

Factor Comparison	Aggrecan	Collagen Type II	Collagen Type I
-TGF- β 1 vs. +TGF- β 1	$p < 0.05$	$p < 0.05$	$p < 0.05$
PCL vs. PCL/ECM	NS	NS	$p < 0.05$
Day 0 vs. Day 9	$p < 0.05$	NS	$p < 0.05$
Day 0 vs. Day 15	$p < 0.05$	$p < 0.05$	$p < 0.05$
Day 0 vs. Day 21	$p < 0.05$	$p < 0.05$	$p < 0.05$
Day 9 vs. Day 15	NS	$p < 0.05$	$p < 0.05$
Day 9 vs. Day 21	$p < 0.05$	$p < 0.05$	$p < 0.05$
Day 15 vs. Day 21	$p < 0.05$	$p < 0.05$	NS

CHAPTER VI

CONCLUDING REMARKS

Biomaterial scaffolds for osteochondral tissue engineering must not only act as a template for tissue growth, but also as instructive microenvironments to guide cellular function. Since mesenchymal stem cells (MSCs) play a vital role in the natural development, maintenance, and repair of cartilage and bone, and are influenced by factors in the native tissue microenvironment, scaffolds for osteochondral regeneration should contain appropriate signals to guide MSC differentiation. This thesis work explored interactions that modulate MSC chondrogenic and osteogenic differentiation in an effort to develop polymer/extracellular matrix (PCL/ECM) composite scaffolds to facilitate osteochondral tissue regeneration.

In an osteochondral defect, interactions exist between bone marrow cell populations within the adjacent bone marrow niche. Since the role of hematopoietic stem and progenitor cells (HSPCs) in regulating the osteogenic differentiation of MSCs is not well understood, the first part of this thesis explored the interaction between HSPCs and MSCs in direct contact co-culture. Results showed that HSPCs played an active role in modulating the development and maintenance of the osteogenic niche. Although this investigation was performed in two-dimensional culture to specifically examine cellular interactions that might take place on bone surfaces, three-dimensional culture using electrospun

microfiber scaffolds could serve as a model for the more porous niche in trabecular bone. Additionally, the incorporation of an initial mineralized matrix could provide insight into how HSPCs regulate bone remodeling for a broader view on the role of HSPCs in bone regeneration.

The second part of this thesis focused on fabricating composite scaffolds consisting of poly(ϵ -caprolactone) (PCL) microfibers coated with mineralized extracellular matrix (ECM). Studies in our laboratory using a titanium fiber mesh base material with a mineralized matrix coating have shown promising results, and thus warranted the transition to a biodegradable scaffolding system. Mineralized PCL/ECM composite scaffolds were fabricated with different matrix maturity and composition via flow perfusion culture. Results showed that mineralized matrix was capable of inducing osteogenic differentiation even in the absence of dexamethasone, with a more rapid and robust differentiation response elicited by a more mature matrix containing higher quantities of collagen and minerals. This investigation was very promising in that osteoblastic differentiation was achieved *in vitro* through specific interactions with the scaffolding material, without the need for external factors such as physical stimulation via bioreactor culture, or soluble signaling including growth factors and dexamethasone. Although this analysis demonstrated how matrix signals modulate osteogenic differentiation while focusing on the osteoinductive ability of the scaffold itself, the bioactive components within the scaffold include more than collagen and minerals, and thus should be further characterized to determine the precise osteoinductive mechanisms. Even though this biodegradable scaffolding

system demonstrated osteoconductivity and osteoinductivity *in vitro*, application of this scaffold *in vivo* would allow more direct evaluation of its potential to enhance bone regeneration, with specific interest in its ability to recruit host progenitor cells and degradation in the physiological environment.

Along with the concept of imparting bioactive properties to an otherwise inert scaffold, the third part of this thesis explored the fabrication of cartilaginous PCL/ECM composite scaffolds. Results showed that although some glycosaminoglycan content was lost during scaffold processing, the remaining cartilaginous matrix served to reduce fibroblastic phenotype and further promoted chondrogenesis in combination with TGF- β 1. While cartilaginous scaffolds did not result in an overwhelming inductive effect as was observed with mineralized scaffolds, mechanisms governing chondrogenic induction may rely more on soluble signals and precise three-dimensional interactions. Further optimization of cartilaginous scaffolds might include varying fabrication parameters to obtain a more uniform cartilaginous matrix coating, and adjusting processing methods to better preserve sensitive matrix components. Flow perfusion culture could increase cellular contact with matrix components for testing, though isolating true scaffold effects *in vitro* remains a challenge and thus, must be addressed in an *in vivo* environment where functional capabilities can be evaluated.

In conclusion, while further investigation is necessary to optimize and test these scaffolds to induce the regeneration of cartilage and bone, this work demonstrates the importance of harnessing signals present in the native microenvironment to modulate chondrogenic and osteogenic differentiation.

CHAPTER VII

BIBLIOGRAPHY

- [1] Schurman DR, Smith RL, Carter DR. Joints: normal structure and function. In: Kelly W, editor. Textbook of internal medicine. New York: Lippincott 1991.
- [2] Buckwalter JA. Articular cartilage: overview. In: Goldberg VM, Caplan AI, editors. Orthopedic tissue engineering: basic science and practice. New York: Marcel Dekker 2004.
- [3] Brittberg M, Lindahl A. Tissue engineering of cartilage. In: van Blitterswijk CA, editor. Tissue engineering. London: Academic Press 2008.
- [4] Buckwalter JA, Mankin HJ. Articular cartilage: tissue design and chondrocyte-matrix interactions. Instr Course Lect 1998; 47: 477-486.
- [5] Mankin HJ. The response of articular cartilage to mechanical injury. J Bone Joint Surg Am 1982; 64(3): 460-466.
- [6] Hunziker EB, Rosenberg LC. Repair of partial-thickness defects in articular cartilage: cell recruitment from the synovial membrane. J Bone Joint Surg Am 1996; 78(5): 721-733.
- [7] De Bari C, Dell'Accio F, Tylzanowski P, Luyten FP. Multipotent mesenchymal stem cells from adult human synovial membrane. Arthritis Rheum 2001; 44(8): 1928-1942.
- [8] Honner R, Thompson RC. The nutritional pathways of articular cartilage. An autoradiographic study in rabbits using ³⁵S injected intravenously. J Bone Joint Surg Am 1971; 53(4): 742-748.
- [9] Mendler M, Eich-Bender SG, Vaughan L, et al. Cartilage contains mixed fibrils of collagen types II, IX, and XI. J Cell Biol 1989; 108(1): 191-197.
- [10] Silver FH. Microscopic and macroscopic structure of tissues. In: Silver FH, editor. Mechanosensing and mechanochemical transduction in extracellular matrix. New York: Springer 2006.
- [11] Maroudas A, Grushko G. Measurement of swelling pressure of cartilage. In: Maroudas A, Kuettner KE, editors. Methods in cartilage research. New York: Academic Press 1990.

- [12] Buckwalter JA, Rosenberg LC. Electron microscopic studies of cartilage proteoglycans. Direct evidence for the variable length of the chondroitin sulfate-rich region of proteoglycan subunit core protein. *J Biol Chem* 1982; 257(16): 9830-9839.
- [13] Wang X, Rackwitz L, Noth U, Rocky ST. Cartilage development, physiology, pathologies, and regeneration. In: Santin M, editor. *Strategies in regenerative medicine: integrating biology with materials design*. New York: Springer 2009.
- [14] Roughley PJ. Articular cartilage and changes in arthritis: non-collagenous proteins and proteoglycans in the extracellular matrix of cartilage. *Arthritis Res* 2001; 3(6): 342-347.
- [15] Outerbridge RE. The etiology of chondromalacia patellae. *J Bone Joint Surg Br* 1961; 43-B: 752-757.
- [16] Hunziker EB. Articular cartilage repair: are the intrinsic biological constraints undermining this process insuperable? *Osteoarthritis Cartilage* 1999; 7(1): 15-28.
- [17] Goldberg VM, Caplan AI. Biologic restoration of articular surfaces. *Instr Course Lect* 1999; 48: 623-627.
- [18] Ulrich-Vinther M, Maloney MD, Schwarz EM, et al. Articular cartilage biology. *J Am Acad Orthop Surg* 2003; 11(6): 421-430.
- [19] Shapiro F, Koide S, Glimcher MJ. Cell origin and differentiation in the repair of full-thickness defects of articular cartilage. *J Bone Joint Surg Am* 1993; 75(4): 532-553.
- [20] Campbell CJ. The healing of cartilage defects. *Clin Orthop Relat Res* 1969; 64: 45-63.
- [21] Grande DA, Singh IJ, Pugh J. Healing of experimentally produced lesions in articular cartilage following chondrocyte transplantation. *Anat Rec* 1987; 218(2): 142-148.
- [22] Coletti JM, Jr., Akeson WH, Woo SL. A comparison of the physical behavior of normal articular cartilage and the arthroplasty surface. *J Bone Joint Surg Am* 1972; 54(1): 147-160.
- [23] Ahmed TA, Hincke MT. Strategies for articular cartilage lesion repair and functional restoration. *Tissue Eng Part B Rev* 2010; 16(3): 305-329.
- [24] Johnson LL. Arthroscopic abrasion arthroplasty: a review. *Clin Orthop Relat Res* 2001; 391 Suppl: S306-317.

- [25] Pridie KH. A method of resurfacing osteoarthritic knee joints. *J Bone Joint Surg Am* 1959; 41: 618-619.
- [26] Steadman JR, Rodkey WG, Briggs KK. Microfracture to treat full-thickness chondral defects: surgical technique, rehabilitation, and outcomes. *J Knee Surg* 2002; 15(3): 170-176.
- [27] Furukawa T, Eyre DR, Koide S, Glimcher MJ. Biochemical studies on repair cartilage resurfacing experimental defects in the rabbit knee. *J Bone Joint Surg Am* 1980; 62(1): 79-89.
- [28] Kim HK, Moran ME, Salter RB. The potential for regeneration of articular cartilage in defects created by chondral shaving and subchondral abrasion. An experimental investigation in rabbits. *J Bone Joint Surg Am* 1991; 73(9): 1301-1315.
- [29] Hangody L, Fules P. Autologous osteochondral mosaicplasty for the treatment of full-thickness defects of weight-bearing joints: ten years of experimental and clinical experience. *J Bone Joint Surg Am* 2003; 85-A Suppl 2: 25-32.
- [30] Brittberg M, Lindahl A, Nilsson A, et al. Treatment of deep cartilage defects in the knee with autologous chondrocyte transplantation. *N Engl J Med* 1994; 331(14): 889-895.
- [31] Langer F, Gross AE, West M, Urovitz EP. The immunogenicity of allograft knee joint transplants. *Clin Orthop Relat Res* 1978; 132: 155-162.
- [32] Stevenson S. The immune response to osteochondral allografts in dogs. *J Bone Joint Surg Am* 1987; 69(4): 573-582.
- [33] Pap K, Krompecher S. Arthroplasty of the knee, experimental and clinical experiences. *J Bone Joint Surg Am* 1961; 43: 523-527.
- [34] Carter DR, Beaupre GS. Skeletal tissue histomorphology and mechanics. In: Carter DR, Beaupre GS, editors. *Skeletal function and form: mechanobiology of skeletal development, aging, and regeneration*. Cambridge: Cambridge University Press 2001.
- [35] Boskey AL. The organic and inorganic matrices. In: Hollinger JO, Einhorn TA, Doll BA, Sfeir C, editors. *Bone tissue engineering*. Boca Raton: CRC Press 2005.
- [36] Burstein AH, Zika JM, Heiple KG, Klein L. Contribution of collagen and mineral to the elastic-plastic properties of bone. *J Bone Joint Surg Am* 1975; 57(7): 956-961.

- [37] Gokhale J, Robey PG, Boskey AL. Osteoporosis. In: Marcus R, Feldman D, Kelsey J, editors. *The biochemistry of bone*. San Diego: Academic Press 2001.
- [38] van der Meulen MC, Jepsen KJ, Mikic B. Understanding bone strength: size isn't everything. *Bone* 2001; 29(2): 101-104.
- [39] Nijweide PJ. The osteocyte. In: Bilezikian JP, Raisz LG, Rodan GA, editor. *Principles of bone biology*. San Diego: Academic Press 1996.
- [40] Vannanen K. Osteoclast function: biology and mechanisms. In: Bilezikian JP, Raisz LG, Rodan GA, editor. *Principles of bone biology*. San Diego: Academic Press 1996.
- [41] Caterson EJ, Tuan RS, Bruder SP. Cell-based approaches to orthopedic tissue engineering. In: Goldberg VM, Caplan AI, editors. *Orthopedic tissue engineering: basic science and practice*. New York: Marcel Dekker 2004.
- [42] Burgeson RE, Nimni ME. Collagen types. Molecular structure and tissue distribution. *Clin Orthop Relat Res* 1992; 282: 250-272.
- [43] Knott L, Bailey AJ. Collagen cross-links in mineralizing tissues: a review of their chemistry, function, and clinical relevance. *Bone* 1998; 22(3): 181-187.
- [44] Lamoureux F, Baud'huin M, Duplomb L, et al. Proteoglycans: key partners in bone cell biology. *Bioessays* 2007; 29(8): 758-771.
- [45] van Gaalen S, Kruyt M, Meijer G, et al. Tissue engineering of bone. In: van Blitterswijk CA, editor. *Tissue engineering*. London: Academic Press 2008.
- [46] Gerstenfeld LC, Einhorn TA. Fracture healing: the biology of bone repair and regeneration. In: Favus MJ, editor. *Primer on the metabolic bone diseases and disorders of mineral metabolism*. Washington DC: American Society for Bone and Mineral Research 2006.
- [47] Sfeir C, Ho L, Doll BA, et al. Fracture repair. In: Lieberman JR, Friedlaender GE, editors. *Bone regeneration and repair*. Totowa: 2005.
- [48] Engel E, Castano O, Salvagni E, et al. Biomaterials for tissue engineering of hard tissues. In: Santin M, editor. *Strategies in regenerative medicine: integrating biology with materials design*. New York: Springer 2009.
- [49] Tsumaki N, Yoshikawa H. The role of bone morphogenetic proteins in endochondral bone formation. *Cytokine Growth Factor Rev* 2005; 16(3): 279-285.

- [50] Kneser U, Schaefer DJ, Polykandriotis E, Horch RE. Tissue engineering of bone: the reconstructive surgeon's point of view. *J Cell Mol Med* 2006; 10(1): 7-19.
- [51] Movassaghi K, Ver Halen J, Ganchi P, et al. Cranioplasty with subcutaneously preserved autologous bone grafts. *Plast Reconstr Surg* 2006; 117(1): 202-206.
- [52] Scaglione S, Quarto R. Clinical applications of bone tissue engineering. In: Santin M, editor. *Strategies in regenerative medicine: integrating biology with materials design*. New York: Springer 2009.
- [53] Kurz LT, Garfin SR, Booth RE, Jr. Harvesting autogenous iliac bone grafts. A review of complications and techniques. *Spine (Phila Pa 1976)* 1989; 14(12): 1324-1331.
- [54] Banwart JC, Asher MA, Hassanein RS. Iliac crest bone graft harvest donor site morbidity. A statistical evaluation. *Spine (Phila Pa 1976)* 1995; 20(9): 1055-1060.
- [55] Friedlaender GE, Sell KW, Strong DM. Bone allograft antigenicity in an experimental model and in man. *Acta Med Pol* 1978; 19(1-2): 197-205.
- [56] Norman-Taylor FH, Santori N, Villar RN. The trouble with bone allograft. *Bmj* 1997; 315(7107): 498.
- [57] Till JE, Mc CE. A direct measurement of the radiation sensitivity of normal mouse bone marrow cells. *Radiat Res* 1961; 14: 213-222.
- [58] Friedenstein AJ, Chailakhjan RK, Lalykina KS. The development of fibroblast colonies in monolayer cultures of guinea-pig bone marrow and spleen cells. *Cell Tissue Kinet* 1970; 3(4): 393-403.
- [59] Jukes J, Both S, Post J, et al. Stem cells. In: van Blitterswijk C, editor. *Tissue engineering*. London: Academic Press 2008.
- [60] Barry FP. Biology and clinical applications of mesenchymal stem cells. *Birth Defects Res C Embryo Today* 2003; 69(3): 250-256.
- [61] Zipori D. Stem cells with no tissue specificity. In: Zipori D, editor. *Biology of stem cells and the molecular basis of the stem cell state*. New York: Humana Press 2009.
- [62] Bosnakovski D, Mizuno M, Kim G, et al. Isolation and multilineage differentiation of bovine bone marrow mesenchymal stem cells. *Cell Tissue Res* 2005; 319(2): 243-253.

- [63] Smith JR, Pochampally R, Perry A, et al. Isolation of a highly clonogenic and multipotential subfraction of adult stem cells from bone marrow stroma. *Stem Cells* 2004; 22(5): 823-831.
- [64] Cancedda R, Castagnola P, Cancedda FD, et al. Developmental control of chondrogenesis and osteogenesis. *Int J Dev Biol* 2000; 44(6): 707-714.
- [65] Bobick BE, Chen FH, Le AM, Tuan RS. Regulation of the chondrogenic phenotype in culture. *Birth Defects Res C Embryo Today* 2009; 87(4): 351-371.
- [66] Cancedda R, Cancedda FD, Dozin B. Chondrocyte culture. In: Beresford JN, Owen ME, editors. *Marrow stromal cell culture*. Cambridge: Cambridge University Press 1998.
- [67] Castagnola P, Moro G, Descalzi-Cancedda F, Cancedda R. Type X collagen synthesis during in vitro development of chick embryo tibial chondrocytes. *J Cell Biol* 1986; 102(6): 2310-2317.
- [68] Gentili C, Cancedda R. Cartilage and bone extracellular matrix. *Curr Pharm Des* 2009; 15(12): 1334-1348.
- [69] Hughes FJ, Collyer J, Stanfield M, Goodman SA. The effects of bone morphogenetic protein-2, -4, and -6 on differentiation of rat osteoblast cells in vitro. *Endocrinology* 1995; 136(6): 2671-2677.
- [70] Aubin JE, Herbertson A. Osteoblast lineage in experimental animals. In: Beresford JN, Owen ME, editors. *Marrow stromal cell culture*. Cambridge: Cambridge University Press 1998.
- [71] Stein GS, Lian JB, Stein JL, et al. Mechanisms regulating osteoblast proliferation and differentiation. In: Bilezikian JP, Raisz LG, Rodan GA, editors. *Principles of bone biology*. San Diego: Academic Press 1996.
- [72] Aubin JE, Liu F, Malaval L, Gupta AK. Osteoblast and chondroblast differentiation. *Bone* 1995; 17(2 Suppl): 77S-83S.
- [73] Aubin JE, Liu F. The osteoblast lineage. In: Bilezikian JP, Raisz LG, Rodan GA, editors. *Principles of bone biology*. San Diego: Academic Press 1996.
- [74] Liu F, Malaval L, Gupta AK, Aubin JE. Simultaneous detection of multiple bone-related mRNAs and protein expression during osteoblast differentiation: polymerase chain reaction and immunocytochemical studies at the single cell level. *Dev Biol* 1994; 166(1): 220-234.
- [75] Zipori D. Historical roots. In: Zipori D, editor. *Biology of stem cells and the molecular basis of the stem cell state*. New York: Humana Press 2009.

- [76] Okada S, Nakauchi H, Nagayoshi K, et al. In vivo and in vitro stem cell function of c-kit- and Sca-1-positive murine hematopoietic cells. *Blood* 1992; 80(12): 3044-3050.
- [77] Matsuzaki Y, Kinjo K, Mulligan RC, Okano H. Unexpectedly efficient homing capacity of purified murine hematopoietic stem cells. *Immunity* 2004; 20(1): 87-93.
- [78] Gunsilius E, Gastl G, Petzer AL. Hematopoietic stem cells. *Biomed Pharmacother* 2001; 55(4): 186-194.
- [79] Kinner B, Spector M. Cartilage: current applications. In: Goldberg VM, Caplan AI, editors. *Orthopedic tissue engineering: basic science and practice*. New York: Marcel Dekker 2004.
- [80] Nehrer S, Breinan HH, Ashkar S, et al. Characteristics of articular chondrocytes seeded in collagen matrices in vitro. *Tissue Eng* 1998; 4(2): 175-183.
- [81] Solchaga LA, Yoo JU, Lundberg M, et al. Hyaluronan-based polymers in the treatment of osteochondral defects. *J Orthop Res* 2000; 18(5): 773-780.
- [82] Liu LS, Thompson AY, Heidarman MA, et al. An osteoconductive collagen/hyaluronate matrix for bone regeneration. *Biomaterials* 1999; 20(12): 1097-1108.
- [83] Temenoff JS, Stein ES, Mikos AG. Biodegradable scaffolds. In: Goldberg VM, Caplan AI, editors. *Orthopedic tissue engineering: basic science and practice*. New York: Marcel Dekker 2004.
- [84] Guo X, Park H, Young S, et al. Repair of osteochondral defects with biodegradable hydrogel composites encapsulating marrow mesenchymal stem cells in a rabbit model. *Acta Biomater* 2010; 6(1): 39-47.
- [85] Sitharaman B, Shi X, Tran LA, et al. Injectable in situ cross-linkable nanocomposites of biodegradable polymers and carbon nanostructures for bone tissue engineering. *J Biomater Sci Polym Ed* 2007; 18(6): 655-671.
- [86] Hutmacher DW. Scaffolds in tissue engineering bone and cartilage. *Biomaterials* 2000; 21(24): 2529-2543.
- [87] Lu L, Mikos AG. The importance of new processing techniques in tissue engineering. *MRS Bull* 1996; 21(11): 28-32.
- [88] Xin X, Hussain M, Mao JJ. Continuing differentiation of human mesenchymal stem cells and induced chondrogenic and osteogenic lineages in electrospun PLGA nanofiber scaffold. *Biomaterials* 2007; 28(2): 316-325.

- [89] Bostman O, Hirvensalo E, Vainionpaa S, et al. Ankle fractures treated using biodegradable internal fixation. *Clin Orthop Relat Res* 1989; 238: 195-203.
- [90] Fu K, Pack DW, Klibanov AM, Langer R. Visual evidence of acidic environment within degrading poly(lactic-co-glycolic acid) (PLGA) microspheres. *Pharm Res* 2000; 17(1): 100-106.
- [91] Middleton JC, Tipton AJ. Synthetic biodegradable polymers as orthopedic devices. *Biomaterials* 2000; 21(23): 2335-2346.
- [92] Li WJ, Tuli R, Huang X, et al. Multilineage differentiation of human mesenchymal stem cells in a three-dimensional nanofibrous scaffold. *Biomaterials* 2005; 26(25): 5158-5166.
- [93] Li WJ, Laurencin CT, Caterson EJ, et al. Electrospun nanofibrous structure: a novel scaffold for tissue engineering. *J Biomed Mater Res* 2002; 60(4): 613-621.
- [94] Kwon IK, Kidoaki S, Matsuda T. Electrospun nano- to microfiber fabrics made of biodegradable copolyesters: structural characteristics, mechanical properties and cell adhesion potential. *Biomaterials* 2005; 26(18): 3929-3939.
- [95] Pham QP, Sharma U, Mikos AG. Electrospinning of polymeric nanofibers for tissue engineering applications: a review. *Tissue Eng* 2006; 12(5): 1197-1211.
- [96] Nair LS, Bhattacharyya S, Laurencin CT. Development of novel tissue engineering scaffolds via electrospinning. *Expert Opin Biol Ther* 2004; 4(5): 659-668.
- [97] Lim SH, Mao HQ. Electrospun scaffolds for stem cell engineering. *Adv Drug Deliv Rev* 2009; 61(12): 1084-1096.
- [98] Huang L, Nagapudi K, Apkarian RP, Chaikof EL. Engineered collagen-PEO nanofibers and fabrics. *J Biomater Sci Polym Ed* 2001; 12(9): 979-993.
- [99] Deitzel JM, Kleinmeyer J, Harris D. The effect of processing variables on the morphology of electrospun nanofibers and textiles. *Polymer* 2001; 42(1): 261-272.
- [100] Demir MM, Yilgor I, Yilgor E. Electrospinning of polyurethane fibers. *Polymer* 2002; 43(11): 3303-3309.
- [101] Xu C, Inai R, Kotaki M, Ramakrishna S. Electrospun nanofiber fabrication as synthetic extracellular matrix and its potential for vascular tissue engineering. *Tissue Eng* 2004; 10(7-8): 1160-1168.

- [102] Wise JK, Yarin AL, Megaridis CM, Cho M. Chondrogenic differentiation of human mesenchymal stem cells on oriented nanofibrous scaffolds: engineering the superficial zone of articular cartilage. *Tissue Eng Part A* 2009; 15(4): 913-921.
- [103] Li WJ, Tuli R, Okafor C, et al. A three-dimensional nanofibrous scaffold for cartilage tissue engineering using human mesenchymal stem cells. *Biomaterials* 2005; 26(6): 599-609.
- [104] Li WJ, Chiang H, Kuo TF, et al. Evaluation of articular cartilage repair using biodegradable nanofibrous scaffolds in a swine model: a pilot study. *J Tissue Eng Regen Med* 2009; 3(1): 1-10.
- [105] Yoshimoto H, Shin YM, Terai H, Vacanti JP. A biodegradable nanofiber scaffold by electrospinning and its potential for bone tissue engineering. *Biomaterials* 2003; 24(12): 2077-2082.
- [106] Shin M, Yoshimoto H, Vacanti JP. In vivo bone tissue engineering using mesenchymal stem cells on a novel electrospun nanofibrous scaffold. *Tissue Eng* 2004; 10(1-2): 33-41.
- [107] Vunjak-Novakovic G, Obradovic B, Madry H, et al. Bioreactors for orthopedic tissue engineering. In: Goldberg VM, Caplan AI, editors. *Orthopedic tissue engineering: basic science and practice*. New York: Marcel Dekker 2004.
- [108] Carter DR, Beaupre GS. Skeletal tissue regeneration. In: Carter DR, Beaupre GS, editors. *Skeletal function and form: mechanobiology of skeletal development, aging, and regeneration*. Cambridge: Cambridge University Press 2001.
- [109] Carver SE, Heath CA. Increasing extracellular matrix production in regenerating cartilage with intermittent physiological pressure. *Biotechnol Bioeng* 1999; 62(2): 166-174.
- [110] Mauck RL, Soltz MA, Wang CC, et al. Functional tissue engineering of articular cartilage through dynamic loading of chondrocyte-seeded agarose gels. *J Biomech Eng* 2000; 122(3): 252-260.
- [111] Lammi MJ, Inkinen R, Parkkinen JJ, et al. Expression of reduced amounts of structurally altered aggrecan in articular cartilage chondrocytes exposed to high hydrostatic pressure. *Biochem J* 1994; 304(Pt 3): 723-730.
- [112] Buschmann MD, Gluzband YA, Grodzinsky AJ, Hunziker EB. Mechanical compression modulates matrix biosynthesis in chondrocyte/agarose culture. *J Cell Sci* 1995; 108(Pt 4): 1497-1508.

- [113] Martin I, Wendt D, Heberer M. The role of bioreactors in tissue engineering. *Trends Biotechnol* 2004; 22(2): 80-86.
- [114] Malda J, Radisic M, Levenberg S, et al. Cell nutrition. In: van Blitterswijk C, editor. *Tissue engineering*. London: Academic Press 2008.
- [115] Gooch KJ, Kwon JH, Blunk T, et al. Effects of mixing intensity on tissue-engineered cartilage. *Biotechnol Bioeng* 2001; 72(4): 402-407.
- [116] Freed LE, Vunjak-Novakovic G. Cultivation of cell-polymer tissue constructs in simulated microgravity. *Biotechnol Bioeng* 1995; 46(4): 306-313.
- [117] Tsao YD, Gonda SR. A new technology for three-dimensional cell culture: the hydrodynamic focusing bioreactor. *Adv in Heat and Mass Transfer in Biotech* 1999; 44: 37-38.
- [118] Pazzano D, Mercier KA, Moran JM, et al. Comparison of chondrogenesis in static and perfused bioreactor culture. *Biotechnol Prog* 2000; 16(5): 893-896.
- [119] Datta N, Pham QP, Sharma U, et al. In vitro generated extracellular matrix and fluid shear stress synergistically enhance 3D osteoblastic differentiation. *Proc Natl Acad Sci U S A* 2006; 103(8): 2488-2493.
- [120] Goldstein AS, Juarez TM, Helmke CD, et al. Effect of convection on osteoblastic cell growth and function in biodegradable polymer foam scaffolds. *Biomaterials* 2001; 22(11): 1279-1288.
- [121] Bancroft GN, Sikavitsas VI, Mikos AG. Design of a flow perfusion bioreactor system for bone tissue-engineering applications. *Tissue Eng* 2003; 9(3): 549-554.
- [122] Martins AM, Saraf A, Sousa RA, et al. Combination of enzymes and flow perfusion conditions improves osteogenic differentiation of bone marrow stromal cells cultured upon starch/poly(epsilon-caprolactone) fiber meshes. *J Biomed Mater Res A* 2010; 94(4): 1061-1069.
- [123] Calvi LM, Adams GB, Weibrecht KW, et al. Osteoblastic cells regulate the haematopoietic stem cell niche. *Nature* 2003; 425(6960): 841-846.
- [124] Jing D, Fonseca AV, Alakel N, et al. Hematopoietic stem cells in co-culture with mesenchymal stromal cells--modeling the niche compartments in vitro. *Haematologica* 2010; 95(4): 542-550.
- [125] Mishima S, Nagai A, Abdullah S, et al. Effective ex vivo expansion of hematopoietic stem cells using osteoblast-differentiated mesenchymal stem cells is CXCL12 dependent. *Eur J Haematol* 2010; 84(6): 538-546.

- [126] Taichman RS, Reilly MJ, Emerson SG. Human osteoblasts support human hematopoietic progenitor cells in vitro bone marrow cultures. *Blood* 1996; 87(2): 518-524.
- [127] Li Z, Li L. Understanding hematopoietic stem-cell microenvironments. *Trends Biochem Sci* 2006; 31(10): 589-595.
- [128] Wilson A, Trumpp A. Bone-marrow haematopoietic-stem-cell niches. *Nat Rev Immunol* 2006; 6(2): 93-106.
- [129] Yin T, Li L. The stem cell niches in bone. *J Clin Invest* 2006; 116(5): 1195-1201.
- [130] Balduino A, Hurtado SP, Frazao P, et al. Bone marrow subendosteal microenvironment harbours functionally distinct haemosupportive stromal cell populations. *Cell Tissue Res* 2005; 319(2): 255-266.
- [131] Taichman RS. Blood and bone: two tissues whose fates are intertwined to create the hematopoietic stem-cell niche. *Blood* 2005; 105(7): 2631-2639.
- [132] Denhardt DT, Guo X. Osteopontin: a protein with diverse functions. *Faseb J* 1993; 7(15): 1475-1482.
- [133] Nilsson SK, Johnston HM, Whitty GA, et al. Osteopontin, a key component of the hematopoietic stem cell niche and regulator of primitive hematopoietic progenitor cells. *Blood* 2005; 106(4): 1232-1239.
- [134] Stier S, Ko Y, Forkert R, et al. Osteopontin is a hematopoietic stem cell niche component that negatively regulates stem cell pool size. *J Exp Med* 2005; 201(11): 1781-1791.
- [135] Adams GB, Chabner KT, Alley IR, et al. Stem cell engraftment at the endosteal niche is specified by the calcium-sensing receptor. *Nature* 2006; 439(7076): 599-603.
- [136] Jung Y, Song J, Shiozawa Y, et al. Hematopoietic stem cells regulate mesenchymal stromal cell induction into osteoblasts thereby participating in the formation of the stem cell niche. *Stem Cells* 2008; 26(8): 2042-2051.
- [137] Shiozawa Y, Jung Y, Ziegler AM, et al. Erythropoietin couples hematopoiesis with bone formation. *PLoS One* 2010; 5(5): e10853.
- [138] Haylock DN, Williams B, Johnston HM, et al. Hemopoietic stem cells with higher hemopoietic potential reside at the bone marrow endosteum. *Stem Cells* 2007; 25(4): 1062-1069.
- [139] Kretlow JD, Jin YQ, Liu W, et al. Donor age and cell passage affects differentiation potential of murine bone marrow-derived stem cells. *BMC Cell Biol* 2008; 9(60).

- [140] Challen GA, Goodell MA. Runx1 isoforms show differential expression patterns during hematopoietic development but have similar functional effects in adult hematopoietic stem cells. *Exp Hematol* 2010; 38(5): 403-416.
- [141] Liao J, Guo X, Nelson D, et al. Modulation of osteogenic properties of biodegradable polymer/extracellular matrix scaffolds generated with a flow perfusion bioreactor. *Acta Biomater* 2010; 6(7): 2386-2393.
- [142] Peter SJ, Liang CR, Kim DJ, et al. Osteoblastic phenotype of rat marrow stromal cells cultured in the presence of dexamethasone, beta-glycerolphosphate, and L-ascorbic acid. *J Cell Biochem* 1998; 71(1): 55-62.
- [143] Gregory CA, Gunn WG, Peister A, Prockop DJ. An Alizarin red-based assay of mineralization by adherent cells in culture: comparison with cetylpyridinium chloride extraction. *Anal Biochem* 2004; 329(1): 77-84.
- [144] Singer VL, Jones LJ, Yue ST, Haugland RP. Characterization of PicoGreen reagent and development of a fluorescence-based solution assay for double-stranded DNA quantitation. *Anal Biochem* 1997; 249(2): 228-238.
- [145] Breaudiere JP, Spillan T. Alkaline phosphatases. In: Grassl M, *Methods of enzymatic analysis*. Deerfield Beach: Verlag Chemie 1984.
- [146] Holtorf HL, Jansen JA, Mikos AG. Flow perfusion culture induces the osteoblastic differentiation of marrow stroma cell-scaffold constructs in the absence of dexamethasone. *J Biomed Mater Res A* 2005; 72(3): 326-334.
- [147] Ogawa M, Livingston AG. Hematopoietic colony-forming cells. In: Jordan CT, *Hematopoietic stem cell protocols*. Totowa: Humana Press 2002.
- [148] Taichman RS, Reilly MJ, Verma RS, Emerson SG. Augmented production of interleukin-6 by normal human osteoblasts in response to CD34+ hematopoietic bone marrow cells in vitro. *Blood* 1997; 89(4): 1165-1172.
- [149] Owen TA, Aronow M, Shalhoub V, et al. Progressive development of the rat osteoblast phenotype in vitro: reciprocal relationships in expression of genes associated with osteoblast proliferation and differentiation during formation of the bone extracellular matrix. *J Cell Physiol* 1990; 143(3): 420-430.
- [150] Kim H, Choi JY, Lee JM, et al. Dexamethasone increases angiopoietin-1 and quiescent hematopoietic stem cells: a novel mechanism of dexamethasone-induced hematoprotection. *FEBS Lett* 2008; 582(23-24): 3509-3514.

- [151] Kriegler AB, Bernardo D, Verschoor SM. Protection of murine bone marrow by dexamethasone during cytotoxic chemotherapy. *Blood* 1994; 83(1): 65-71.
- [152] Datta N, Holtorf HL, Sikavitsas VI, et al. Effect of bone extracellular matrix synthesized in vitro on the osteoblastic differentiation of marrow stromal cells. *Biomaterials* 2005; 26(9): 971-977.
- [153] Holtorf HL, Datta N, Jansen JA, Mikos AG. Scaffold mesh size affects the osteoblastic differentiation of seeded marrow stromal cells cultured in a flow perfusion bioreactor. *J Biomed Mater Res A* 2005; 74(2): 171-180.
- [154] Sikavitsas VI, Bancroft GN, Holtorf HL, et al. Mineralized matrix deposition by marrow stromal osteoblasts in 3D perfusion culture increases with increasing fluid shear forces. *Proc Natl Acad Sci U S A* 2003; 100(25): 14683-14688.
- [155] Borgen E, Beiske K, Trachsel S, et al. Immunocytochemical detection of isolated epithelial cells in bone marrow: non-specific staining and contribution by plasma cells directly reactive to alkaline phosphatase. *J Pathol* 1998; 185(4): 427-434.
- [156] Jaiswal N, Haynesworth SE, Caplan AI, Bruder SP. Osteogenic differentiation of purified, culture-expanded human mesenchymal stem cells in vitro. *J Cell Biochem* 1997; 64(2): 295-312.
- [157] Kao ST, Scott DD. A review of bone substitutes. *Oral Maxillofac Surg Clin North Am* 2007; 19(4): 513-521, vi.
- [158] Holtorf HL, Jansen JA, Mikos AG. Modulation of cell differentiation in bone tissue engineering constructs cultured in a bioreactor. *Adv Exp Med Biol* 2006; 585: 225-241.
- [159] van den Dolder J, Bancroft GN, Sikavitsas VI, et al. Flow perfusion culture of marrow stromal osteoblasts in titanium fiber mesh. *J Biomed Mater Res A* 2003; 64(2): 235-241.
- [160] Sikavitsas VI, van den Dolder J, Bancroft GN, et al. Influence of the in vitro culture period on the in vivo performance of cell/titanium bone tissue-engineered constructs using a rat cranial critical size defect model. *J Biomed Mater Res A* 2003; 67(3): 944-951.
- [161] Castano-Izquierdo H, Alvarez-Barreto J, van den Dolder J, et al. Pre-culture period of mesenchymal stem cells in osteogenic media influences their in vivo bone forming potential. *J Biomed Mater Res A* 2007; 82(1): 129-138.

- [162] Pham QP, Sharma U, Mikos AG. Electrospun poly(epsilon-caprolactone) microfiber and multilayer nanofiber/microfiber scaffolds: characterization of scaffolds and measurement of cellular infiltration. *Biomacromolecules* 2006; 7(10): 2796-2805.
- [163] Maniatopoulos C, Sodek J, Melcher AH. Bone formation in vitro by stromal cells obtained from bone marrow of young adult rats. *Cell Tissue Res* 1988; 254(2): 317-330.
- [164] Medalie DA, Eming SA, Collins ME, et al. Differences in dermal analogs influence subsequent pigmentation, epidermal differentiation, basement membrane, and rete ridge formation of transplanted composite skin grafts. *Transplantation* 1997; 64(3): 454-465.
- [165] Stegemann H, Stalder K. Determination of hydroxyproline. *Clin Chim Acta* 1967; 18(2): 267-273.
- [166] Vunjak-Novakovic G, Martin I, Obradovic B, et al. Bioreactor cultivation conditions modulate the composition and mechanical properties of tissue-engineered cartilage. *J Orthop Res* 1999; 17(1): 130-138.
- [167] Farndale RW, Buttle DJ, Barrett AJ. Improved quantitation and discrimination of sulphated glycosaminoglycans by use of dimethylmethylene blue. *Biochim Biophys Acta* 1986; 883(2): 173-177.
- [168] Park H, Temenoff JS, Tabata Y, et al. Injectable biodegradable hydrogel composites for rabbit marrow mesenchymal stem cell and growth factor delivery for cartilage tissue engineering. *Biomaterials* 2007; 28(21): 3217-3227.
- [169] Young S, Patel ZS, Kretlow JD, et al. Dose effect of dual delivery of vascular endothelial growth factor and bone morphogenetic protein-2 on bone regeneration in a rat critical-size defect model. *Tissue Eng Part A* 2009; 15(9): 2347-2362.
- [170] Breaudiere JP, Spillman T. Alkaline phosphatases, routine method. In: Grassl M, *Methods of enzymatic analysis*. Deerfield Beach, FL: Verlag Chemie 1984.
- [171] Sikavitsas VI, Bancroft GN, Lemoine JJ, et al. Flow perfusion enhances the calcified matrix deposition of marrow stromal cells in biodegradable nonwoven fiber mesh scaffolds. *Ann Biomed Eng* 2005; 33(1): 63-70.
- [172] Gomes ME, Sikavitsas VI, Behravesh E, et al. Effect of flow perfusion on the osteogenic differentiation of bone marrow stromal cells cultured on starch-based three-dimensional scaffolds. *J Biomed Mater Res A* 2003; 67(1): 87-95.

- [173] Gomes ME, Bossano CM, Johnston CM, et al. In vitro localization of bone growth factors in constructs of biodegradable scaffolds seeded with marrow stromal cells and cultured in a flow perfusion bioreactor. *Tissue Eng* 2006; 12(1): 177-188.
- [174] Keller JC, Collins JG, Niederauer GG, McGee TD. In vitro attachment of osteoblast-like cells to osteoceramic materials. *Dent Mater* 1997; 13(1): 62-68.
- [175] Dalby MJ, Gadegaard N, Tare R, et al. The control of human mesenchymal cell differentiation using nanoscale symmetry and disorder. *Nat Mater* 2007; 6(12): 997-1003.
- [176] Dalby MJ, Andar A, Nag A, et al. Genomic expression of mesenchymal stem cells to altered nanoscale topographies. *J R Soc Interface* 2008; 5(26): 1055-1065.
- [177] Simon TM, Jackson DW. Articular cartilage: injury pathways and treatment options. *Sports Med Arthrosc* 2006; 14(3): 146-154.
- [178] Keeling JJ, Gwinn DE, McGuigan FX. A comparison of open versus arthroscopic harvesting of osteochondral autografts. *Knee* 2009; 16(6): 458-462.
- [179] Brittberg M. Autologous chondrocyte implantation--technique and long-term follow-up. *Injury* 2008; 39(Suppl 1): S40-49.
- [180] Philp D, Chen SS, Fitzgerald W, et al. Complex extracellular matrices promote tissue-specific stem cell differentiation. *Stem Cells* 2005; 23(2): 288-296.
- [181] Farrell E, O'Brien FJ, Doyle P, et al. A collagen-glycosaminoglycan scaffold supports adult rat mesenchymal stem cell differentiation along osteogenic and chondrogenic routes. *Tissue Eng* 2006; 12(3): 459-468.
- [182] Cheng NC, Estes BT, Awad HA, Guilak F. Chondrogenic differentiation of adipose-derived adult stem cells by a porous scaffold derived from native articular cartilage extracellular matrix. *Tissue Eng Part A* 2009; 15(2): 231-241.
- [183] Li WJ, Danielson KG, Alexander PG, Tuan RS. Biological response of chondrocytes cultured in three-dimensional nanofibrous poly(epsilon-caprolactone) scaffolds. *J Biomed Mater Res A* 2003; 67(4): 1105-1114.
- [184] Liao J, Guo X, Nelson D, et al. Modulation of osteogenic properties of biodegradable polymer/extracellular matrix scaffolds generated with a flow perfusion bioreactor. *Acta Biomater* 2010; 6(7): 2386-2393.

- [185] Hu JC, Athanasiou KA. Low-density cultures of bovine chondrocytes: effects of scaffold material and culture system. *Biomaterials* 2005; 26(14): 2001-2012.
- [186] Solchaga LA, Gao J, Dennis JE, et al. Treatment of osteochondral defects with autologous bone marrow in a hyaluronan-based delivery vehicle. *Tissue Eng* 2002; 8(2): 333-347.
- [187] Solchaga LA, Johnstone B, Yoo JU, et al. High variability in rabbit bone marrow-derived mesenchymal cell preparations. *Cell Transplant* 1999; 8(5): 511-519.
- [188] Pham QP, Kasper FK, Scott Baggett L, et al. The influence of an in vitro generated bone-like extracellular matrix on osteoblastic gene expression of marrow stromal cells. *Biomaterials* 2008; 29(18): 2729-2739.
- [189] Livak KJ, Schmittgen TD. Analysis of relative gene expression data using real-time quantitative PCR and the 2^{(-Delta Delta C(T))} method. *Methods* 2001; 25(4): 402-408.
- [190] Freyria AM, Yang Y, Chajra H, et al. Optimization of dynamic culture conditions: effects on biosynthetic activities of chondrocytes grown in collagen sponges. *Tissue Eng* 2005; 11(5-6): 674-684.
- [191] Raimondi MT, Moretti M, Cioffi M, et al. The effect of hydrodynamic shear on 3D engineered chondrocyte systems subject to direct perfusion. *Biorheology* 2006; 43(3-4): 215-222.
- [192] Heng BC, Cao T, Lee EH. Directing stem cell differentiation into the chondrogenic lineage in vitro. *Stem Cells* 2004; 22(7): 1152-1167.
- [193] Sobajima S, Shimer AL, Chadderdon RC, et al. Quantitative analysis of gene expression in a rabbit model of intervertebral disc degeneration by real-time polymerase chain reaction. *Spine J* 2005; 5(1): 14-23.
- [194] Mahmood TA, Shastri VP, van Blitterswijk CA, et al. Tissue engineering of bovine articular cartilage within porous poly(ether ester) copolymer scaffolds with different structures. *Tissue Eng* 2005; 11(7-8): 1244-1253.
- [195] Wang L, Seshareddy K, Weiss ML, Detamore MS. Effect of initial seeding density on human umbilical cord mesenchymal stromal cells for fibrocartilage tissue engineering. *Tissue Eng Part A* 2009; 15(5): 1009-1017.
- [196] Campbell MA, Handley CJ, Hascall VC, et al. Turnover of proteoglycans in cultures of bovine articular cartilage. *Arch Biochem Biophys* 1984; 234(1): 275-289.

- [197] Bolis S, Handley CJ, Comper WD. Passive loss of proteoglycan from articular cartilage explants. *Biochim Biophys Acta* 1989; 993(2-3): 157-167.
- [198] von Rechenberg B, Akens MK, Nadler D, et al. Changes in subchondral bone in cartilage resurfacing--an experimental study in sheep using different types of osteochondral grafts. *Osteoarthritis Cartilage* 2003; 11(4): 265-277.
- [199] Yang Z, Shi Y, Wei X, et al. Fabrication and repair of cartilage defects with a novel acellular cartilage matrix scaffold. *Tissue Eng Part C Methods* 2009; 16(5): 865-876.
- [200] Elder BD, Eleswarapu SV, Athanasiou KA. Extraction techniques for the decellularization of tissue engineered articular cartilage constructs. *Biomaterials* 2009; 30(22): 3749-3756.